ABSTRACT

Title of Document: THE FUNCTIONAL REGULATION OF FCRN EXPRESSION AND FCRN-MEDIATED ANTIGEN PRESENTATION

Xindong Liu, Doctor of Philosophy, 2009

Directed By: Associate Professor Xiaoping Zhu, College of Veterinary Medicine

The neonatal Fc receptor for IgG (FcRn), a major histocompatibility complex (MHC) class I-related molecule, plays an important role in IgG transport and protection. The transport of IgG across epithelial and endothelial barriers and the IgG homeostasis maintained by FcRn contributes to the effective humoral immunity. Thus, the level of FcRn itself will affect the IgG-associated immune responses.

Although FcRn is expressed in a variety of tissues and cell types, the extent to which FcRn expression is regulated by immunological and inflammatory events remains unknown.I showed here that FcRn was up-regulated by the stimulation of inflammatory cytokines or Toll-like receptor ligands in human peripheral blood mononuclear cell (PBMC) and THP-1 cell line. By chromatin immunoprecipitation, I identified three NF-κB binding sites within introns 2 and 4 of the human FcRn gene. These intronic binding sites boost FcRn transcription activities through looping with the promoter region. In contrast, FcRn expression was down-regulated by Th1 cytokine IFN-γ, and the down-regulation of FcRn was not caused by apoptosis or the instability of FcRn mRNA. It

has been demonstrated that IFN-γ activated STAT1 bound with GAS sequence in human FcRn promoter, and which blocked the transcriptional machinery.

Fc gamma receptors (FcγRs) expressed in macrophages (MΦ) and dendritic cells (DCs) can mediate antigen presentation in both MHC class II and MHC class I pathways. We tested here the role for FcRn in antigen presentation of IgG-restricted Immune complexes (ICs). It was observed that the expression of FcRn in MΦ, but not in DC enhanced the phagosomal ICs antigen presentation to CD4 T cells. A low pH value in phgosome of MΦ facilitated FcRn binding to ICs, stabilizing the antigens and promoting the efficient MHC II –peptide assembly. However, the alkalized phagosomes in DC failed FcRn to enhance the antigen presentation of ICs.

THE FUNCTIONAL REGULATION OF FCRN EXPRESSION AND FCRN-MEDIATED ANTIGEN PRESENTATION

By

Xindong Liu

Dissertation submitted to the Faculty of the Graduate School of the
University of Maryland, College Park, in partial fulfillment
of the requirements for the degree of
Doctor of Philosophy
2009

Advisory Committee:
Associate Professor Xiaoping Zhu, Chair
Professor David M. Mosser
Assistant Professor Kenneth Frauwirth
Professor Siba K, Samal
Associate Professor Wenxia Song

Dedication

This dissertation is dedicated to my parents, my sister, my wife, my baby girl Sheila. I couldn't have done this without you. Thank you so much for everything you've given me. I love you all very much!

Acknowledgements

First, I would like to thank my advisor, Xiaoping Zhu. His support and guidance throughout the years has given me the knowledge and abilities to explore the unknown. His true passion for science has impressed me. What he has done sets up the great example leading me through my future endeavors. Also, I would like to thank the members of my dissertation committee: Kenneth Frauwirth, Wenxia Song, David Mosser, and Sibal Samal. I appreciate all of your suggestions, constructive criticism, and encouraging remarks throughout my graduate study.

I would like to thank all of members of the Zhu lab for their help, kindness and support. I am grateful to Lilin Ye, his valuable protein handling skills and advices helps me so much over the years. The IgG-transcytosis experiments benefit me and the lab a lot; even though I am the only one in the lab don't know how to handle this experiment. Dr.Li Lu, Dr.Zili Li and Yu Bai, Thank you for everything. I appreciated it more than you know. I am grateful to Rongyu Zengand Senthilkumar for all your help. I will not finish my thesis without your support on mouse housing and bedding changes.

My sincere appreciation goes to Ireen Dryburgh-Barry, Daniel Rockmann and Kadavil Kumar for their support and friendship.

I extend my thanks to my colleagues in Dr. Mosser's lab, Xia Zhang, Jinshan Cao and Ziyan Yang. Your support and friendship keep me sane in all these years. I am lucky to have friends like you. You are the best!

Finally, I'd like to thank my family. I don't know where I'd be without the love and support you have given me all these years. I am especially grateful to my wife, Yun Yun, for her patience and support.

TABLE OF CONTENTS

LIST OF TABLES

LIST OF FIGURES

LIST OF ABBREVIATIONS

antibody dependent immune enhancement	ADE
antigen presenting cell	APC
β_2-microglobulin	β_2m
bone marrow derived dendritic cell	BMDC
bone marrow derived macrophage	BMM
$CD4_+$ T helper cell	Th
carboxyfluorescein succinimidyl ester	CFSE
chromatin immunoprecipitation	ChIP
chromosome conformation capture	3C
cycloheximide	CHX
cytotoxic T lymphocyte	CTL
delayed-type hypersensitivity	DTH
dendritic cell	DC
dulbecco's modification of eagle's medium	DMEM
electrophoretic mobility-shift assay	EMSA
enzyme Linked Immunosorbent Assay	ELISA
Fc gamma receptor	FcγR
fluorescein isothiocyanate	FITC
heat inactivated fetal calf serum	HI-FCS
horseradish peroxidase	HRP
IFN-γ activated sequence	GAS

IFN-stimulated response elements	ISRE
immune complex	IC
immunoglobulin G	IgG
immunoreceptor tyrosine-based activation motif	ITAM
immunoreceptor tyrosine-based inhibitory activation motif	ITIM
inhibitor of NF-κB	IκB
interleukin	IL
interferon gamma	IFN-γ
intestinal epithelial cell	IEC
Janus tyrosine kinase	Jak
lipopolysaccharide	LPS
macrophage	MΦ
macrophage colony stimulating factor	m-CSF
major histocompatibility complex	MHC
neonatal Fc receptor	FcRn
Nuclear factor-kappa B	NF-κB
ortho-Nitrophenyl-β-galactoside	ONPG
ovalbumin	OVA
pathogen associated molecular pattern	PAMP
peripheral blood mononuclear cell	PBMC
protein inhibitor of activated Stat	PIAS
reverse transcription-PCR	RT-PCR
signal transducers and activators of transcription	STAT

suppressor of cytokine signaling	SOCS
systemic lupus erythematosus	SLE
T cell receptor	TCR
T regulatory cell	Treg
toll-like receptor	TLR
tumor necrosis factor	TNF
Terminal deoxynucleotidyl transferase dUTP nick end labeling	TUNEL

CHAPTER 1: INTRODUCTION

OVERVIEW

Immunoglobulins

Immunoglobulin is the crux of humoral immune responses. Membrane immunoglobulins on B cell surface serve as receptors to antigen for B cell. The secreted immunoglobulins are able to bind antigen, receptors, and complement to arm and recruit effector systems in defense of invading pathogens. Such a wide array of duties performed by immunoglobulin is attributed to the feature of its high binding affinity to antigen and Fc receptors (1, 2).There are five isotypes of immunoglobulins in mammals: IgM, IgD, IgG, IgA and IgE. IgM and IgD, the major component of B cell receptor (BCR), are co-expressed on the surface of naive B cells share a number of commonalities to mediate activation, deletion and anergy of B cell (3). Pentameic IgM is the first antibody to be secreted upon challenge by antigen. The secreted IgD is very rare in the plasma comparing with other isotypes. IgG is the predominant immunoglobulin in blood, lymph, peritoneal fluid and cerebrospinal fluid. It makes up 75% of serum immunoglobulin (over 30 mg/kg/d). IgG is the only isotype that can pass through the human placenta, thereby providing protection to the fetus in utero. The majority of synthesized IgA is in the secreted form, which coats the mucosal surface. The synthetic rate of IgA is the highest, roughly double that of IgG (4). IgE is the present in serum in the lowest concentration of all immunoglobulins. It plays a vital role in the clearance of parasites and the unfortunate consequence of allergy.

IgG and FcγRs

IgG is the most abundant and stable isotype of immunoglobulin in serum. The presence of high affinity IgG is the hallmark of the secondary humoral immune responses. There are four subclasses in the IgG family (human IgG1, IgG2, IgG3, and IgG4; mouse IgG1, IgG2a, IgG2b and IgG3). The selection of IgG subclasses does not occur randomly. In human, IgG1 and IgG2 tend to be against polysaccharide immunogens, while IgG1, IgG3 and IgG4 are biased to anti-protein and anti-viral responses (5, 6). In mouse, IgG3 tends to be against carbohydrate, IgG1 and IgG2a is for anti-protein and anti-viral (7, 8). This skewness is greatly affected by cytokines. These characteristics signify the function of the IgG molecule in humoral and cell-mediated immune response (Table I.I) (1).

IgG communicates with the effector arms of immune system via the Fc receptors (FcγR), thereby bridging the cellular and humoral arms of the immune response. Macrophages, polymorphonuclear cells and lymphocytes are implicated as important binders of IgG. Interaction of IgG with FcγRs on these immunological cells triggers many functional effects, such as antibody-dependent cell-mediated cytotoxicity (ADCC), phagocytosis, antigen presentation and inflammation (9). Signals through FcγRs cytoplasmic tail or their associated chains also modulate antigen presentation, cytokine secretion, and cytokine receptors or co-stimulatory expression in lymphocyte. The activating Fc receptors, FcγRI, FcγRIIa FcγRIII and FcγRIV, contain an immunoreceptor tyrosine-based activation motif (ITAM) in their cytoplasmic region or in their associated subunit (9, 10). The inhibitory receptor, FcγRIIb contains an immunoreceptor tyrosine-based inhibitory motif (ITIM) (9, 11). FcγRI is able to bind both monomeric IgG and IgG-antigen complex

Table I.I Characteristics of the IgG Isotype. Compilation of the various characteristics and functions of the IgG subclasses.

CHARACTERISTICS OF IgG	
Subclasses	**IgG1, IgG2, IgG3, IgG4 (human)** **IgG1, IgG2a, IgG2b, IgG3 (mouse)**
Concentration in Sera	**IgG1 > IgG2 > IgG3 > IgG4 (human)**
FcγR Binding	**High affinity receptor -can bind monomeric IgG** **FcγRI: IgG3, IgG1 >IgG4>>IgG2 (human)** **IgG2a>IgG2b, IgG3>>IgG1 (mouse)** **Low affinity receptors –bind IgG-immune complexes** **FcγRII: IgG1, IgG2, IgG3 (human)** **FcγRIII:IgG1, IgG3 (human)** **FcγRIV:IgG2a, IgG2b >> IgG1, IgG3 (mouse)**
FcRn Binding	**IgG4>IgG1>IgG3>IgG2 (human)** **IgG2a>IgG1>IgG2c>IgG2b (rat)** **IgG2a>IgG1>IgG3>IgG2b (mouse)**
Th Response	**Th1: IgG1, IgG3 (human)** **IgG2a (mouse)** **Th2: IgG4 (human)** **IgG1 (mouse)**

with high affinity in dendritic cells (DCs), monocytes and macrophages (MΦ). However FcγRs bind to different IgG subclasses with different affinity. In humans, high affinity Fc receptor FcγRI preferentially binds IgG1 and IgG3 (12). The high affinity of FcγRI depends on a third extracellular Ig-like domain. Low affinity FcγRs, FcγRII and III are only capable of binding immune complexes. FcγRI and FcγRIII are homodimers that associated with the subunit (FcRγ) chain. The formation of homodimer is required for their cell surface expression. FcRγ chain is essential for triggering activation signals through FcγRI and FcγRIII. FcγRII, in contrast, is a single-chain receptor (9, 11). FcγRs are important immune regulators, FcRγ knockout (KO) mice fail to induce IgG-mediated phagocytosis by MΦ, and they also exhibit severe reduction in the autoantibody-dependent experimental hemolytic anemia and thrombocytopenia (13), anti-glomerular basement membrane IgG-induced glomerulonephritis (14), and immune complex-induced vasculitis syndrome (15). Therefore, FcγRs play important roles in shaping the immune response (16-20) and determining the outcome of immunopathology (21-25).

The Neonatal Fc Receptor (FcRn).

FcRn belongs to MHC class I family

It has long been known that passive immunity can be transferred from mother to offspring. The neonatal Fc receptor (FcRn) is the first receptor identified in rodent to carry out the specific transport of IgG. IgG is the only immunoglobulin transferred from mother to the fetus. The gene encoding FcRn was first isolated from rat by Simister & Mostov in 1989. FcRn is a heterodimer of β_2-microglobulin and a 45- to 53-kDa heavy chain, associating with

each other noncovalently. The sequencing analysis of the heavy-chain confirmed that all three extracellular and transmembrane domains of FcRn share homology with the corresponding regions of MHC class I molecules (26). This thereby expand the functions of MHC class I molecules beyond their known roles in antigen presentation. The fact that cytoplasmic domains of FcRn share much less homology with MHC class I molecules is consistent with the different functional activities of the two types of proteins (27).

The structural similarity between FcRn and MHC class I molecules was confirmed by the X-ray crystallographic structure (28). Notably, the antigen-binding groove where peptide or glycolipid ligand binds is occluded in FcRn (Fig. 1.1). This occlusion is primarily caused by a kink which is introduced by the presence of proline at position 165 of the $\alpha 2$ domain helix (29). However, the introduction of a proline at the corresponding position in the MHC class I molecule H-2d does not affect peptide MHC class I-mediated antigen presentation to (30), suggesting that additional structural features of FcRn cause the closed groove. It is interesting to explore whether groove on FcRn might be opened up in the acidic condition, based on the finding that groove on CD1b can opened up by low pH (31).

Both mouse and human FcRn alpha chains have been isolated later on (32, 33). FcRn from mouse and rat is highly related and the human form is more divergent, although the rodent and human genes share homology. Human FcRn was first identified in human syncytiotrophoblast (33-35). This suggests that it plays a role in the transfer of IgGs from the maternal circulation to the fetal capillaries of the placental villi (34, 36, 37). The isolation and characterization of human FcRn links the studies of FcRn in rodents and humans.

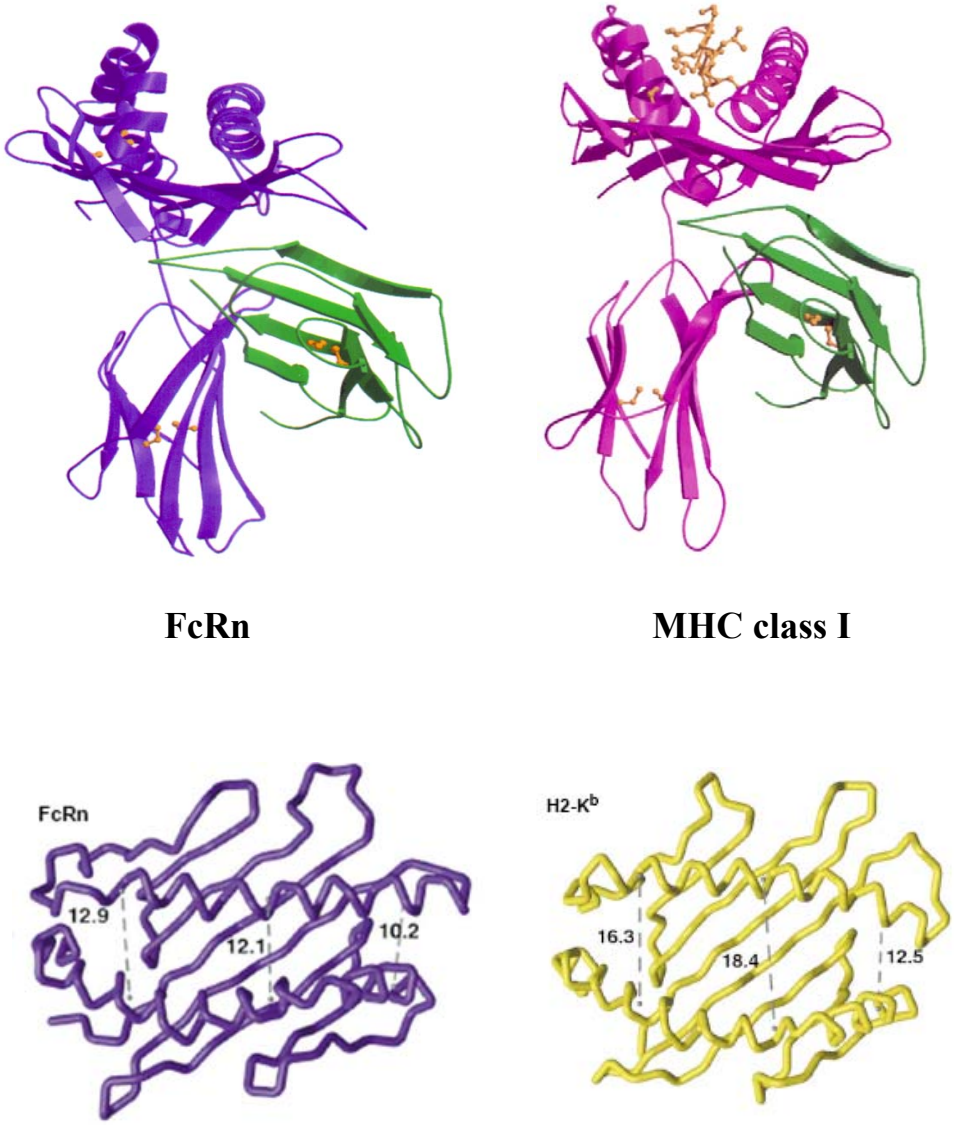

Figure 1.1 The structural comparison of FcRn and MHC class I

From Zeng et al., 1997, Science: 277:339-345. and Bennett et al., 2000, Nature 403:46.

The interaction of IgG with FcRn

Characterization of FcRn-IgG interaction sheds light on the mechanism of IgG transport. A combination of approaches has been used to identify the IgG interaction site for FcRn. Several conserved amino acids located at the CH2-CH3 domain interface of IgG has been identified playing a central role in the interaction with rat or mouse FcRn. Ile253, His310 in CH2 domain of IgG are key players in the interaction of IgG with FcRn (38-40), although the His435 in CH3 plays a minor but significant role in the mouse FcRn-IgG interaction (40). Also, the sequence -H-N-H-Y (AA 433-436) of the CH3 domain is important for pH-dependent binding. These residues are highly conserved across species, and the lack of conservation of this amino acid across species is consistent with more limited involvement (40). Further analyses of resulting recombinant Fc fragments demonstrated that amino acids at position 257 and, to a lesser extent, positions 307 and 309 in proximity to the CH2-CH3 domain interface play a role in the FcRn-Fc interaction. The role of residues 257, 307, and 309 is less marked than that of Ile253, His310, and His435 (40, 41). However, sequence variations at 257, 307, and 309 can be used to explain the different affinities of rat IgGs for FcRn. Furthermore, fragment B of staphylococcal protein A is known to bind to amino acids at this interdomain interface; it competes with IgG for binding to FcRn (42) (Table I.II).

The IgG binding site on rat FcRn was mapped using site-directed mutagenesis, the mutants were then analyzed by in vitro binding assays (42, 43). These studies identify α2 domain and β2m for interacting with IgG. The α2 domain residues (Glu117, Glu132,

Table I.II Variations of IgG sequences in the region involved in the binding of FcRn (27)

	Position	252	253	254	255	256	257	307	308	309	310	311	433	434	435	436
Human	IgG1	Met	Ile	Ser	Arg	Thr	Pro	Thr	Val	Leu	His	Gln	His	Asn	His	Tyr
	IgG2	Met	Ile	Ser	Arg	Thr	Pro	Thr	Val	Val	His	Gln	His	Asn	His	Tyr
	IgG3	Met	Ile	Ser	Arg	Thr	Pro	Thr	Val	Leu	His	Gln	His	Asn	Arg	Phe
	IgG4	Met	Ile	Ser	Arg	Thr	Pro	Thr	Val	Leu	His	Gln	His	Asn	His	Tyr
Mouse	IgG1	Thr	Ile	Thr	Leu	Thr	Pro	Pro	Ile	Met	His	Gln	His	Asn	His	His
	IgG2a	Met	Ile	Ser	Leu	Thr	Pro	Pro	Ile	Gln	His	Gln	His	Asn	His	His
	IgG2b	Met	Ile	Ser	Leu	Thr	Pro	Pro	Ile	Gln	His	Gln	Lys	Asn	Tyr	Tyr
	IgG3	Met	Ile	Ser	Leu	Thr	Pro	Pro	Ile	Gln	His	Gln	His	Asn	His	His
Rat	IgG1	Thr	Ile	Thr	Leu	Thr	Pro	Pro	Ile	Leu	His	Gln	His	Asn	His	His
	IgG2a	Thr	Ile	Thr	Leu	Thr	Pro	Pro	Ile	Val	His	Arg	His	Asn	His	His
	IgG2b	Leu	Ile	Ser	Gln	Asn	Ala	Pro	Ile	Gln	His	Gln	His	Asn	His	His
	IgG2c	Met	Ile	Thr	Leu	Thr	Pro	His	Ile	Gln	His	Gln	His	Asn	His	His

Trp133, Glu135, and Asp137) and one β2m residue (Ile1) are shown playing a direct role in the interaction, and these residues are reasonably well conserved across species (26, 33, 44). FcRn binds to IgG is a pH dependent manner. The IgG binding occurs at pH<6.5, and the dissociation happens at pH>7.5. The highly conserved histidines (His 310 and His 435) in IgG, together with acidic residues in FcRn (Glu117, Glu132, Trp133, Glu135, and Asp137) provide an explanation for the strict pH dependence of the FcRn-IgG (or Fc) interaction (26).

The interaction of IgG with FcRn occurs in a mode distinct from that reported for T-cell receptor-peptide-MHC class I interactions (45, 46), in which the T-cell receptor footprint covers the surface of the two MHC helices and binds antigenic peptide in a diagonal orientation. A ‘‘lying-down’’ model has been proposed for FcRn-IgG binding where an FcRn dimer binds to one IgG molecule. This is supported by in vitro studies showing that FcRn dimerizes upon binding to IgG in a higher afffinity (47).

The interaction of FcγRs with IgG is different from FcRn

Mutagenesis studies indicate that the FcγR interaction sites of IgG are different from the region of IgG binding with FcRn. The residues in the lower hinge region of IgG are important for binding to FcγRI, FcγRIIa and FcγRIII (48-52). Other residues close to lower hinge spatially, such as FcγRI (Pro331) and FcγRII (Glu318), glycocylation of IgG are also important for FcγR binding(49, 53-55). The binding of both FcγRI and FcγRII to IgG was not inhibited by recombinant soluble FcRn, indicating that FcγR interaction site does not encompass the CH2-CH3 domain surface covering FcRn binding sites (27).

The FcRn-mediated transportation of IgG

FcRn, was initially identified as a receptor transporting maternal IgGs across placenta to the fetus and from the proximal small intestine to the newborn animals (36, 56). In other words, FcRn transcytoses IgG across a polarized cell layer from the mother to the offspring. In the gut of neonatal rodents, FcRn functions most efficiently in the neonatal period. Maternal IgG from ingested milk passes through the stomach, goes into the duodenum, where IgG binds to FcRn on the apical surface of an epithelial cell with the slightly acidic environment (57). The FcRn-IgG complexes are taken up by receptor-mediated endocytosis. The complexes are then transcytosed across the cells and delivered via exocytosis at the basolateral surface of the cells. FcRn then releases IgG into the underlying extracellular space, due to an increase in pH. In β2-microglobulin-/- or FcRn -/- mice, no maternal IgG was transported (58). These studies confirm that FcRn is the receptor involved in the transport of IgG from mother's milk to newborns.

There is also a minor route for IgG transport in rodent. The successful cloning FcRn from rat yolk sac endoderm indicates that this Fc receptor is also involved in the maternal IgG transfer (59). However, the barely detectable FcRn on the cell surface led to the suggestion that FcRn binding to IgG occurs only after nonspecific uptake via fluid-phase pinocytosis by yolk sac.

In human, transporting maternal antibodies across placenta antenatally is the major route of IgG delivery to the fetus. Although the relative transfer efficiency of maternal IgG still remains controversial, the proposed model of FcRn-mediated IgG transfer is that the

syncytiotrophoblast internalizes fluid containing maternal IgG into endosomes; the IgG-containing endosome is then gradually acidified thereby allowing IgG to bind tightly to FcRn present in this compartment. The vesicle then fuses with the membrane on the fetal side of the syncytiotrophoblast, where the physiological pH promotes the dissociation of IgG from FcRn. The FcRn molecule may then be recycled to the maternal membrane to perform additional rounds of transcytosis (57).

FcRn in human is different from that in rodents. In humans, FcRn is expressed by intestinal epithelial cells in both the fetus and adult (60, 61). However, intestinal expression of FcRn in rodent is highest on the epithelial cells of the proximal small intestine during the neonatal period and then decline rapidly after weaning. The level of FcRn in the intestine of adult rodent is very low (62, 63). The intestinal expression of FcRn in adult human suggests the additional role of FcRn besides the maternal IgG transfer. This hypothesis was proven by the study from Blumberg's group. They showed that IgG–bacteria complexes were transcytosed across the epithelium by using a transgenic mice carrying human FcRn. FcRn in the mouse intestine delivered the immune complexes back to lamina-propria DCs, which then efficiently process and present antigen to the antigen-specific T‑cell in the draining lymph node (57).

Consistent with the observation that significant amount of IgG exist on the mucosal surface of lung, FcRn is highly expressed in the bronchiolar and alveolar epithelium in rats. Different from rat, FcRn is expressed predominantly in the upper airway epitheliumof primate (64). Given the large surface area of the lung epithelium, a role for FcRn is being

taken for consideration seriously. FcRn is proposed to transport IgGs from the circulation to the lumen of lung airway, where IgGs provide protection against the pathogens from the air (64). Similarly, IgG absorption by the epithelium should not be ignored in these systems.

FcRn-mediated IgG/albumin protection from catablism.

FcRn also acts as salvage receptors binding and protecting IgGs from lysosomal degradation. It has been demonstrated that the IgGs in both β_2m and FcRn knockout (KO) mice have short serum half-lives (27, 58, 65-68). In FcRn-deficient mice, the serum IgG level is ~20–30% of wild-type animals, the half-lives of IgG and albumin are reduced from ~6–8 days to ~1 day, similar to the typical half-life of other serum proteins that are not freely filtered by the kidneys (57). Consistent with these, other studies showed that a good correlation between affinity for binding IgG and serum half-life for IgG. The mechanism for FcRn-mediated IgG protection is likely through uptaken of IgG by cells expressing FcRn. Following entry into an acidic compartment such as endosome, IgG molecules bind to FcRn. Enzymes present in the vesicles downstream of endosomes, such as in lysosomes, digest unbound IgG; whereas, the IgG bound to FcRn is protected and recycled back out of the cells (69)(Fig. 1.2).

Recently, FcRn has also been shown to bind albumin and extend its half-life. In FcRn-deficient mice, the serum albumin concentration is about 40% of the normal level. It is important to note that IgG and albumin make up ~90% of the protein content of serum. Therefore, through a pH-dependent binding, FcRn rescues IgG and albumin from degradation, and thereby selectively extends their half-lives in the circulation.

The exact tissure location of FcRn to protect serum IgG remains an open question, and the dual functions of FcRn also complicated this issue. At present, FcRn expressed on vascular endothelium is considered as the main player for IgG protection (70, 71). Expression of FcRn in the vascular endothelium of skeletal muscle and the skin in mice provides a large contact area for FcRn to contactwith blood (46, 71, 72). As these endothelial cells efficiently internalize serum proteins, FcRn is proposed to capture IgG and return it to the circulation, thereby prolonging the persistence of IgG in the serum. Alternatively, IgG may be saved from lysosomal catabolism when IgG is transcytosed into tissues through the polarized cells (57).

The expression of FcRn on monocytes, including MΦs and DCs provides additional candidates for the IgG protection (73, 74).When WT bone marrow cells are adoptively transferred to FcRn deficient mouse, it partially rescued the serum half-life of IgG (72). Most likely, myeloid-derived monocytes contribute to this protection by recycling the internalized IgG, as phagocytes and monocytes can ingest significant quantities of fluid. Additional functions for FcRn were found in professional antigen-presenting cells (APCs). The recent two reports describing the recycle of intact IgG immune complexes (ICs) in DCs and the impaired function of antigen presentation for ICs in FcRn -/- DC provide evidence for the divergent faces of FcRn (75, 76).

FcRn, as therapeutic target for autoimmune diseases

As FcRn functions as salvager to maintain IgG homeostasis in the serum, and as transporter to deliver IgG to different tissue and organs (Fig. 1.2), many studies have been

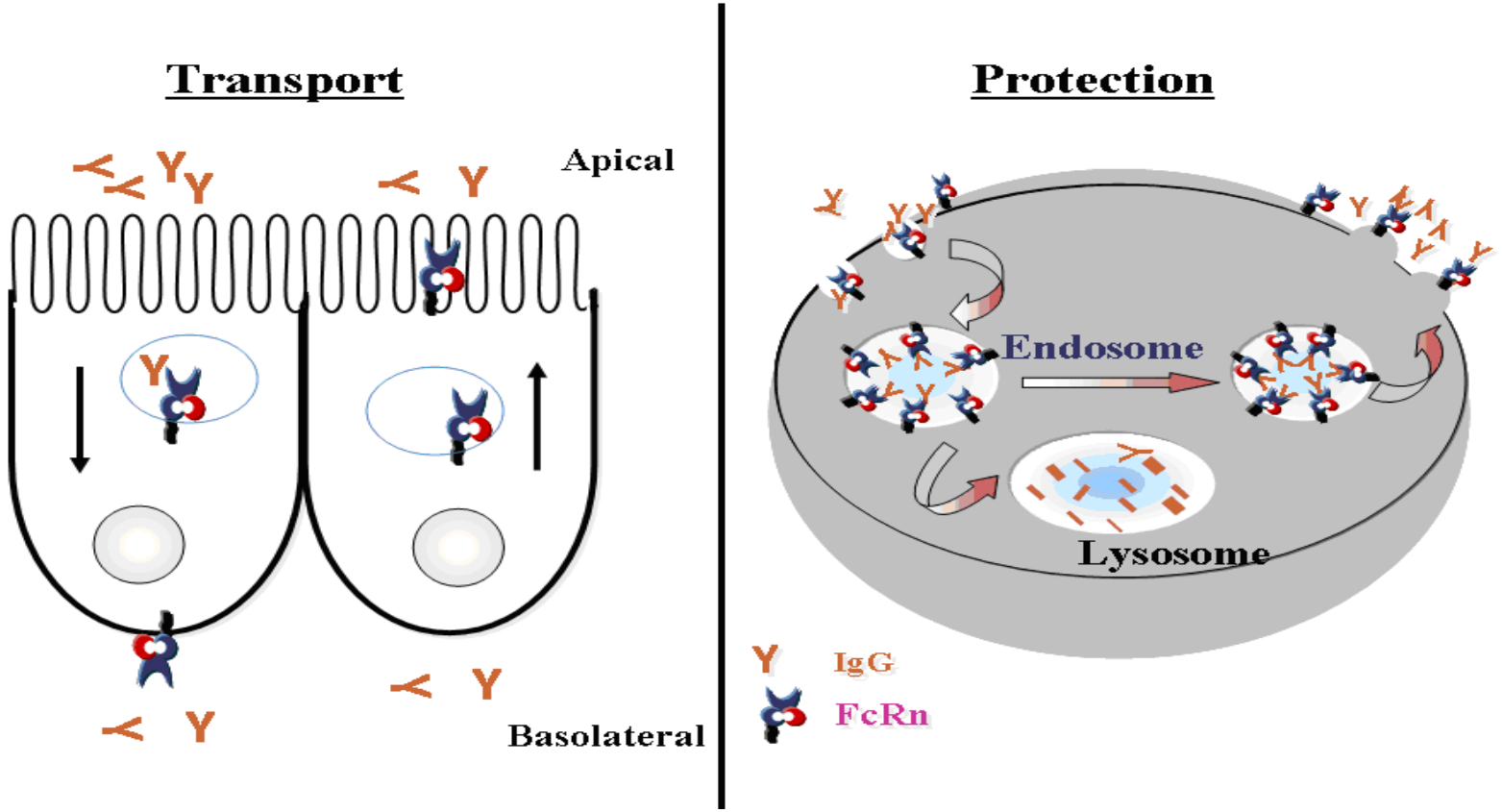

Figure 1.2 The functions of FcRn in transport and protection of IgG. IgG is pinocytosed into vesicles along with membrane. FcRn binds the Fc portion of IgG at the acidic compartment and transcytoses IgG across the cellular layer (left panel). FcRn can also act as salvager to bind the uptaken IgG in the endosome and recycle the bound IgG to the cell surface. The unbound IgG is degraded in the lysosome (right panel).

done in the IgG-mediated diseases by taking advantage of these characteristics of FcRn (57). In autoimmune diseases model (Table I.III), such as myasthenia gravis, bullous pemphigoid, idiopathic thrombocytopenic purpura (ITP) and systemic lupus erythematosus (SLE), the endogenously pathogenic IgG level was reduced by administration of high-dosage of intravenous immunoglobulins (IVIG) as a consequence of FcRn saturation (77, 78). Blocking FcRn-IgG interaction by using FcRn specific antibody is a more direct approach to reduce the titer of pathogenic IgG (78, 79). Alternatively, administration of humanized IgG monoclonal antibodies with Fc regions that bind to FcRn with an unusually high affinity results in the rapid degradation of non-bound endogenous antibodies (80).

Transcriptional regualtion

The nuclear factor-κB (NF-kB) and inhibitors of NF-kB (IkBs)

The mamalian NF-kB family has many members including RELA (p65), NF-kB1 (p50; p105), NF-kB2 (p52; p100), c-REL and RELB (81, 82). These proteins have a structural conserved amino terminal region, which contains the dimerization, nuclear localization and DNA-binding domains. The RELA, RELB and c-REL also have a carboxy-terminal domain which can activate transcription. The p50 and p52 is generated respectively from precursor p105 and p100 by proteolytic digestion, they lack transcription activation domain, but they still are able to bind to NF-kB consensus sites in DNA. Each member of NF-kB family can form homodimers as well as heterodimers with one another, except for RELB. The main activated form of NF-kB is the heterodimer of p65/p50 or p65/p52. p50 and p65 are expressed in a wide varities of cell types, whereas the expression of RELB is

Table I.III IgG-mediated autoimmune diseases

IgG-mediated Autoimmune Diseases	
Organ-specific  **Systemic**	**Addison's disease** **Insulin dependent diabetes mellitus** **myasthenia gravis** **bullous pemphigoid** **Multiple sclerosis** **Autoimmune haemolytic anaemia** **Idiopathic thrombocytopenic purpura** **Rheumatoid arthritis** **Scleroderma** **Systemic lupus erythematosis (SLE)**

restricted to thymus, lymph nodes and Peyer's patches. The c-REL is confined to haematopoietic cells and lymphocytes (81, 83).

It has been well documented that the association of IkBs with NF-kB proteins in the cytoplasm results in the inactivation of NF-kB. Most commonly, IkBs are composed of IkBα, IkBβ and IkBε, which are defined by the presence of ankyrin repeats, a 33-amino-acid motif that mediates protein-protein interactions. Another unusual member of IkBs is BCL-3, which specifically interacts with p50 or p52 homodimers and can enhance the NF-kB-regulated genes. This is in contrast to the inhibitory function of IkBs (83). The subsequent phosphorylation, ubiquitination and proteasome-mediated degradation of IkBs result in the liberation of NF-kB heterodimers follwed by rapid translocation to the nucleus. IkBs are phosphorylated by IkB kinases (IKKs) including IKKα, IKKβ and IKKγ. IKKs mediate site-specific phosphorylation of the IkBs, which triggers the degradation of NF-kB inhibitors. Once in the nucleus, NF-kB bind to the consensus sequence (5'-GGGRNYYYCC-3', R: purine, Y: pyrimidine, N: any nucleic acid) and activate gene transcription (84).

NF-κB signalling pathways through TLR ligands and cytokines

The NF-kB/REL family of transcriptional factors has an essential role in regulating the expression of a wide variety of genes that control both innate and adaptive immune response. NF-kB is activated rapidly in response to a wide range of stimuli, including pathogens, stress, and inflammatory cytokines. Many pathogens are recognized by specific pathogen-recognition receptors (PRR). These pathogens are consistently found bearing small molecular motifs named as pathogen-associated molecular patterns (PAMPs). Bacterial

lipopolysaccharide (LPS), peptidylglycans, lipoproteins, unmethylated bacterial DNA and double strand RNA are considered as PAMPs. The best known PRRs are Toll-like receptors (TLRs), a group of transmembrane proteins that mediates the intracellular signalling after recognizing the extracellular pathogens. The binding of PAMPs with TLRs will activate an intracellular signaling cascade through TLR cytoplamsic Toll/IL-1 receptor (TIR)-homology domain. The TLR family signaling pathway is highly homologous to that of IL-1 receptor (IL-1R) family in mammals. Both TLR and IL-1R interact with an adaptor protein MyD88 (myeloid differentiation primary response gene 88). Upon stimulation, MyD88 recruits IL-1R associated Kinase (IRAK), IRAK is activated by phosphorylation and then associates with TRAF6 (TNF receptor associated factor 6), leading to activation of NF-kB (85). The complex of transforming-growth-factor-β-activated kinase 1 (TAK1), TAK-binding protein (TAB1) and TAB2 was considered as an integral component that linked TRAF6 and downstream IKK complexes, but recent observation from TAB1-andTAB2-knockout mice did not support the roles for these proteins in NF-kB signalling (83). Another candidate molecule that links TRAF6 and NF-kB was identified in a screen of TRAF6-interacting molecules, designated ECSIT (evolutionarily conserved signaling intermediate in Toll pathways), and the roles for ECSIT need more studies (86, 87).

Cytokines, such as TNF and IL-1, are another important class of NF-kB inducers. TNF and IL-1 activate signaling cascade that lead to the activation of activitor protein1 (AP1) and NF-kB, which regulates the expression of inflammatory cytokine genes. IL-1 activates NF-kB in a similar manner to LPS, because both IL-1R and TLR 4 contain homology domain (TIR) in the cytoplasmic tail. The engagement of TNF and TNF receptor

results in the receptor trimerization and recruitment of adaptor protein TRADD (TNF receptor-associated via death domain) to the cytoplamic tail. TRADD interacts with carboxyl terminus of TRAF2. Mitogen-activated protein (MAP)/extracellular signal-regulated kinase ERK) kinase kinase 3 (MEKK3) and receptor interacting serine/throenine kinase (RIP) are likely to relay the signal from TNF to IKKs (88, 89).

JAKs (Janus family tyrosine kinases)-STATs (Signal transducer and activitor of transcription)

JAKs and STATs pathway is integral to both type I (IFN-α/β) and type II (IFN-γ) interferons and to all type I cytokines which share a similar four-α-helix bundle strutures. This pathway represents a rapid membrane-to-nucleus signaling system to induce many important biological responses in the target cell (90).

Jaks are relatively large kinases of approximately 1150 amino acids with molecular weight 120-130 kDa. Jak family is recognized by the existance of tandem kinases domain (JH1) and pseudokinase domains (JH2) in the C-terminal. In addition, five other Jak homology (JH3-JH7) domains were defined in Jaks. The N-terminal of Jaks seems to associate with receptor subunits. Four Jaks have been identified in mamalian: Jak1, Jak2, Jak3 and Tyk2 (Tyrosine kinase 2). The essential functions of Jaks are established in many cytokine signaling pathways. Specially, IFN-α/β requires Jak1 and Tyk2, whereas IFN-γ requires Jak1 and Jak2 (91).

Mamalian STATS comprises seven member proteins: Stat1, Stat2, Stat3, Stat4, Stat5,

Stat6 and Stat7. STATs are approximately 750-850 amino acids in length. They have a conserved tyrosine (~700 residues), whose phosphorylation allows STATs dimerization, a Src homology (SH2) domain and an N-terminal domain known to play a role in the dimerization of STATs, and the DNA binding domain located in the middle region (91). Following the interferons binding to their receptors, Jak kinase is rapidly induced and phosphorylates the interferon receptors. Such phosphorylation provides docking sites for STATs. The recruited STATs are phosphorylated, dimerized and released from the receptors. The dimric form then translocates into the nucleus and binds with STATs binding sites to mediate gene expression.

Interferons have potent antiviral and growth inhibitory effects, which provide the first line in defence against viral invasion and have important roles in immunosurveilance for malignant cells. The binding of type I interferons (mainly IFN-α/β) with their receptors (IFNAR1 and IFNAR2) results in the phosphorylation and activation of Jak1 and Tyk2. Activated Jak1 and Tyk2 in turn regulate the phosphorylation and activation of Stat1 and Stat2. Together with IRF-9 (Interferon-regulatory factor 9), the dimerized Stat1 and Stat2 is delivered to the nuclues and binds to specific elements known as interferon-stimulated response element (IRES), thereby initate the gene expression (90, 92). Other Stats, such as Stat3, Stat5, Stat4 and Stat5 can also be activated by type I interferon. In contrast, the association of type II interferon (IFN-γ) with its receptor (IFNGR1 and IFNGRII) triggers activation of Jak1 and Jak2, which induce the phosphorylation of Stat1. Phosphorylated Stat1 forms homodimer, translocates into the nucleus and binds to GAS sites (Interferon-γ-activated sites) (90).

The phosphorylation of tyrosine residues (Tyr 701) in STATs by JAKs is a crucial step in IFN-mediating sigaling, as it is required for the dimerization and translocation of STATs (93). However, in Stat1 and Stat3, serine residue at position 727 (Ser 727) is also found phosphorylated by the induction of type I and type II interferons. The Ser727 is located in the C-terminal domain. Such phosphorylation is not required for their translocation, but it is essential for full transcriptional activaties (94, 95).

IFN-activated STATs can interact with other proteins to enhance the transcriptional precisement. For examples, the protein inhibitor of activated STAT-1 (PIAS1) and suppressor of cytokine signaling (SOCS) have been shown to negatively regulate STAT-1 signaling in cytosol (96). The association of STATs with p300 and CBP (cAMP-responsive elements-binding protein (CREB) binding protein) in nucleus increase IFN-α- or IFN-γ-inducible transcription. P300 and CBP are acetyltransferases which remodel the chromatin and regulate the gene expression on epigenic level (97).

Antigen presentation

MHC class I-restricted antigen presentation.

Endogenous proteins destined to presentation on MHC-I molecules are ubiquitinated in cytosol and degradated by proteasome. The resulting peptides are transferred to the ER by TAP (Transporter associated protein) and loaded on the newly synthesized MHC-I molecules under the help of loading complex comprised of several chaperones (tapasin, calnexin, and calreticulin) (98). After the MHC-I-peptide loaded, MHC-I is rapidly transferred through

Golgi apparatus to the plasma membrane, where MHC-I molecules interact with TCR of CD8+ T cells and activate CD8+ T cells. The sources for endogenous proteins vary, incuding cytosolic proteins, alternative translation products and defective ribosomal translation, proteins retranslocated to the cytosol from ER, and internalized proteins transferred to the cytosol (99).

Exogenous proteins can also be presented on MHC-I molecules, a recently discribed antigen presentation route denoted as “Cross-presentation”. Exogenous proteins are internalized by various ways. Macropinocytosis allows the soluble antigen cross-presented in DCs. Phagocytosis has been shown a major route for antigen uptake and cross-presentation in both MΦ and DC. Interestingly, phagocytosis of apoptosic cells also results in efficient cross-presentation of viral and tumor antigens. In addition, FcR-mediated uptake of immune complexes enhances the cross presentation efficiently. The MHC class I peptide loading for cross presentation occurs at two main sites, either endocytic compartment or ER lumen. Endocytic compartments pathway is sensitive to proteases inhibitors and TAP-independent, this requires the presence of MHC-I molecules in the endocytic compartments. By contrast, ER lumen pathway is sensitive to proteasome inhibitor and requires TAP, and the antigen transport pathway from endocytic lumen to cytosol is essentially required for TAP-dependent cross presentation.

MHC class II-restricted antigen presentation

Antigens loading on MHC class II molecules occur through a different pathway (APC). Soon after synthesis in ER, three a/b MHC-II dimers bind to one trimers of invariant

chains (Ii). Ii chain will escort MHC-II from ER to the endocytic pathways under the tranport signal present in the cytoplasmic tail of Ii chain. Once in the endosomes and lysosomes, the acidic environment facilitates proteolytic enzyme to digest Ii chain. MHC-II dimers become competent to bind antigenic peptide under the control of two nonpolymorphic MHC-II molecules HLA-DM/HLA-DO (human). MHC-II peptide complexes reach to the plasma surface after peptide loading onto the MHC-II molecules. Antigen loaded onto MHC-II molecules are typically generated from exogenous proteins internalized by antigen presenting cells (APC). The internalization of exogenous proteins is mainly through four pathways, including phagocytosis, micropinocytosis, clathrin-meditaed endocytosis and non clathrin endocytosis.

Macrophage and DC

MΦ has long been considered the prototypical APC, simply due to the fact that they are associated with microoganisms endocytosis in innate immune response. MΦ owns extraordinary capacity for endocytosis. It can internalize cell-associated or soluble antigens, either nonspecifically or via specific receptors (FcR, lectins, etc.), allowing them to stimulate T cells. MΦ express MHC-I, MHC-II, and costimulatory molecules, and their expression level can be upregulated by the stimulation of inflammatory cytokines or bacterial products. Although the level of MHC II and costimulators expressed on MΦ are lower than that of DCs and B cells. the large number of MΦ at the sites of infection and chronic inflammation contribute to the T cell stimulation (22, 99).

DCs are the most efficient antigen-presenting cells to the T cell stimulation. Both MΦ and DCs are originated from bone marrow-derived precursor and take residence in peripheral tissue. Nearly all the tissues contain MΦ and DCs, but the primary function for DCs is antigen presentation. DCs exhibit a variety of features that greatly enhance the capacity as APCs. First, DCs have unique surveillance and migratory properties to carry antigen acquired in the periphery to lymph node and then activate the naïve T cells . Second, DCs can endocytose and present virtually any form of protein antigen on MHC I and II molecules. Third, exceptionally high level of MHC-II and co-stimulatory molecule is expressed on DCs. Fourth, DCs own the capacity to tightly control the antigen degradation (99).

The function of DCs can be regulated by maturation, and the maturation induces a dramatic structural reorganization. Immature DCs express low levels of surface MHC II and co-stimulatory molecules, together with high capacity of endocytosis. Upon stimulation by TLR ligand, inflammatory cytokines, DCs begin to mature with several changing features. First, MHC II is transported to the plasma membrane associated with high levels of costimulatory molecules (100, 101). Second, endocytosis rates decrease dramatically following a transient increase (102). Finally, DCs change the morphology with extended dendrites and more folded membrane. Concomitant with these features, DCs switch the function from antigen handling to T cell activation (100).

QUESTIONS TO BE ADDRESSED IN MY PROJECT

In our study, we want to know whether FcRn can be regulated in the context of inflammation. In other words, how is the IgG controller controlled? We found that human

FcRn can be regulated by inflammatory cytokines, toll-like receptor ligands, and interferons. This will be described in detail in **Chapter 2** and **Chaper 3**. Furthermore, the phagosomal pH difference in DC and MΦ leads to a new discovery of FcRn-mediated antigen presentation of immune complexes (**Chapter 4**).

CHAPTER 2: NF-κB SIGNALING REGULATES FUNCTIONAL EXPRESSION OF FcRn VIA INTRONIC BINDING SEQUENCES

ABSTRCT

The neonatal Fc Receptor for IgG (FcRn) functions to transport maternal IgG to a fetus or newborn and to protect IgG from degradation. Although FcRn is expressed in a variety of tissues and cell types, the extent to which FcRn expression is regulated by immunological and inflammatory events remains unknown. Stimulation of intestinal epithelial cell lines, macrophage-like THP-1, and freshly-isolated human monocytes with cytokine tumor necrosis factor-α (TNF-α) rapidly up-regulated FcRn gene expression. In addition, Toll-like receptor ligands lipopolysaccharides and CpG-oligodeoxynucleotide enhanced the level of FcRn expression in macrophage-like THP-1 and freshly-isolated human monocytes. Treatment of TNF-stimulated THP-1 cells with nuclear factor-kappa B (NF-κB) specific inhibitor, or over-expression of a dominant negative mutant inhibitory nuclear factor-kappa B (IκBα, S32A/S36A) resulted in down-regulation of FcRn expression. By chromatin immunoprecipitation, we identified three NF-κB binding sites within introns 2 and 4 of the human FcRn gene. The intronic NF-κB sequences in combination with the promoter or alone regulated the expression of a luciferase reporter gene in response to TNF-α stimulation or over-expression of NF-κB p65 and p50. DNA looping interactions potentially occurred after the stimulation between intronic NF-κB sequences and FcRn promoter, as shown by chromosome conformation capture assay. Together,

these data provide the first evidence that NF-κB signaling via intronic sequences regulates FcRn expression and function.

INTRODUCTION

The neonatal Fc receptor for IgG (FcRn) differs from FcγRs because it is structurally related to the MHC class I family, with a membrane-bound heavy chain (HC) in nonconvalent association with β_2-microglobulin (β_2m) (26, 47). The overall exon-intron organization of the FcRn gene is similar to that of MHC class I molecules, with the exception of a very large 10-kb intron between exons 4 and 5. In addition, FcRn displays pH-dependent binding of IgG; specifically, FcRn preferentially binds IgG at acidic pH (6-6.5) and releases it at neutral pH (7-7.4). FcRn is a transport receptor involved in controlling the movement of IgG from the maternal to the fetal blood of rodents and humans in placental and/or intestinal tissues. FcRn, therefore, plays a major role in the passive acquisition of neonatal immunity to newborn mammals. FcRn also functions in the maintenance of IgG homeostasis in mammals of all ages by salvaging IgG from degradation. In the proposed model, IgG is taken up into cells by pinocytosis or endocytosis from the surrounding tissue fluid or blood. FcRn in acidic compartments, such as the endosome, binds and recycles IgG out of the cell to avoid IgG degradation in the lysosome. The IgG transport and protective functions of FcRn are evidenced by several studies in which mice deficient in either β_2m or the FcRn HC fail to transport maternal IgG and show a significant reduction in the serum half-life of IgG (27, 103-105).

Although first observed in the intestinal epithelial cells of the neonatal rodent, FcRn has more recently been shown to express in a variety of cell types and tissues, including epithelial cells, endothelial cells, macrophages and dendritic cells in adult life (73). The level of FcRn expression appears to be critical for controlling IgG levels in tissues and blood (106). In autoimmune situations, FcRn expression may act as a rheostat that enables sufficient levels of pathogenic IgG to permit downstream conventional FcγR-mediated immune responses, immune complexes and inflammatory cascades. Indeed, FcRn has been shown to be associated with the development of pathogenic IgG-mediated autoimmune diseases (107, 108)). Although an understanding of the operative mechanism of FcRn function is emerging, evidence of how FcRn is regulated, especially under immune responses or inflammatory reactions, is not understood. The central roles that FcRn plays in the protection and transportation of IgG under normal or inflammatory situations have led to an increased interest in the mechanism that controls FcRn expression with regard to both the constitutive and stimuli-mediated receptor expression.

Nuclear factor kappa B (NF-κB) is a family of transcription factors that coordinate the expression of numerous genes in the innate and adaptive immune responses and development of inflammatory and autoimmune diseases. NF-κB is composed of five members of the Rel family, including NF-κB1 (p50), NF-κB2 (p52), RelA (p65), RelB, and c-Rel (Rel) (83). These proteins form homo- and heterodimers, which are usually sequestered in the cytosol of unstimulated cells via non-covalent

interactions with specific inhibition proteins known as IκBs. Upon stimulation, signals that induce NF-κB activity subsequently cause the phosphorylation of IκBs by IκB kinase complex. As a result, ubiquitin ligase complex interacts with the phosphorylated IκB, mediates poly-ubiquitination of IκB, and leads to its subsequent proteasomal degradation (109, 110) . The degradation of IκB proteins, thereby, allows NF-κB dimers to translocate to the nucleus and bind cognate NF-κB sequences of target genes.

In the present study, we investigate the involvement of NF-κB activation in the regulation of human FcRn expression and function. Our study showed that NF-κB specific inhibitor significantly down-regulated expression of human FcRn gene. Using several complementary strategies, we have further identified direct involvement of NF-κB specific binding sites located in human FcRn introns 2 and 4 that may function as modulators that are responsive to immunologic and inflammatory stimuli, such as agonists of toll like receptor and proinflammatory cytokines TNF-α.

MATERIALS AND METHODS

Cell lines, antibodies, reagents

Human intestinal epithelial cell lines HT-29 and Caco-2, and THP-1 cells (kind gifts from Dr. Richard S. Blumberg, Harvard Medical School, Boston, MA) were maintained in DMEM or RPMI 1640 medium (Invitrogen, CA) supplemented

with 10 mM HEPES, 10% fetal calf serum, L-glutamine (1:100 dilution), nonessential amino acids, and penicillin/streptomycin (1:100 dilution) in a humidified atmosphere of 5% CO_2 incubator at 37°C.

The anti-human FcRn monoclonal antibodies DVN24 and ADM31 were made by immunizing C57BL/6 mFcRn -/- mice first with $2x10^7$ spleen cells from C57BL/6 human FcRn transgenic mice in complete Freund's adjuvant (Sigma, St Louis, Mo), followed 2 weeks later with the same cells in incomplete Freund's adjuvant (Sigma). Spleen cells from seropositive responder mice were fused with SP2-0 cells using established procedures to make hybridomas. HRP-conjugated donkey anti-rabbit antibody was purchased from Pierce (Rockford, IL), and purified human IgG from Jackson ImmunoResearch Laboratories (West Grove, PA). Antibodies against NF-κB p65, p50, Rel B, p52 were obtained from Santa Cruz Biotechnology (Santa Cruz, CA), and IL-1β and TNF-α from R&D Systems (Minneapolis, MN). Affinity-purified rabbit anti-FcRn antibody has been described (9). Phosphorothionate CpG ODN (5′-TCGTCGTTTTGTCGTTTTGTCGTT-3′) and mutant GpC ODN (5′-TCTGGCTTTTCTCATTTTCTGGTT-3′) were from Operon (San Francisco, CA).

Semi-quantitative RT-PCR and quantitative real-time RT-PCR

Total RNA was isolated from cells (2×10^6/ml) in TRIzol (Invitrogen). cDNA was generated by amplification of total RNA using the FcRn-specific primers (5'CCGGAATTGGAGCCCCCCTCCAT-3', 5'-TGCTCTAGAGGAGGACTTGGCTGGAGATT-3') with a one-step RT-PCR kit (Qiagen). GAPDH was amplified by primers (5'-GAGAAGGCTGGGGCTCAT-3',

5'-TGCTGATGATCTTGAGGCTG-3'). Thirty cycles of PCR amplification were performed under optimized conditions. The total RNA samples were extracted from freshly-isolated human CD14+ CD11+ monocytes (Cambrex, Baltimore, MD). The 10^6 cells/ml monocytes were stimulated with TNF-α (50 ng/ml) or LPS (1μg/ml). Total RNA (150 ng/reaction) was reversely transcribed to yield first-strand cDNA using Superscript III (Invitrogen). Real-time RT-PCR was performed using FcRn and GAPDH primers and the SYBR Green Supermix Kit (Bio-Rad) in Chromo 4 (MJ Research, MA). FcRn expression was calculated following normalization to GAPDH levels by the comparative delta delta CT method. All reactions were performed for 40 cycles: 15 s at 94°C, 15 s at 58°C, and 20 s at 72°C. The specificity of the amplification reactions was confirmed by melt curve analysis. Software Opticon Moniter 3.1 was used for real time RT-PCR.

Gel electrophoresis, Western blot, and IgG binding assay

Gel electrophoresis and Western blots were performed as previously described (108, 111). In brief, cell lysates were prepared in PBS with 0.5% CHAPS by adding a protease inhibitor cocktail (Sigma, St. Louis). A post-nuclear supernatant was analyzed for total protein concentrations by the Bradford method with BSA as a standard (BioRad, Hercules, CA). The proteins were separated on 12% SDS-PAGE gels under reducing conditions and transferred onto nitrocellulose (Schleicher & Schuell, Keene, NH). The membranes were blocked with 5% non-fat milk and probed with affinity-purified anti-human FcRn antibody, then with HRP-conjugated Goat anti-rabbit or -mouse antibody. All washing steps were performed in 5% milk

containing 0.05% Tween-20. The final product was visualized by ECL (Pierce, Rockford, IL).

IgG binding assay was performed as previously described (20). Cells were lysed in PBS (pH 6.0 or 7.5) with 0.5% CHAPS (Sigma) and protease inhibitor cocktail. Post-nuclear supernatants containing 0.5–1 mg of soluble proteins were incubated with human IgG-Sepharose (Amersham Pharmacia Biotech). The unbound proteins were washed away with PBS (pH 6.0 or 7.5) containing 0.1% CHAPS. The adsorbed proteins were boiled with reducing electrophoresis sample buffer. The eluted proteins were subjected to 12% SDS-PAGE gel electrophoresis. Proteins were visualized by Western blot.

Chromatin immunoprecipitation (ChIP)

ChIP experiments were performed according to the manufacturer recommendations (Upstate Biotechnology Inc, Lake Placid, NY). In brief, THP-1 cells (5 x 10^6 cells) were incubated with or without TNF-α (50 ng/ml) for 20-60 min. The cells were fixed with formaldehyde. The nuclei were isolated and sonicated. Chromatin was immunoprecipitated overnight at 4°C by mild agitation with 5 μg of antibody specific for p65, p50, or with 5 μg of normal IgG as negative control. Immune complexes were collected by incubation with protein-A-agarose. The DNA samples were amplified by PCR primers in an optimized condition.

Construction of expression or reporter plasmids and mutagenesis

The pLUC-MCSFcRn vectors were constructed by cloning the pairs of complementary oligonucleotides encompassing the three tandem NF-κB binding sequences from the FcRn introns (Fig. 2.4 A, +1104, +5561, +9651). An FcRn DNA sequence (+3463) was also used as negative control. Double-stranded oligonucleotide was cloned into the pLUC-MCS plasmid (Stratagene, La Jolla, CA) digested with *Hind* III and *Xho* I. All plasmids were verified by DNA sequencing analysis.

Transient transfection and Luciferase assay

THP-1 and HT-29 cells were transiently transfected with Effectene (Qiagen, Valencia, CA). In each co-transfection, 2×10^6 cells were transfected with a DNA mix containing 0.95μg firefly luciferase reporter plasmid and 0.05 μg *Renilla* luciferase pRL-TK control plasmid. In the following day, the cells were cultured with or without TNF-α (10-50 ng/ml). The cells were harvested 24 hr after stimulation and assayed for the expression of renilla and firefly luciferase using the dual luciferase kit (Promega, Madison, WI). The values for firefly luciferase were normalized to the renilla luciferase activity and expressed as fold activation over the vector background.

Chromosome conformation capture (3C) assay

The 3C experiment was modified according to previously-described procedures (112, 113). Briefly, THP-1 cells ($1 \text{ X } 10^7$) were fixed with 2% formaldehyde. The nuclei were harvested and suspended in the *Hind* III digestion buffer containing 0.3% SDS at 37°C for 1 hr. Triton X-100 was added to a 1.8% final concentration to sequester the SDS. Samples were digested with *Hind* III overnight at

37°C. Samples were then diluted with ligase buffer. Trinton X-100 was added to a final concentration of 1%. T4 DNA ligase was then added for incubation at 16°C for 4.5 hr. The intramolecular ligation of cross-linked fragments was optimized, and ligation product was monitored by PCR. Proteinase K was added at 200 μg/ml final concentration. The samples were incubated at 65°C overnight to reverse cross-linking and the DNA was isolated**.**

The PCR amplifications were determined by primer pairs in Table II.I. Primer pairs were designed to span each of six *Hind* III sites positioned along the 15-kb region of the human FcRn gene. Primers were used for cross-linked and control templates in all pairwise combinations. In general, DNA amplifications were done in 20-μl reaction mixtures by an initial denaturing step for 5 min at 94 °C, then 35 cycles of PCR. PCR products were cloned and sequenced to confirm the presence of the FcRn DNA fragments ligated in a *Hind* III site.

RESULTS

Up-Regulation of FcRn expression by TNF-α

The NF-κB is well known to be activated by exposure of cells to proinflammatory mediators, such as TNF-α (114). To show the possibility that TNF-α regulate the gene expression of human FcRn, we treated human freshly isolated monocytes treated with TNF-α (50 ng/ml), FcRn mRNA was increased 12-fold over the mock-stimulated cell after 20 min and about 17-fold after 1 hr, as assessed by real time RT-PCR (Fig. 2.1 A). To determine whether newly-synthesized proteins,

including transcription factors, are required for TNF-dependent induction of FcRn mRNA, we treated THP-1 cells with cycloheximide (CHX, 25 μg/ml) and then subsequently with cytokines for 20 minutes and 1 hr. CHX failed to inhibit the TNF-α-dependent induction of FcRn expression from both semi-quantitative or real time RT-PCR.These data indicate that *de-novo* protein biosynthesis was not required for the induction of FcRn transcription by TNF-α. The enhanced expression of FcRn protein in THP-1 cells was shown by Western blot in TNF-α-stimulated cells (Fig.2.1B, lanes 4-5) in comparison with mock-stimulated cells (lane 3). Lysates from Hela and Hela-FcRn were used as a negative (Fig 2.1 B *lane 1*) and positive (*lane 2*) controls in Western blot. Furthermore, induction of FcRn protein could be significantly detected by staining with flow cytometry or immunofluorence microscope with FcRn-specific antibodies in THP-1 cells.

FcRn binds IgG at acidic pH 6.0 and releases IgG at neutral pH (27). We tested whether the enhanced expression of FcRn after TNF-α stimulation affects its ability to bind to its natural ligand IgG. We incubated cell lysates from cells at either pH 6.0 or pH 8.0 with human IgG-Sepharose. Cell lysates from Hela cells transfected with FcRn were used as positive control. As expected, FcRn from Hela-FcRn cells bound IgG at pH 6.0, but not pH 8.0 (Fig. 2.1 C, *lanes 5-6*). Our result showed that TNF-α stimulation enhanced cellular FcRn binding to IgG at pH 6.0 (Fig. 2.1C, *lane 3*) in comparison with mock-stimulated cells (Fig. 2.1C, *lanes 1*), suggesting the enhanced level of FcRn led to increased FcRn-IgG complexes. To evaluate other cell types in response to TNF-α induction, human intestinal HT-29 cells were treated with

TNF-α (10 ng/ml). The mRNA level of FcRn was increased about 2.5-fold over the unstimulated level (Fig. 2.1 D).

Regulation of FcRn expression in THP-1 cells by a TLR-mediated signaling pathway

Similar to TNF-α receptor engagement, activation of Toll-like receptors (TLR) by their cognate ligands can effectively result in NF-κB activation (115). We investigated the activation of TLR on cells in the induction of human FcRn expression. The TLR9 binds nonmethylated CpG-containing DNA and the TLR4 in association with CD14 recognizes ligand LPS. THP-1 cells express both TLR4 and TLR9 (115). FcRn mRNA appeared to be rapidly augmented in response to CpG in comparison to the mutant GpC treatment (Fig. 2.2 A). CpG increased the FcRn mRNA level 1.7-fold and 2-fold over the unstimulated cell after 60 and 120 min, respectively. THP-1 cells expressed nearly undetectable levels of CD14 expression on the surface. The phorbol 12-myristate 13-acetate (PMA) and 1,25-dihydroxy vitamin D3 are known to increase the expression of CD14 (116). Thus, THP-1 cells were first stimulated with 100 nM PMA and 100 nM 1,25-dihydroxy vitamin D3. THP-1 cells were then mock-treated (Fig. 2.2 B*, lane 1*) or treated by LPS (1μg/ml) (Fig. 2.2 B, enhanced 1.8 fold after 1 hr (*lane 3*) and up to 2-fold after 3 hr (*lane 5*) following LPS stimulation. Furthermore, human freshly isolated monocytes treated with LPS (1 μg/ml) increased FcRn mRNA level 6-fold over the mock-stimulated cells after 1 h and 12-fold after 2 h as measured by real-time RT-PCR (Fig. 2C). As such,

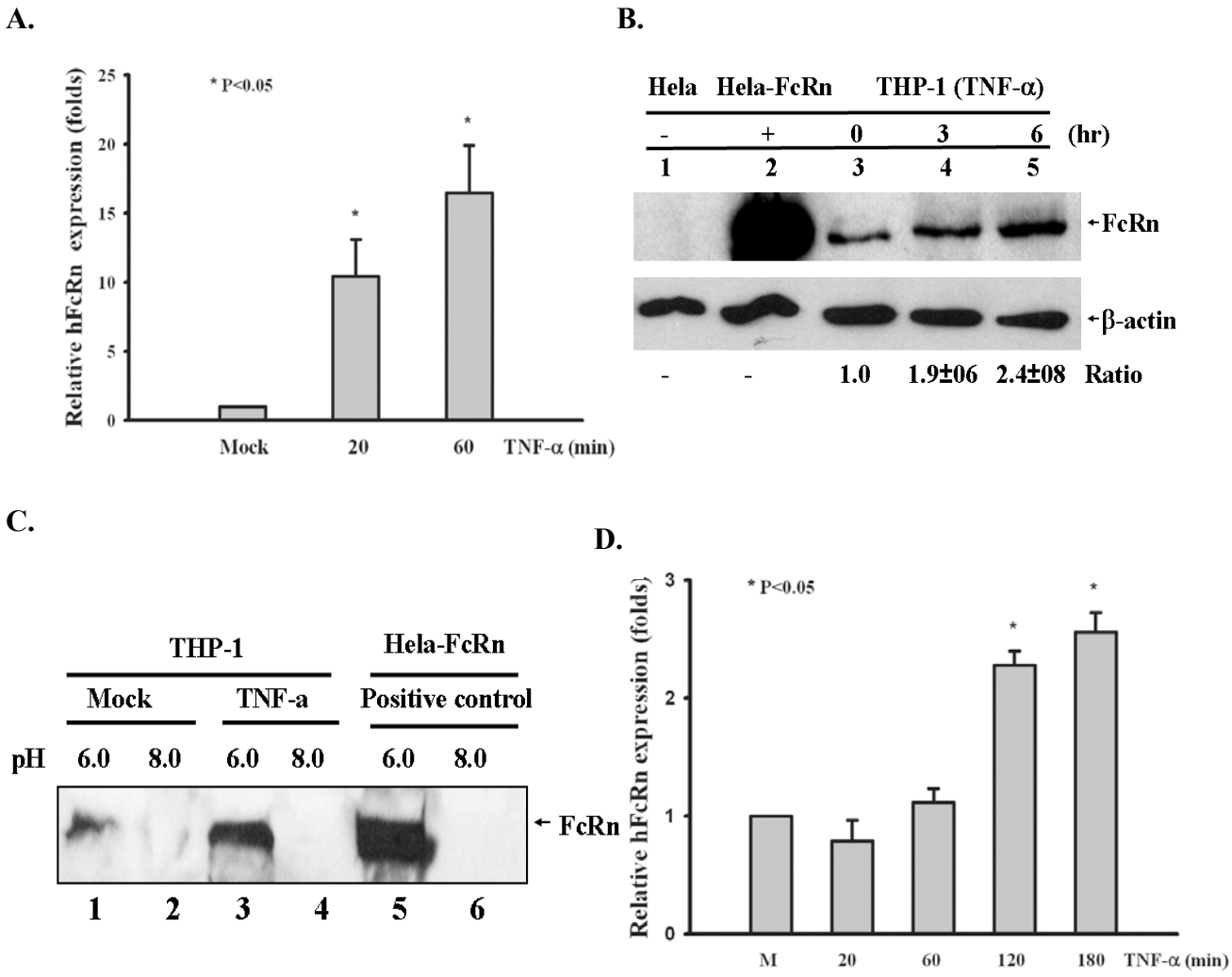

Figure 2.1 FcRn expression in response to cytokine stimulation. A. Quantitative real-time RT-PCR analysis of FcRn mRNA in freshly isolated human monocytes treated with TNF-α (50 ng/ml) for indicated time or mock treated. **B.** Western blot. The cell lysates (10 μg) from Hela (lane 1), Hela-FcRn (lane 2), TNF-stimulated THP-1 (lanes 3-5) was blotted with FcRn- (top panel) or β-actin- (bottom panel) specific antibody (bottom panel). The ratio of the mock group is assigned a value of 1.0, and the values from other groups are normalized to this value. **C.** The pH-dependent FcRn binding of IgG. **D.** Quantitative real-time RT-PCR analysis of FcRn mRNA by analyzing total RNA extracted from HT-29 cells treated with TNF-α (10 ng/ml) as indicated time. Data are mean ± SD of three independent experiments.

the studies in Fig. 2 suggest that activation of TLR signal pathways, similar to TNF- and IL-1β, can also enhance FcRn expression.

Effect of NF-κB inhibition on FcRn expression

Because downstream activation of TNF-α, IL-1β, and Toll-like receptors undergoes the similar NF-κB-mediated signaling pathway, we further study the function of NF-κB signaling in FcRn transcription. Several steps of the NF-κB activation pathway, such as IκB kinase activation, IκB phosphorylation and degradation, and NF-κB nuclear translocation, can be targeted by a variety of inhibitors (117). Caffeic acid phenethyl ester (CAPE) has an inhibitory effect on the translocation of NF-κB p65 to the nucleus and inhibition of NF-κB binding to DNA (117). THP-1 cells were pretreated with CAPE (25 μg/ml) for 2 hr, subsequently stimulated by TNF-α. Treatment with CAPE significantly reduced TNF-α-stimulated FcRn levels to that of the mock-stimulated THP-1, as assessed by semi-quantitative RT-PCR (Fig. 2.3 A). We further tested the effects of CAPE on CpG-stimulated THP-1 cells, and similar inhibitions were observed. Treatment with CAPE significantly reduced CpG-stimulated FcRn yield to the level of the mutant GpC-stimulated THP-1. In addition, CAPE did not exert the obvious toxicity to cells in our assay.

NF-κB can be activated by phosphorylation of its inhibitory subunit, IκB-α, on serine residues 32 and 36 by IκB kinases (109). Signaling through the TNF-α or IL-1β receptor can cause rapid phosphorylation of IκBα. The substitution of alanine

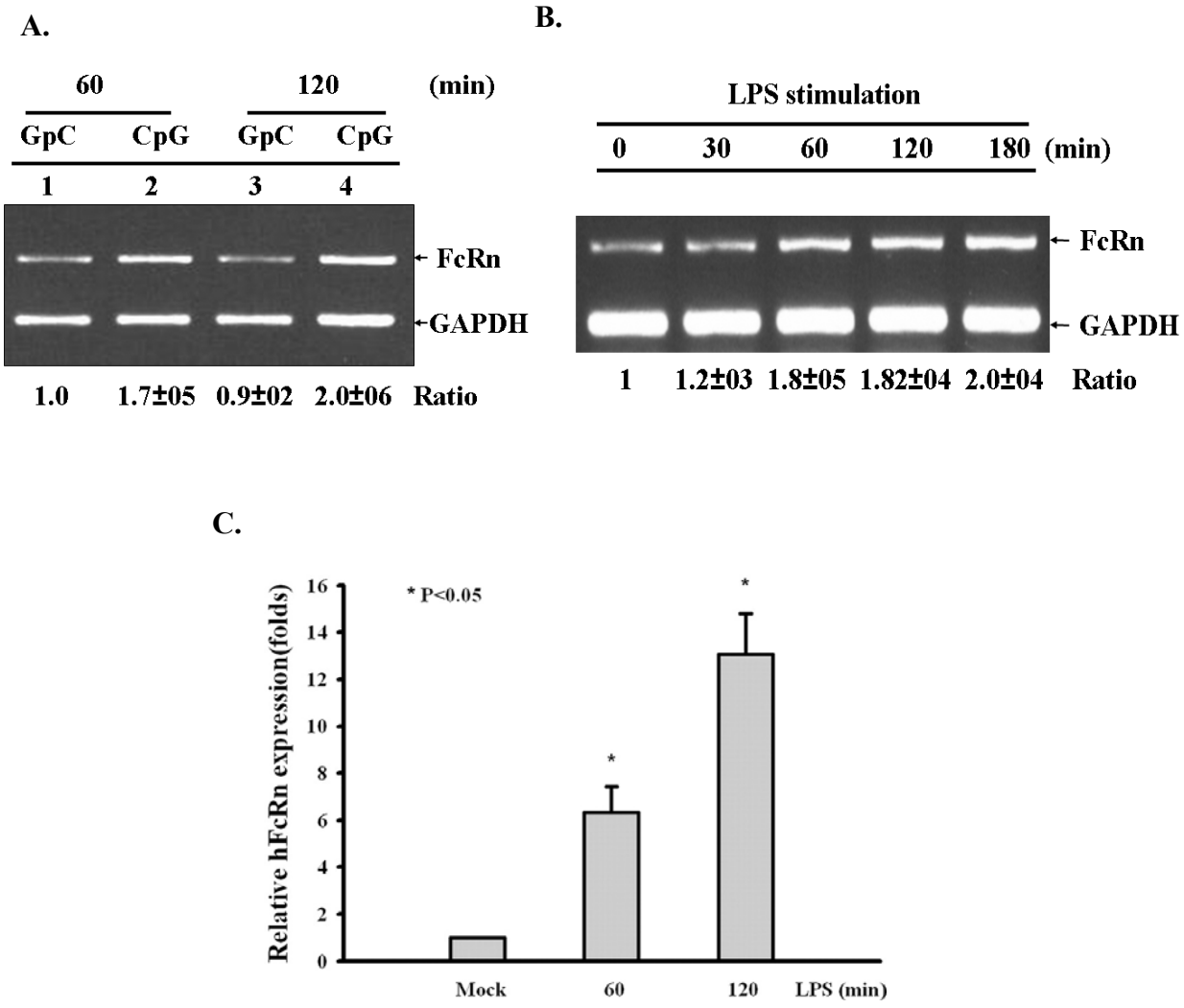

Figure 2.2 FcRn expression in response to CpG or LPS stimulation.
A.THP-1 cells were stimulated with 4 μg/ml CpG or mutant GpC for 60 and 120 min. A representative sample for RT-PCR analysis using total RNA extracted from the cells is shown for FcRn and GAPDH. **B.** THP-1 cells were pretreated with PMA and 1,25-dihydroxy vitamin D3 for 6 days, then stimulated with 1 μg/ml LPS for the indicated time. A representative sample for RT-PCR analysis using total RNA extracted from the cells is shown for FcRn and GAPDH. **C.**Quantitative real-time RT-PCR analysis of FcRn mRNA from freshly isolated human monocytes treated with LPS (1 μg/ml) for the indicated times or left untreated. Data are mean ± SD of three independent experiments. *, $p < 0.05$.

residues for serines 32 and 36 within the *N*-terminal signal response domain can abolish the signal-induced IκBα phosphorylation and ubiquitination for degradation, resulting in a blockage of NF-κB activation. Over-expression of this IκBα (S32A/S36A) decreased FcRn expression in response to TNF-α by at least 80% (Fig. 2.3 B, *lane 3*), compared to cells transfected with a control plasmid (Fig. 2.3 B, *lanes 1 and 2*). Overall, this selective NF-κB inhibition by CAPE in conjunction with the over-expression of dominant IκB mutant indicates that the blockade of NF-κB activation inhibited the FcRn transcription in response to TNF-α.

Screening for NF-κB binding sites adjacent to the FcRn gene

The canonic NF-κB DNA binding sequence is a common 10-bp consensus DNA element, which has been identified as 5'-GGGRNNYYCC-3' or 5'-HGGARNYYCC-3' (where H is A, C, or T; R is an A or G purine; and Y is a C or T pyrimidine) (83). We hypothesized that NF-κB regulates FcRn expression through a mechanism that involves direct binding to a putative regulatory NF-κB binding sequence (s) located in the FcRn gene. To test this hypothesis, we searched for putative NF-κB-binding sequence (s) along the entire human FcRn genomic sequence (Fig. 2.4 A) (GenBank accession No. AC010619). Computational inspection revealed that the promoter and introns of FcRn gene contained sequences with a similarity to the NF-κB consensus sequence (Fig 2.4 B). To verify that these putative NF-κB binding sequences do have the capability to directly bind NF-κB proteins in living cells, we employed a ChIP assay to precipitate the NF-κB-DNA complexes with antibody specific for p65 or p50 after cross-linking the DNA with bound NF-κB

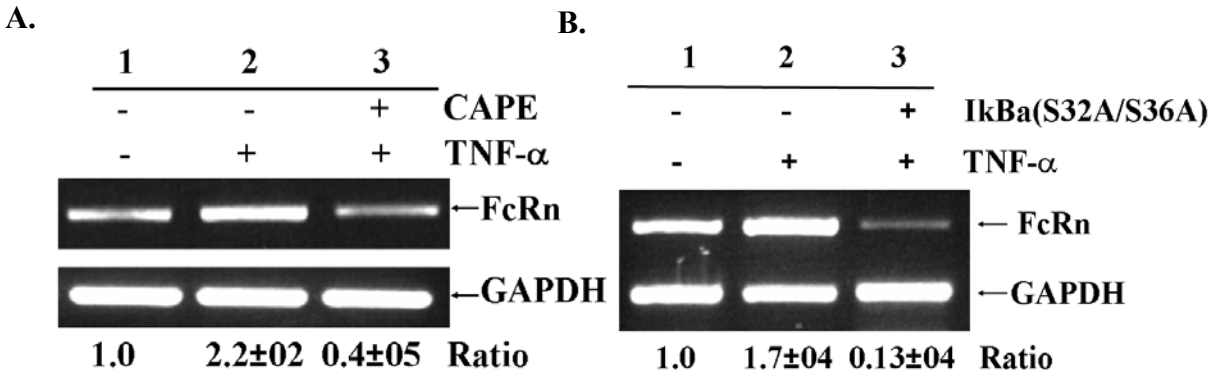

Figure 2.3 Effect of NF-κB inhibitors on the expression of FcRn. A Effects of CAPE on expression of FcRn mRNA. **B.** Effect of NF-κB blockage by IκBα on expression of FcRn. Human THP-1 cells were transfected with the dominant-negative construct pCMV-IκBα (S32A/S36A). RNA was isolated and analyzed by semi-quantitative RT-PCR.

proteins *in situ* in TNF-stimulated verus unstimulated THP-1 cells. The DNA fragments containing the putative NF-κB binding sequences in FcRn gene were measured by PCR. As shown in Fig. 2.4 C, PCR with primers flanking the putative NF-κB binding sequences (Fig 2.4 C, +1104, +5561, +9651) produced a band from DNA coprecipitated with p65 or p50. In a negative control, immunoprecipitation with normal rabbit IgG did not generate any corresponding PCR products (Fig 2.4 C, *lane 6*). The NF-κB binding sequence in the IκB gene promoter was used as a positive control. These data suggest that NF-κB p65 and p50 interacted with the three NF-κB binding sequences of FcRn gene in THP-1 cells.

NF-κB binding sequences in FcRn introns can regulate the expression of the luciferase

We constructed luciferase reporter plasmid in which three tandem copies of NF-κB binding sequences (+1104, +5561, +9651) were respectively linked to a minimal promoter containing only a TATA box (Fig. 2.5 A). The pLuc-MCS plasmids (Fig. 2.5 A) were transiently transfected into intestinal HT-29 cells with or without co-transfection of the NF-κB p50/p65 plasmid in order to validate the results obtained from THP-1 cells. The data showed that each NF-κB binding sequence significantly amplified the luciferase signal from 2-12 folds in cooperation with p65/p50 proteins (Fig. 2.5 B). A relevant DNA sequence (Fig. 2.4 B) that did not bind p50 or p65 *in vivo* from our ChIP assay was used a negative control, and it failed to enhance the luciferase activity over vector alone (Fig. 2.5 B). However, NF-κB binding sequence (+1104) from the intron 2 supported the strongest induction (12

A.

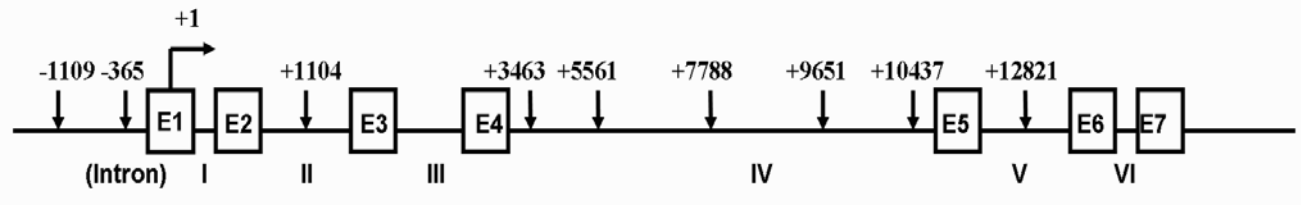

B.

Site	Sequence
-1109	GGAGGTTGAG
-365	GGGTGTCACC
+1104	GGGAACCACC
+3463	GGAGGCCCCC
+5561	GGGAGTCACC
+7788	GGGTTTCACC
+9651	GGATTCCTCC
+10437	GGGTTTCACC
+12821	TGGAATCTCC
IkBα	**GGGAATTTCC**
NF-κB consensus	**GGGRNNYYCC**

C.

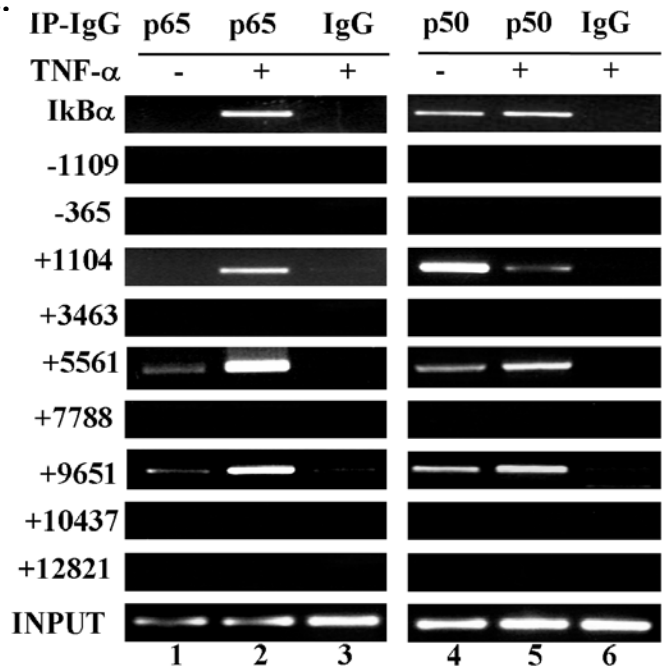

Figure 2.4 Mapping of NF-κB binding sequence (s) in human FcRn gene by chromatin immunoprecipitation (ChIP). A. Organization of the human FcRn gene. Arrowheads indicate the position of candidate NF-κB sequences. Exons (E) are drawn as *boxes* and intron numbers are shown as *Roman* numerals. **B.** The putative NF-κB binding sequences in FcRn gene are listed. Numbers represent the putative NF-κB binding sequences relevant to the transcription start site of the FcRn gene. The consensus NF-*k*B sequence is bolded. R is an A or G purine; and Y is a C or T pyrimidine. **C.** NF-κB p65 and p50 components are present at FcRn introns *in vivo* in response to TNF-α. THP-1 cells were treated with TNF-α (50 ng/ml) for 30 min. ChIP assays were performed using p65- (lanes 1-3 and p50- (lanes 4-6) specific antibodies. IgG was used as a negative control (lanes 3 and 6). Immunoprecipitated chromatin was prepared and subjected to PCR analysis using primer pairs

fold) in comparison with the other intronic NF-κB binding sequences (2.1 fold). Overall, the results support the notion that these NF-κB binding sequences are functional.

Mutual interactions between promoter and intronic NF-κB of human FcRn gene

Considering that NF-κB-dependent induction of genes involves the cooperative interactions between NF-κB and other transcription factors (118, 119), we speculated that the intronic NF-κB binding sequences might also act upon the upstream FcRn promoters through a DNA looping mechanism. The chromosome conformation capture (3C) assay has proven to be an effective method to analyze the interactions between genomic regions, such as promoter-enhancer or enhancer-enhancer interactions, in gene regulation (112). We used the 3C assay to investigate the mechanism through which the distant NF-κB binding sequences regulate the FcRn gene. Intact nuclei isolated from live THP-1 cells were cross-linked with formaldehyde to fix segments of genomic DNA that are in close physical proximity (Fig 2.6 A). The cross-linked DNA was then digested with *Hind* III (Fig. 2.6 B) and ligated at a low concentration of DNA, and the ligated DNA was then analyzed by PCR using primers in all possible combinations (1F + 2R, 1F + 3R, 1F + 4R, 1F + 5R) (Fig. 2.6 B). The appearance of a positive PCR product signals successful ligation and DNA looping.

As shown in Fig. 2.6 B, the primer H1F (Table II.I) which anneals to the promoter region sequence of the FcRn gene was used as an anchor primer to pair with

A.

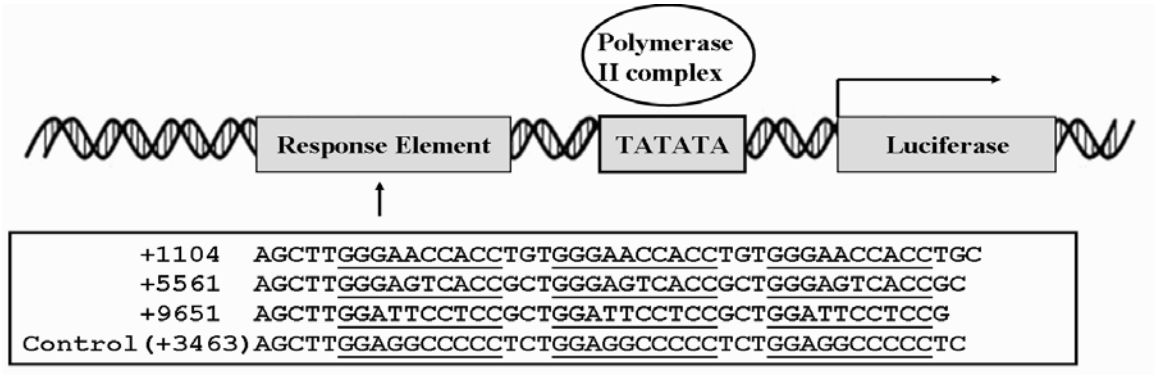

B.

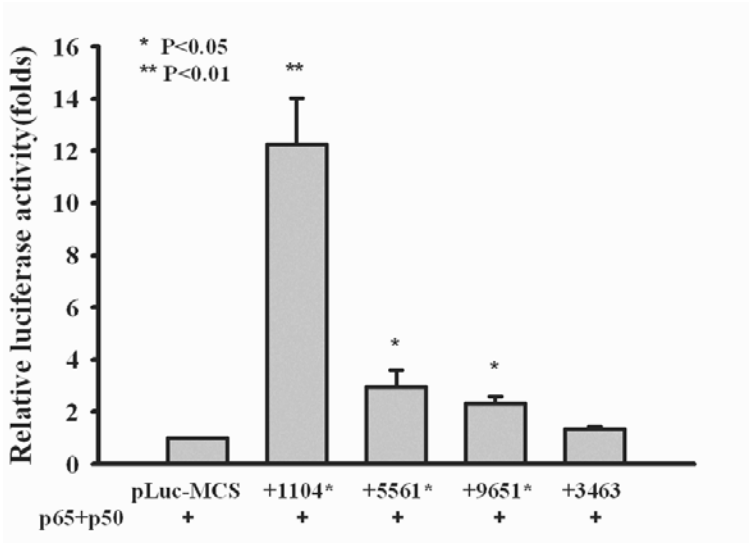

Figure 2.5 NF-κB binding sequences from FcRn introns can enhance the transcription of luciferase gene. A. A schematic representation of constructs pLuc-MCS containing NF-κB binding sequences from human FcRn introns 2 and 4. The pLuc-MCS plasmid has the minimal promoter with a TATA box. The plasmids, pLuc-MCS+1104, pLuc-MCS+5561, pLuc-MCS+9651, and pLuc-MCS+3463, were constructed as described in *Materials and Methods*. NF-κB sequences are underlined. Numbers represent the locations of NF-κB sites in the human FcRn gene. A DNA sequence corresponding +3463 was used as a negative control. **B**. HT-29 monolayers were cotransfected with the pLuc-MCS reporter plasmids as indicated, and the NF-κB transactivator plasmid p50/65 in addition to *Renilla* luciferase pRL-TK control plasmid. The pLuc-MCS backbone serves as a negative control. Luciferase activity was measured 24 hr post-transfection. The results represent the mean of three independent experiments.

A.

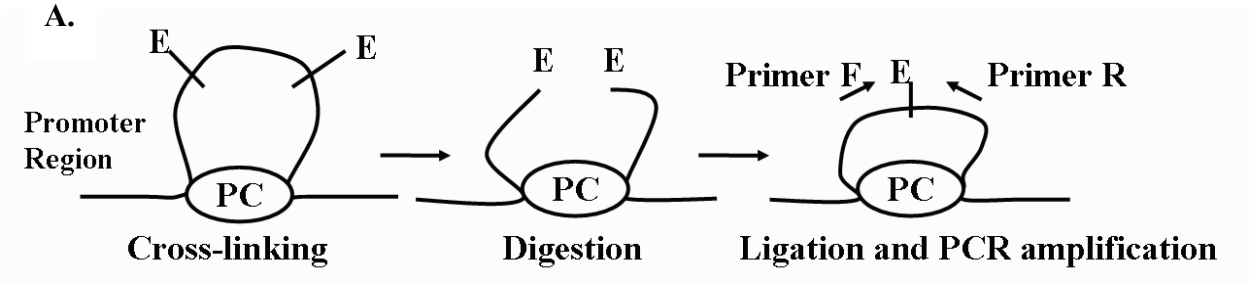
E
E
Promoter Region
PC
Cross-linking
E
E
PC
Digestion
Primer F
E
Primer R
PC
Ligation and PCR amplification

B.

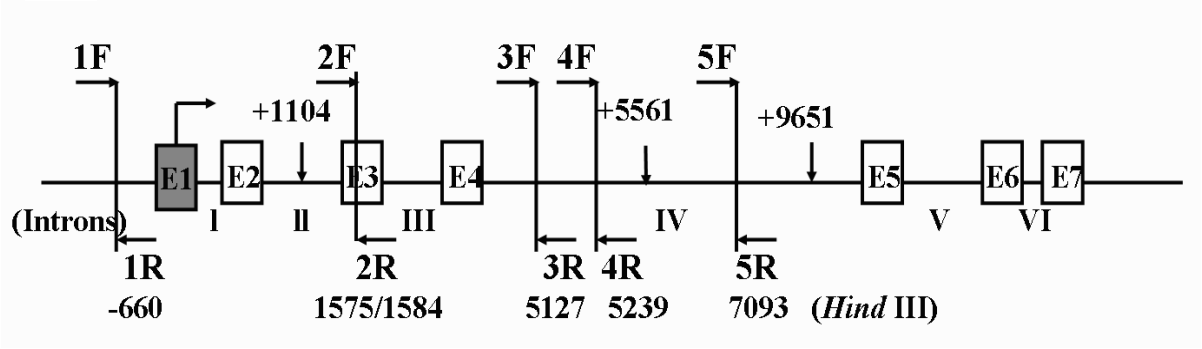
1F
2F
3F
4F
5F
+1104
+5561
+9651
E1
E2
E3
E4
E5
E6
E7
(Introns)
I
II
III
IV
V
VI
1R
2R
3R
4R
5R
-660
1575/1584
5127
5239
7093
(Hind III)

C.

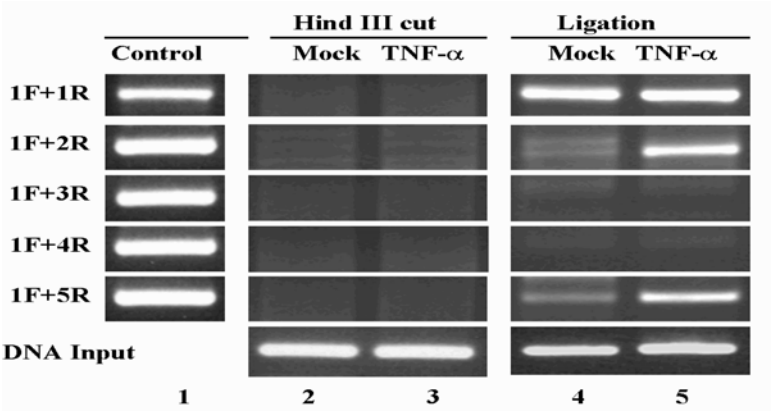
Hind III cut
Ligation
Control
Mock
TNF-α
Mock
TNF-α
1F+1R
1F+2R
1F+3R
1F+4R
1F+5R
DNA Input
1
2
3
4
5

D.

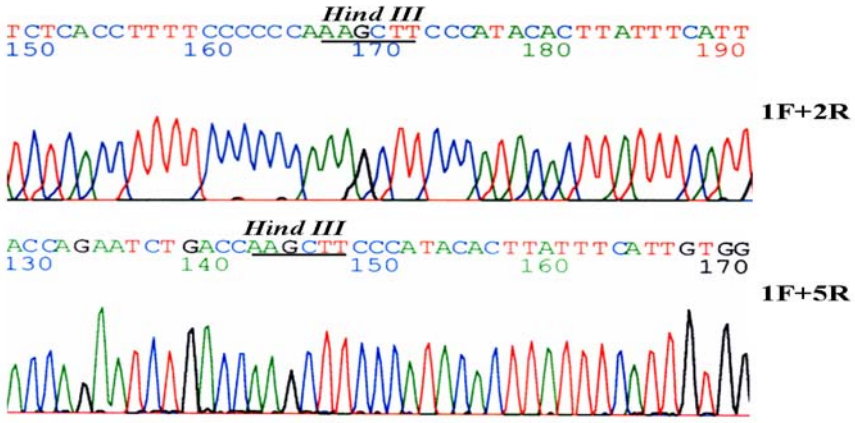
Hind III
TCTCACCTTTTCCCCCCAAAGCTTCCCATACACTTATTTCATT
150
160
170
180
190
1F+2R
Hind III
ACCAGAATCTGACCAAGCTTCCCATACACTTATTTCATTGTGG
130
140
150
160
170
1F+5R

Figure 2.6 Chromosome conformation capture (3C) analysis of interaction between promoter and downstream human FcRn gene. A. Schematic representation of the 3C technology in analyzing human FcRn gene regulation.PC, protein complexes. **B.** Locations of *Hind* III sites and PCR primers in the 15-kb FcRn gene are shown. Positions of the six *Hind* III restriction sites (perpendicular bars) from the transcriptional start site of the FcRn gene are indicated. **C. The 3C assay**. THP-1 cells were mock-treated (lanes 2 and 4) or stimulated by TNF-α (50 ng/ml) for 20 minutes (lanes 3 and 5). Chromatin material was cross-linked and digested with excessive amounts of *Hind* III, ligated, and amplified by PCR. Primer 1F was the anchor primer, and the others amplified from 5' to 3'. In lane 1, random ligation control templates were generated by amplifying the genomic DNA fragment with primers that amplify across the *Hind* III sites. Equimolar amounts of five different PCR products were mixed and digested with *Hind* III overnight at 37 °C. Ligated DNA was used to generate control PCR products by using a combination of primer pairs listed in Table II.I to monitor the efficiency of ligation. *Hind* III-digested chromosomal DNA were used as template for PCR to examine the efficiency of *Hind* III digestion (Lanes 2 and 3). Ligated templates after dilution were used to PCR amplify after *Hind* III digestion and ligation (Lanes 4 and 5). Input DNA was used as an internal control for PCR reaction. **D.** Sequence analysis of PCR products from 3C analysis. PCR products were sequenced to confirm the fidelity of *Hind* III digestion and ligation. The *Hind* III sites were underlined in ligated products.

other test primers (Table II.I) in the Hind III-digested and ligated fragments. In Fig. 8C, PCR reactions from three primer pairs (1F+1R, 1F+2R, 1F+5R) yielded positive products (Fig. 2.6 C, *lanes 4 and 5*). The PCR product from the primer pair 1F+2R and 1F+5R was sequenced to confirm the fidelity of ligations and PCR amplifications (Fig. 2.6 D). The primer 1F+1R produced positive products from the ligated DNA template in both stimulated and unstimulated cells (Fig. 2.6 C, *lanes 4 and 5*). To exclude the possibility that the observed PCR products were a result of random collisions as the result of the inherent flexibility of chromatin (112, 113) and of independent of the *Hind* III digestion, we also analyzed unligated samples after *Hind* III treatment for overnight (Fig. 2.6 C, *lanes 2+3*). We failed to detect corresponding bands amplified by PCR from the non-ligated DNA template. To monitor the differences in PCR amplification and ligation efficiencies, an additional control was used by mixing all restriction fragments from *Hind* III-digested PCR fragments (1F+1R, 2F+2R, 3F+3R, 4F+4R, 5F+5R) in equimolar amounts. After ligation at a high DNA concentration, all possible ligation products were present in the sample and amplified by PCR (Fig. 2.6 C, *lanes 1*). Taken together, we conclude that there were specific looping-interactions between NF-κB binding sequences and FcRn promoters.

DISCUSSION

Activation or inhibition of NF-κB signaling pathway can regulate human FcRn expression. Proinflammatory cytokines TNF-α as well as TLR ligands, are well known to activate NF-κB signaling pathway. Our results showed that stimulation by

Table II.I 3C primers used in this study

H1F	5’-GAACTCGGATAGAGGTGACAGTTGCAC-3’
H1R	5’-CCGAGATTGCACCACTGCACTCCAGAC-3’
H2F	5’-CGCAGCAGTACCTGAGCTACAATAGC-3’
H2R	5’-GAGGTGTTGTCAGGGCCCAGTTCACAG-3’
H3F	5’-AGGAAGCGAGCATCCCATCACTGAGAC-3’
H3R	5’-GCAGTGAGCCGAGACTGAGCCACTACAC-3’
H4F	5’-GCTTTGGTAAATCTCAGACATCACAGTG-3’
H4R	5’-GTCAGGAGTTCAAGACCAGCCTGGCC-3’
H5F	5’-GCCCTTTGCATCCTGTGATGTTGCTG-3’
H5R	5’-GTCCACAGAACAGCACAGAAGCAAGC-3’

TNF-α, CpG, and LPS augmented the FcRn expression in THP-1 and HT-29 cell lines, or freshly-isolated human monocytes in both mRNA and protein level (Figs 2.1&2.2). This result is in concordance with studies that TNF-α induces MHC class I and polymeric IgA receptor (114, 120) expression. Interestingly, we observed that the activation dynamics of FcRn expression exhibited an oscillatory behavior when cells were stimulated by TNF-α but lengthened period when stimulated by LPS treatment. This observation is in agreement with the NF-κB expression patterns induced by TNF-α and LPS (121). Furthermore, we observed that FcRn expression induced by TNF-α was strongly counteracted by the NF-κB specific inhibitor CAPE. This was corroborated by the fact that over-expression of the dominant-negative IκBα (S32A/S36A) almost completely abrogated FcRn transcriptional activation induced by TNF-α (Fig 2.3 B). This complementary experiment lessens concern of specificity or toxicity of the chemical inhibitor. Interestingly, over-expression of either NF-κB did not affect FcRn basal expression in the absence of TNF-α stimulation. It is possible that TNF-α treatment may modify the chromatin structure, allowing NF-κB, or NF-κB+IκBα, to become more accessible to their binding sites. It has been shown that TNF-α stimulation can remodel chromatin by histone acetylation (118, 122). More importantly, TNF-α also induces the binding of NF-κB to κB-like sequences in the promoter of human β2m gene (123). Therefore, activation of NF-κB by TNF-α, and possibly other NF-κB activators, could coordinately up-regulate the expression of both FcRn and β2m genes. This balanced regulation of both genes through an NF-κB-mediated signaling pathway may have functional

significance, since the noncovalent association of FcRn heavy chain and β2m is critical for FcRn to exit the endoplasmic reticulum (111).

NF-κB binding sequences were identified in the intronic regions of human FcRn gene. It was unclear whether NF-κB regulates FcRn expression directly or through an indirect mechanism by inducing other transcription factors which, in turn, could bind to the FcRn gene. Our data showed FcRn mRNA exhibited the rapid kinetics, usually within 20–30 min, in response to stimuli in our experiments. Our inhibition experiment by cyclohexmide further showed that the induction of FcRn mRNA was mediated without newly-synthesized protein factors. In fact, three NF-κB binding sequences were mapped in our ChIP experiment to the second and fourth introns of the human FcRn gene (Fig. 2.4). This is in concert with the observed TNF-α-induced expression of other genes through intronic NF-κB-dependent mechanisms (111, 119, 120, 123). Notably, a large number of studies identify NF-κB binding sequences within noncoding introns (124, 125). The data presented here extend this concept and support an inducer-specific role for intronic regulatory elements in the transcription of human FcRn. Several interesting aspects should be perceived. First, the NF-κB binding sequences identified in the introns of human FcRn were not completely conserved, based on the NF-κB consensus binding sequence (Fig. 2.4 B). However, the apparent binding sequence for NF-κB is very broad and displays a certain degree of degeneration (126). Second, multiple NF-κB isoforms can be detected in nuclear extracts of activated cells. These isoforms may compensate for each other and/or induce gene expression in a sequence-dependent manner.

NF-κB *per se* is clearly involved in the transcriptional regulation of many genes. Its activity can be modulated significantly by factors that bind to motifs adjacent to, overlapping with or distant from that of NF-κB binding sequences (110). In this regard, Sp1 elements may be strong candidates because they are often found in the enhancers or promoters of NF-κB-regulated genes (118, 127, 128). Additional studies have suggested that NF-κB dimers can act synergistically with NF-IL-6, AP-1, and Ets transcriptional factors to influence gene regulation (129, 130). Most importantly, the 5'-proximal promoter region of human and rodent FcRn shares numerous putative consensus sequences that are recognized by Sp1, AP-1, Ets, and NF-IL6 (131, 132). These protein-protein interactions may be involved in mediating the transcriptional regulation of FcRn gene in response to stimuli and can functionally cooperate to elicit maximal activation of the promoter. Further studies are needed to determine whether and how NF-κB and other transcriptional factors in the introns and promoter cooperatively regulate FcRn expression.

What might be the biological significance of regulation of FcRn by NF-κB signaling via intronic binding sequences? NF-κB is activated by exposure of cells to many physiological and non-physiological stimuli. Thus, regulation of FcRn expression *in vivo* likely involves the coordinated action of numerous modulatory factors. Tight control of FcRn may be especially important because FcRn plays a critical role in maintaining IgG homeostasis. This function results in the maintenance of much higher serum concentrations of immunoprotective IgG. However, FcRn also

extends the life span of pathogenic or autoimmune IgG, potentially promoting the progression of autoimmune diseases. Humans with lupus have been shown to have elevated TNF serum levels (133), which could exacerbate their condition based on these findings. Therefore, the level of FcRn expression may be directly coupled to the pathogenesis and treatment of autoimmune diseases. NF-κB-based regulation of FcRn expression may have certain advantages. Since the promoter of IκBα gene contains NF-κB binding sites, NF-κB is able to autoregulate the transcription of its own inhibitor. As a result, the NF-κB activation of gene expression is transient in nature. Therefore, this autoregulatory control of NF-κB and IκBα expression may, in turn, maintain FcRn expression and be the basis of IgG homeostasis. Additionally, FcRn transports normal or neutralizing IgG across polarized epithelial cells potentially 'seeding' neonatal and mucosal immunity. FcRn expression elevated from the basal level by cytokines or TLR ligands, or during mucosal infections, could facilitate a local immune response and/or promote the transport of IgG to mucosal surfaces and, thereby, allow rapid eradication of infectious agents. This result is further supported by the fact that the activated macrophages are a major source of TNF-α in intestinal inflammation. By examining the molecular mechanisms by which NF-κB regulates FcRn expression using human cell lines or freshly-isolated cells, our studies may contribute toward the general understanding of FcRn-mediated mucosal immunity and IgG-mediated autoimmune diseases. The *in vitro* results described in the present study are likely paralleled by *in vivo* events when NF-κB activation causes enhanced FcRn-mediated transport and protection of IgG. These questions are being further investigated.

In summary, the unusually-long intron of the FcRn gene contains sequences that bound either p65/p50 heterodimers or p50/p50 homodimers of the NF-κB transcription factors. The presence of NF-κB binding sequences located in distant intronic regions suggests NF-κB complexes may play an important role in the regulated expression of FcRn, possibly in cooperation with other transcriptional elements in the FcRn promoter. Because the FcRn protein may exert both beneficial and detrimental effects in a variety of infectious and autoimmune diseases, FcRn biosynthesis may be under the control of multiple complex regulatory mechanisms in response to an extracellular stimulus. Understanding the complex regulation of this critically-important receptor will require additional studies both *in vivo* and *in vitro*.

CHAPTER 3: TRANSCRIPTIONAL REPRESSION OF FcRn BY INTERFERON-γ THROUGH JAK-STAT-1 SIGNALING PATHWAY

ABSTRACT

Expression of many MHC genes is enhanced at the transcriptional or posttranscriptional level following exposure to the cytokine IFN-γ. However, we here found that IFN-γ down-regulated the constitutive expression of the neonatal Fc receptor (FcRn), a MHC class I-related molecule that functions to transport IgG across polarized epithelial cells and protect IgG and albumin from degradation. Epithelial cell exposure to IFN-γ resulted in significant decrease of human FcRn expression, as assessed by real-time RT-PCR and Western blot. The down-regulation of FcRn was not caused by apoptosis or the instability of FcRn mRNA. Chromatin immunoprecipitation and gel mobility shift assays showed that STAT-1 bound to an IFN-γ activation site (GAS) in the human FcRn promoter region. Luciferase expression from an FcRn promoter-luciferase reporter gene construct was not altered in JAK1- and STAT-1-deficient cells following exposure to IFN-γ. Furthermore, the repressive effect of IFN-γ on the FcRn promoter was selectively reversed or blocked by mutations of the core nucleotides in the GAS sequence. Functionally, IFN-γ stimulation dampened bidirectional transport of IgG across a polarized Calu-3 lung epithelial monolayer. Taken together, our results indicate that JAK-STAT-1 signaling pathway was necessary and sufficient to mediate the down-regulation of FcRn gene expression by IFN-γ.

INTRODUCTION

IFNs are multifunctional cytokines that have antiviral, antiproliferative, antitumor, and immunomodulatory effects (90, 134). In the case of IFN-γ, the cell membrane receptor for IFN-γ is composed of two subunits, IFN-γR1 and IFN-γR2. Upon binding to IFN-γ, the IFN-γ receptor rapidly associates with the Janus tyrosine kinases JAK1 and JAK2. JAK enzymes phosphorylate one another and then subsequently phosphorylate the IFN-γ receptor, which results in the formation of a docking site for the latent cytoplasmic transcription factor named STAT-1, a member of the STAT (signal transducer and activator of transcription) protein family (92). Upon phosphorylation, STAT-1 homodimerizes, translocates to the nucleus, and regulates gene transcription by binding to IFN-γ-activated sequences (GAS) in the IFN-γ-inducible genes. Homodimerization of STAT-1 is mediated by the binding of the phosphorylated tyrosine 701 of one STAT-1 monomer to the Src homology 2 domain of another. However, maximal transcriptional activity by active STAT-1 homodimers also requires STAT-1 phosphorylation at serine 727 (135, 136). It has been found that STAT-1 phosphorylation plays a critical role in IFN-mediated innate immunity to microbial infection (137). STAT-1 signaling can also be negatively regulated by the protein inhibitor of activated STAT-1 (PIAS1) and suppressor of cytokine signaling (SOCS) (96). IFN-γ can also regulate expression of its inducible genes in a STAT-1-independent manner (138, 139), suggesting that multiple signaling pathways in parallel play important roles in the biological response to IFN-γ.

The pivotal roles in the protection and transport of IgG have led to an increasing interest in the mechanism that regulates FcRn expression regarding both constitutive and stimulated expression. MHC class I and related molecules include HLA-A, HLA-B, HLA-C, HLA-F, HLA-G, HLA-H, MR1, MIC A/B, CD1, and FcRn. Expression of several MHC class I genes significantly increases at the transcriptional or posttranscriptional level following exposure to IFN-γ in a variety of tissues and cells (140-145). Although the transactivating roles of IFN-γ in MHC class I and its related molecules are well established, at present little is known about whether and how IFN-γ regulates FcRn gene expression. In an effort to identify the role of IFN signaling in regulation of the FcRn receptor, we unexpectedly found, for the first time, that IFN-γ down-regulated human FcRn expression and function. Furthermore, our study showed that activation of STAT-1 is required for IFN-γ-induced down-regulation of FcRn expression. STAT-1-repressed FcRn transcription may act through sequestering the transcriptional coactivator CREB binding protein (CBP)/p300, thus reducing the level of CBP/p300 at the human FcRn promoter.

MATERIALS AND METHODS

Cell lines, Abs, reagents

Human lung-derived Calu-3 adenocarcinoma cells were obtained from American Type Culture Collection (HTB-55) and maintained in a 1:1 mixture of DMEM and Ham's F-12 medium (Invitrogen). Human 2fTGH cells, a cell line derived from the human fibrosarcoma HT1080 cell line, and the 2fTGH-derived cell lines U3A (STAT-1 deficient) and U4A (JAK1 deficient) were gifts from Dr. G. Stark (Cleveland Clinic Foundation, Cleveland, OH). HeLa-

E2A4 (JAK1 deficient) was from Dr. R. A. Flavell (Yale University School of Medicine, New Haven, CT). The human intestinal epithelial cell lines HT-29 and Caco-2 and the macrophage-like THP-1 cells were obtained from Dr. R. S. Blumberg (Harvard Medical School, Boston, MA). The human intestinal epithelial cell line T84 was from Dr. W. Song (University of Maryland, College Park, MD). All epithelial and fibrosarcoma cells were maintained in DMEM complete medium (Invitrogen). All complete medium was supplemented with 10 mM HEPES, 10% FCS, 2 mM L-glutamine, nonessential amino acids, and penicillin (0.1 μg/ml)/streptomycin (0.292 μg/ml) in a humidified atmosphere of 5% CO2 at 37°C.

HRP-conjugated donkey anti-rabbit or rabbit anti-mouse Ab was purchased from Pierce, and purified human IgG was from Jackson ImmunoResearch Laboratories. Anti-STAT-1α, anti-phospho-STAT-1 (tyrosine 701), anti-phospho-STAT-1 (serine 727), and anti-p300 Abs were from Cell Signaling Technology. Human recombinant IFN-γ was from R&D Systems. All DNA-modifying enzymes were purchased from New England Biolab.

Semiquantitative RT-PCR and quantitative real-time RT-PCR

Semiquantitative RT-PCR and real-time RT-PCR were performed as previously described (146). In brief, total RNA was isolated from stimulated and mock-stimulated cells (2×10^6/ml) in TRIzol reagents (Invitrogen) according to the manufacturer's instructions. Semiquantitative RT-PCR was performed using a one-step RT-PCR kit (Qiagen). Primers for amplification of FcRn and GAPDH have been previously described (146). Thirty cycles of PCR amplification were performed in a 20-μl volume. Each cycle consisted of denaturation

at 94°C for 30 s, annealing at 58°C for 30 s, and extension at 72°C for 30 s. An additional 10 min was applied for the final extension. PCR products were resolved on 1.5% agarose gels and visualized by staining with ethidium bromide. Integrated density values for the FcRn binds were normalized to the GAPDH values to yield a semiquantitative assessment.

The freshly isolated human PBMCs (106 cells/ml) were stimulated with IFN-γ (25 ng/ml) for 24 h. The total RNA samples were extracted. The RNA (400 ng/reaction) was reverse transcribed to yield first-strand cDNA using SuperScript III (Invitrogen). Real-time RT-PCR was performed using FcRn and GAPDH primers (146) and the SYBR Green Supermix kit (Bio-Rad Laboratories) in a Chromo 4 thermocycler (MJ Research). FcRn expression was calculated following normalization to GAPDH levels by the comparative ΔΔ threshold cycle method. All reactions were performed for 40 cycles: 15 s at 94 °C, 15 s at 58 °C, and 20 s at 72 °C. The specificity of the amplification reactions was confirmed by melt curve analysis. The Opticon Monitor 3.1 software package (Bio-Rad Laboratories) was used for real time RT-PCR.

Construction of expression or reporter plasmids and mutagenesis

Construction of the human FcRn promoter-luciferase reporter plasmid phFcRnLuc containing sequences from –1801 to +863 of the human FcRn promoter has been previously described (146). The mutant derivative plasmids pM1 and pM2 were constructed by overlapping PCR mutagenesis to disable the putative GAS sequence (see Fig. 3.3 B), using phFcRnLuc as a template. The primer pairs for pM1 (5'-GGAAGCCAACTACTCATATGAATCTCTTTCTGTG-3' and 5'-

AGGATTAGTGGACGTTCAGCTGGTTCAGAG-3') or pM2 (5'-TTATATGATTCAATGGCTTAGACATGTGCAGAATAG-3' and 5'-TATGAAGTCTTTCCTTCCTTCCTTCCTTGCCTC) were used (the mutations are underlined). The expression plasmid encoding wild-type STAT-1 (pSTAT-1) and the phosphorylation site mutant plasmid pSTAT-1Y701F were kindly provided by Dr. K. Nakajima (Osaka City University Medical School, Osaka, Japan) and Dr. D. Geller (University of Pittsburgh, Pittsburgh, PA). The FLAG-tagged STAT-1 and PIAS1 expression plasmids were kind gifts from Dr. K. Shuai (University of California, Los Angeles, CA). The FLAG-tagged pSTAT-1Y701F, pSTAT-1S727A, or pSTAT-1Y701F/S727A was constructed by the overlapping PCR mutagenesis method. The primer pair (5'-AGGAACTGGATTTATCAAGACTGAGTTGAT-3' and 5'-TTAGGGCCATCAAGTTCCATTGGCTCTGGT-3') was used to substitute tyrosine 701 with a phenylalanine residue (underlined). The primer pair (5'-GACAACCTGCTCCCCATGGCTCCTGAGGAG-3' and 5'-TGTGGTCTGAAGTCTA GAAGGGTGAACTTC-3') was used to change serine 727 to alanine (underlined). The murine JAK1 expression construct was obtained from Dr. J. Ihle (St Jude Children's Research Hospital, Memphis, TN). The integrity of the DNA fragments in the plasmids was confirmed by DNA sequence analysis.

Immunoprecipitation, gel electrophoresis, and Western blotting

Immunoprecipitation was done as described previously (111). Protein was precipitated with anti-FLAG Ab. The immunoreactive products were eluted from the protein G complex with gel loading buffer at 95°C. Gel electrophoresis and Western blot were performed as

previously described (108) (111). Protein concentrations were determined by the Bradford method. The cell lysates were resolved by electrophoresis on a 12% SDS-polyacrylamide gel under reducing conditions. Proteins were electrotransferred onto a nitrocellulose membrane (Schleicher & Schuell). The membranes were blocked with 5% nonfat milk, probed separately with affinity-purified rabbit anti-FcRn peptide (CLEWKEPPSMRLKARP) Ab for 1 h, followed by incubation with HRP-conjugated donkey anti-rabbit Ab. All blocking, incubation, and washing were performed in PBST solution (PBS and 0.05% Tween 20). Proteins were visualized by an ECL method (Pierce).

Determination of mature FcRn mRNA stability

Stability of the mature FcRn mRNA transcript was determined by using an actinomycin D inhibition assay as described previously(147, 148). Briefly, after 24 h of HT-29 cells being treated with or without IFN-γ, 5 μg/ml actinomycin D (Sigma-Aldrich) was subsequently added to each culture to stop the further production of mature FcRn transcript. Following the addition of actinomycin D, cell viability was analyzed by trypan blue exclusion and did not significantly change over the course of the experiment. HT-29 cells were collected from the cultures at 0, 1, 2, 4, 8, and 10 h following the addition of actinomycin D, and total RNA was isolated. The level of FcRn mRNA was quantified for each time point by semiquantitative RT-PCR or quantitative real-time PCR as described above.

Nuclear run-on assay

The rate of mature FcRn transcription was determined by nuclear run-on as described in detail previously (148). Briefly, 5×10^7 THP-1 cells were collected 24 h following

stimulation in the presence or absence of IFN-γ and washed twice with PBS before resuspension in 5 ml of cell lysis buffer containing 10 mM Tris-HCl (pH 7.4), 10 mM NaCl, 3 mM $MgCl_2$, and 0.5% Nonidet P-40 for 5 min at 4°C. Nuclei were collected by centrifugation at 300 x *g* for 10 min at 4°C, resuspended in 500 µl of nuclear freezing buffer containing 50 mM Tris-HCl (pH 8.3), 40% glycerol, 5 mM $MgCl_2$, and 0.1 mM EDTA, and stored at –80°C until use for nuclear run-on. Nuclear run-on and RNA isolation were preformed in the presence of biotin-16-UTP (Roche). To control for the possibility of nonbiotin-labeled RNA contamination, replicate sets of nuclei were used in the nuclear run-on that did not contain biotin-16-UTP. Dynabeads M-280 (Invitrogen) were used to capture the biotin-labeled RNA molecules from the purified nuclear RNA, and beads were washed twice with 2x SSC plus 15% formamide and once with 2x SSC and resuspended in 30 µl of RNase-free H_2O before the preparation of random hexamer-primed cDNA as described in the paragraph titled *Semiquantitative RT-PCR and quantitative real-time RT-PCR* above except for the primer pair used for GAPDH (5'-GCCACTAGGCGCTCACTGTTCTCTC-3' and 5'-CTCCTTGCGGGGAACAGCTACCCTGC-3') and FcRn (5'-GAGCCTGGGCGCAGGTGAGGGCCGC-3' and 5'-GCGACAGGTGGTTCCCAGCCTCAGGC-3'). Primers located in the intronic region are underlined. All samples that did not contain biotin-16-UTP were found to be negative for the presence of GAPDH and mature FcRn transcripts.

Immunofluorescence and detection of apoptosis by TUNEL

HT-29 cells were cultivated on coverslips for 24 h. The coverslips were rinsed in PBS and cells were cold-fixed in 4% paraformaldehyde in PBS for 30 min at 4°C. Subsequent

procedures were done at room temperature. After two washings with PBS, the coverslips were permeabilized (3% BSA and 0.2% Triton in PBS) for 30 min. Cells were incubated with affinity-purified rabbit anti-STAT-1 in PBST (0.05% Tween 20 and PBS) with 3% BSA for 1 h. Cells were then incubated with Alexa 458 Fluor-conjugated AffiniPure goat anti-rabbit IgG (Jackson ImmunoResearch Laboratories) in PBST with 3% BSA. Cell nuclei were counterstained with 5 μg/ml 4',6'-diamidino-2-phenylindole (DAPI; Molecular Probes) in PBS. After each step the cells were washed three times with 0.1% Tween 20 in PBS. To mount coverslips, the ProLong antifade kit was used (Molecular Probes). Images were captured using a x100 oil-immersion objective on a Zeiss inverted microscope linked to a DeltaVision deconvolution imaging system.

In situ detection of apoptotic cells was performed with the TUNEL kit from Roche. After IFN-γ (50 ng/ml) treatment, HT-29 cells undergoing cell death were identified. Briefly, IFN-γ- or mock-treated cells were fixed with a freshly prepared fixation solution (4% paraformaldehyde in PBS (pH 7.4)) for 1 h at room temperature, and then incubated in permeabilization solution (0.1% Triton X-100 in 0.1% sodium citrate) for 2 min on ice, and the TUNEL procedure was conducted according to the manufacturer's instructions. For the correlation of TUNEL with nuclear morphology, cells were counterstained with DAPI. To confirm the specificity of TUNEL, cells were treated with 3000 U/ml DNase I at room temperature for 10 min to induce DNA strand breaks before labeling procedures. In negative controls, terminal TdT was omitted from the labeling reaction mixture. Samples were viewed by fluorescence microscopy with excitation at 320–580 nm.

Transient transfection and luciferase assay

Transient transfection and luciferase assay were done as previously described (146). Briefly, cells were transiently transfected with Effectene according to instructions from the manufacturer (Qiagen). In each cotransfection, 2×10^6 cells were transfected with a DNA mix containing 0.95 μg of firefly luciferase reporter plasmid and 0.05 μg of *Renilla* luciferase pRL-TK control plasmid. The following day, the cells were cultured with or without IFN-γ. The cells were harvested 24 h after treatment and assayed for the expression of *Renilla* and firefly luciferase using the dual luciferase kit (Promega) according to the recommended protocol in a Victor 3 luminometer (PerkinElmer). The values for firefly luciferase were normalized to the *Renilla* luciferase activity and expressed as fold activation over the vector background.

Chromatin immunoprecipitation (ChIP)

ChIP experiments were performed according to the manufacturer's recommendations (Upstate Biotechnology) and as previously described(146). In brief, HT-29 cells (5×10^6 cells) were incubated with or without IFN-γ (25 ng/ml) for 1–12 h. The cells were fixed with 1% formaldehyde. The nuclei were isolated and sonicated 20 times on ice for 10–20 s with 90-s breaks (Sonifier 350; Branson) between each sonication interval to shear the DNA to 200-1000 bp. A small aliquot (20 μl) was saved as "input DNA" for PCR analysis by reversing histone-DNA crosslinks by heating at 65°C for 4 h. Chromatin was immunoprecipitated from 200-μl aliquots at 4°C by mild agitation overnight with 5 μg of Ab specific for STAT-1, phospho-STAT-1 (tyrosine 701), and phospho-STAT-1 (serine 727) or with 5 μg of normal rabbit IgG as negative control. Immune complexes were collected by

incubation with protein A-agarose. To analyze the target region, the immunoprecipitated chromatin DNA samples were amplified by PCR with primer pairs for FcRn (5'-GGAAAGACTTCATATTATATGATTC-3' and 5'-GCAACTGTCACCTCTATCCGAGTTC) or ICAM-1 (5'-GATTGCTTTAGCTTGGAAATTC-3' and 5'-GGAGCCATAGCGAGGCTGAG-3'). DNA samples or input DNA fractions were analyzed by 35 cycles of PCR (94°C for 30 s, 58°C for 30 s, and 72°C for 30 s) in 20-μl reaction mixtures. PCR products were subjected to electrophoresis by using 2% agarose gels in TAE (Tris-acetate-EDTA) buffer and visualized by ethidium bromide.

Preparation of nuclear extracts and EMSA

Nuclear extracts were prepared using a nuclear and cytoplasmic extraction kit according to the manufacturer's instructions (Pierce). IFN-γ (25 ng/ml)-treated HT-29 cells (1 x 10^7) were used. The double-stranded oligonucleotides (5'-TGATTCAATTTCTTTGAAATGTGCAG-3') containing a putative GAS sequence (underlined) from the FcRn promoter was used. The double-stranded oligonucleotides (5'-CCCTTTCTGGGAAGTCCGGGT-3') containing the GAS sequence (underlined) from the c-*myc* promoter were used as a positive control. The DNA was labeled with a biotin 3'-end DNA labeling kit (Pierce). In brief, 4 μg of nuclear extracts were incubated in binding buffer (10 mM Tris (pH 7.9), 50 mM NaCl, 5 mM $MgCl_2$, 50 mM KCl, and 50% glycerol) with 50 ng/ml poly(deoxyinosinic-deoxycytidylic acid) (poly(dI-dC)) and a 20-fmol final concentration of biotin-labeled, double-stranded oligonucleotide for 20 min at room temperature. For competition assays, samples were preincubated with a 100-fold excess of a

nonlabeled oligonucleotide. For the supershift assay, 0.8 µg of each Ab specifically directed against STAT-1 was preincubated with the nuclear extracts in the absence of poly(dI-dC) for 30 min at 22°C. Subsequently, poly(dI-dC) was added and incubated for 5 min, followed by the addition of a probe for an additional 20 min. The samples were loaded on a 5% native polyacrylamide gel in 0.5x Tris-borate-EDTA buffer at 80 volts for 2 h. The gels were blotted onto a nylon membrane (Bio-Rad Laboratories), blocked, incubated with HRP-avidin, and developed using the LightShift chemiluminescent EMSA kit (Pierce) according to the manufacturer's instruction. Visualization of the chemiluminescent signal on the membrane was achieved by exposing to X-ray film (Kodak).

IgG transcytosis

IgG transport was performed with a modification of previously described methods (149, 150). Calu-3 cells were grown onto Transwell filter inserts (Corning Costar) to form a monolayer exhibiting transepithelial electrical resistances (700 ohms/cm^2). Transepithelial electrical resistance was measured using a tissue-resistance measurement equipped with planar electrodes (World Precision Instruments). Monolayers were equilibrated in HBSS and mock-treated or stimulated with IFN-γ (25 ng/ml) for 24 h. Thereafter, human IgG at a final concentration of 0.5 mg/ml was added to the apical or basolateral medium. Monolayers were incubated for 1 h with IgG or chicken IgY at 37°C. An aliquot of the buffer was collected into which apically and basolaterally directed IgG or IgY transport was conducted. Transported proteins were analyzed by reducing SDS-PAGE and Western blot-ECL. NIH Image software (National Institutes of Health, Bethesda, MD) was used to determine the relative band intensities of a blot.

Statistical analysis

Data from three independent experiments were initially analyzed by ANOVA to detect significant changes between the stimulated and mock-stimulated cells. Additional statistical evaluation of the differences in expression of FcRn genes was measured by Student's *t* test with a Bonferroni correction. All results are expressed as mean values. A value of $p < 0.05$ was considered significant.

RESULTS

Exposure of cells with IFN-γ *down-regulates the expression of FcRn*

IFN-γ has been shown to enhance the expression of the MHC genes at the transcriptional or posttranscriptional level (140, 141). To determine whether IFN-γ regulates human FcRn gene expression, we treated human intestinal epithelial cell lines that express FcRn (61, 149) with IFN-γ (50 ng/ml). Our data showed that FcRn gene expression in T84 and HT-29 cells was down-regulated in response to IFN-γ treatment as shown by semiquantitative RT-PCR (Fig. 3.1A). To rule out whether this decrease in FcRn was the result of general transcriptional decreases in the cell, we also measured the transcript for the MHC class II-associated invariant (Ii) chain, a molecule highly up-regulated by IFN-γ. Transcript levels for Ii (Fig. 3.1A, *bottom panel*) were significantly increased by IFN-γ, suggesting that the transcriptional down-regulation of FcRn is specific. The decreased expression of FcRn protein in HT-29 cells was shown by Western blotting in IFN-γ-stimulated cells (Fig. 3.1B, *top panel*, *lanes 2–4*) in comparison with mock-stimulated cells (*lane 1*). Lysates from HeLa-FcRn and HeLa were used as a positive (Fig. 3.1B, *lane 3*) and negative (*lane 4*) controls. To establish whether this transcriptional repression requires new

protein synthesis, we performed additional experiments where the levels of FcRn mRNA were determined following treatment with cycloheximide (CHX), an established inhibitor of protein synthesis. In these experiments we used a concentration of CHX (25 μg/ml) at which >95% of protein synthesis is blocked within 1 h (151). The results showed that the IFN-γ-induced transcriptional repression was totally independent of new protein synthesis. Specifically, by RT-PCR analysis we observed ~60% reduction in FcRn mRNA synthesis following 24 h of exposure to IFN-γ in the presence of CHX, an overall inhibition comparable with that obtained in the absence of CHX (Fig. 3.1C). these data indicated that preexisting proteins were modified in a ligand-dependent manner to repress the FcRn gene.

Effect of IFN-γ on FcRn mRNA stability, rate of mRNA transcription, and apoptosis

The primary mechanisms that regulate the amount of mRNA produced in mammalian cells are transcript stability and/or the rate of mRNA transcription. As such, we ascertained whether either of these mechanisms was involved in regulating the decrease in mature FcRn mRNA in the absence or presence of IFN-γ. Using an actinomycin D inhibition assay as shown by semiquantitative RT-PCR (Fig. 3.2 A, *left panel*) and quantitative real-time PCR (Fig. 3.2 A, *right panel*), the half-lives of FcRn mRNA appeared to be similar between mock- and IFN-γ-treated cells for the indicated time period. This suggests that a stability mechanism was not likely responsible for the decrease in FcRn mRNA. In contrast, nuclear run-on analysis indicated that the rate of FcRn mRNA transcription was decreased ~80% in THP-1 cells exposed to IFN-γ (Fig. 3.2 B). Thus, this finding suggests that the decrease in

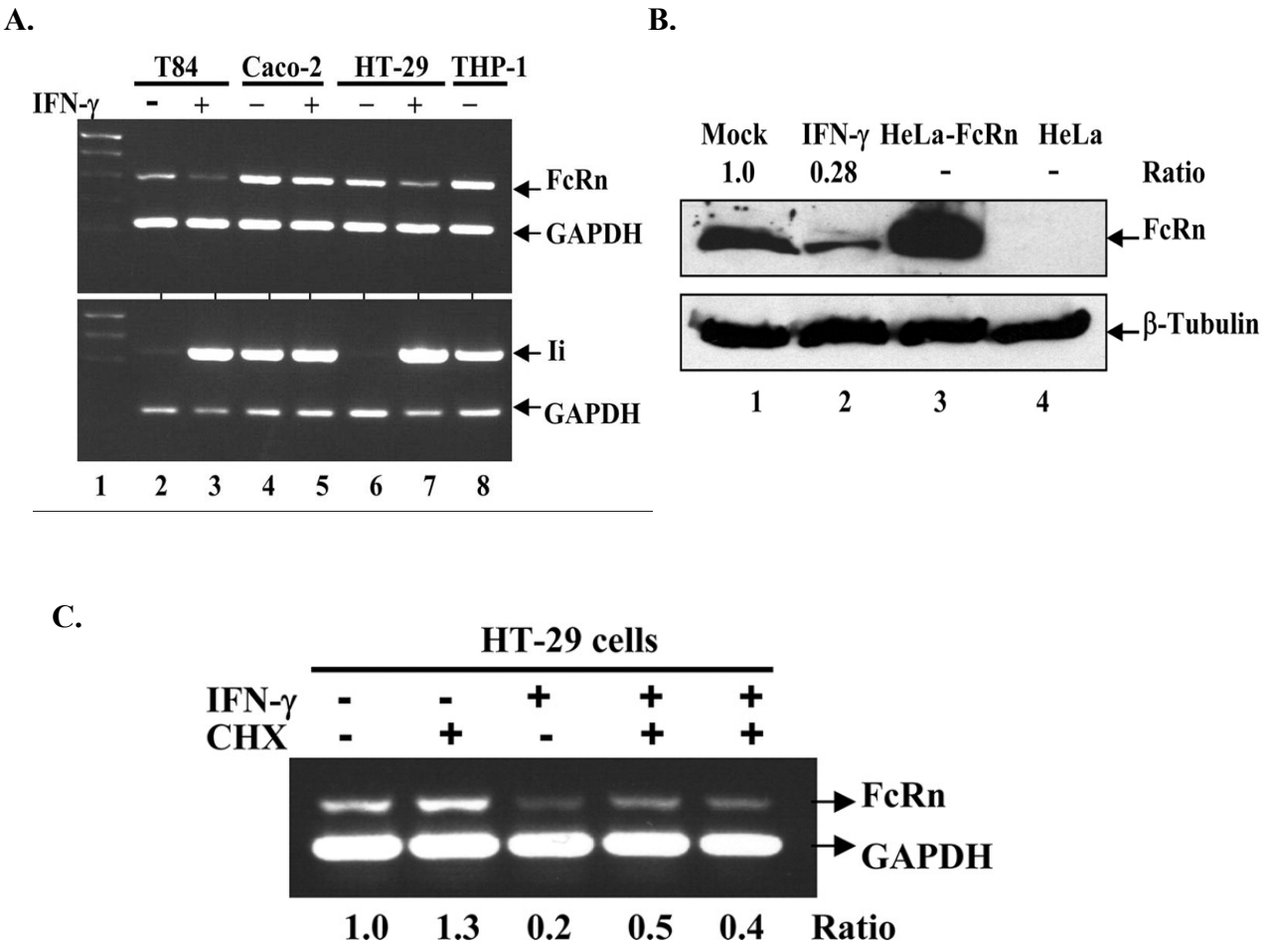

Figure 3.1 Down-regulation of human FcRn expression in epithelial cells by IFN-γ. *, $p < 0.05$. **A**. Down-regulation of human FcRn and up-regulation of Ii occur concomitantly in response to IFN-γ treatment. Human intestinal cell lines were treated with (+) IFN-γ (*lanes 3*, *5*, and *7*) or without (–) IFN-γ (*lanes 2, 4*, and *6*) (50 ng/ml) for 48 h. GAPDH amplification was used as an internal control. **B**.Western blot analysis of FcRn expression. The cell lysates (20 μg) from mock-treated (*lane 1*) and IFN-γ-stimulated HT-29 (*lane 2*) Cell lysates from HeLa-FcRn (*lane 3*) and HeLa (*lane 4*) were used as positive or negative controls, respectively. The ratio of the mock group is assigned a value of 1.0, and the values from other groups are normalized to this value. The ratios of FcRn and β-tubulin are shown as indicated. **C.** Effects of CHX on IFN-γ -mediated repression of FcRn expression. Human intestinal HT-29 cells were incubated with (+) or without (–) the protein synthesis inhibitor CHX (25 μg/ml) for 2 h as indicated. HT-29 cells were subsequently stimulated with (+) or without (–) IFN-γ (25 ng/ml) for 24 h. At the end of the incubation period, total RNA was isolated and analyzed by RT-PCR for FcRn and GAPDH.

FcRn mRNA induced by IFN-γ-stimulation on a HT-29 or THP-1 cell is due to a decrease in the rate of primary FcRn RNA transcription.

In addition, activation of the STAT-1 signaling pathway can cause expression of caspase 1 and subsequent apoptosis (152). To further assess the possible role of IFN-γ in inducing apoptosis in our experiment, HT-29 cells were pretreated with or without IFN-γ (50 ng/ml) for the indicated time periods (Fig. 3.2 C). A TUNEL assay demonstrated that IFN-γ induced detectable apoptosis in a small fraction of HT-29 cells only following 120 h of incubation (Fig. 3.2 C). Mock-treated HT-29 cells were stained TUNEL negative at 120 h; cells stained after treatment with DNase I were used as a positive control (Fig. 3.2 C, panel labeled "PC"), and cells without IFN-γ treatment or those stained without TdT were used as a negative control (Fig. 3.2 C, panel labeled "NC"). Collectively, neither instability of FcRn mRNA nor significant apoptosis was induced by IFN-γ when used for this period of time (24–48 h) and at these concentrations (50 ng/ml) in our experiments.

Identification of STAT-1 binding site in the FcRn promoter

IFN-stimulated response elements (ISRE) and IFN-γ activation site (GAS) motifs are present in a variety of IFN-inducible genes (90, 134). ISRE (consensus sequence AGTTTCNNTTTCNY) and GAS (consensus sequence TTNCNNNAA, TTCNNNG/TAA) binding motifs have been mapped (90, 134, 153). We searched for putative ISRE and GAS sequences along the entire human FcRn promoter (GenBank accession no. AC010619). Computational inspection revealed that the FcRn gene promoter contained no sequence similarity to typical ISRE consensus sequences;

A.

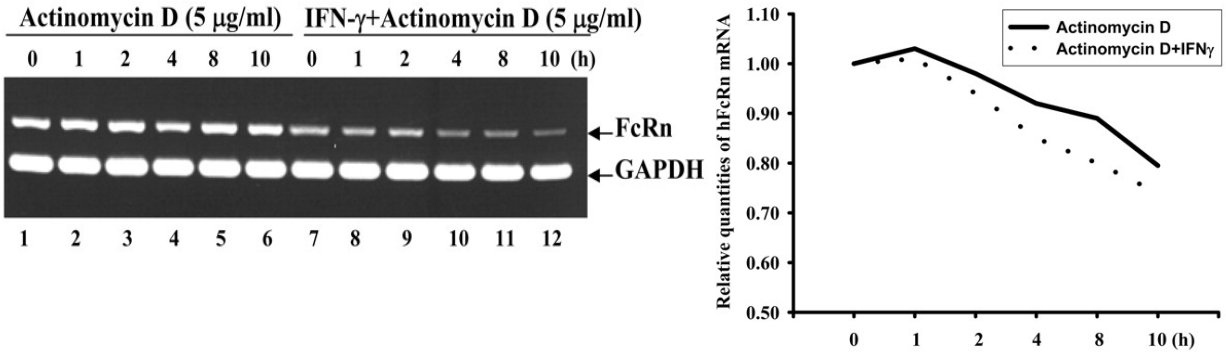
Actinomycin D (5 μg/ml)
IFN-γ+Actinomycin D (5 μg/ml)
0 1 2 4 8 10 0 1 2 4 8 10 (h)
FcRn
GAPDH
1 2 3 4 5 6 7 8 9 10 11 12
Relative quantities of hFcRn mRNA
1.10
1.00
0.90
0.80
0.70
0.60
0.50
0 1 2 4 8 10 (h)
Actinomycin D
Actinomycin D+IFNγ

B.

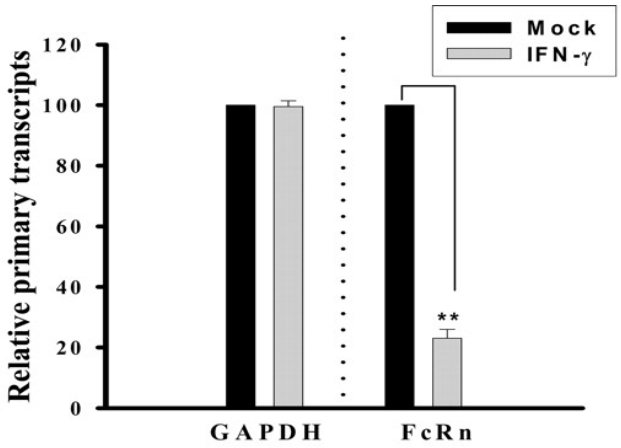
Relative primary transcripts
120
100
80
60
40
20
0
Mock
IFN-γ
**
GAPDH
FcRn

C.

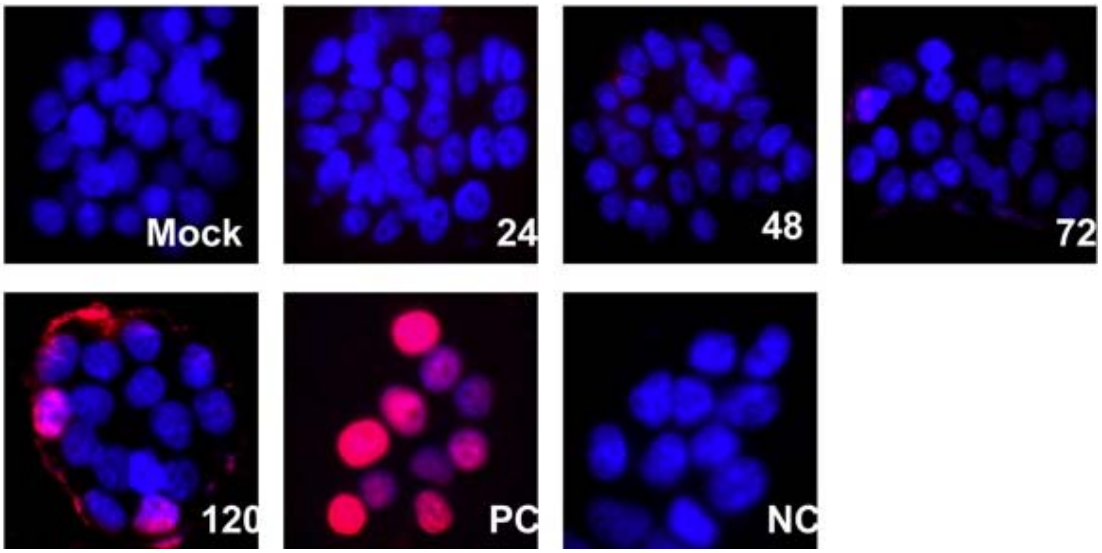
Mock
24
48
72
120
PC
NC

Figure 3.2. **Kinetic studies of FcRn mRNA levels and apoptosis in the absence or presence of IFN-γ. A.** Human intestinal HT-29 cells were preincubated for 24 h in the absence or presence of IFN-γ (25 ng/ml). Actinomycin D (5 μg/ml) was then added; total cellular RNA was harvested at the indicated time points (1–10 h). Ten nanograms of total RNA were reverse transcribed to cDNA in a final volume of 20 μl. Subsequently, 30 cycles of semiquantitative RT-PCR (A, *left panel*) or a real-time RT-PCR (A, *right panel*) were performed. Electrophoresis of 10 μl of PCR product was done on 1.5% agarose gel *(left panel*). FcRn values were normalized for GAPDH with each sample. FcRn product at time 0 before the addition of actinomycin D was plotted as 100%. **B,** Nuclear run-on analysis was performed on THP-1 nuclei isolated in the presence of biotin-16-UTP for 30 min. Biotinylated RNA was collected using streptavidin magnetic beads, and the level of FcRn or GAPDH RNA was determined by quantitative real-time RT-PCR. Data are mean ± SD of three independent experiments. **C.** TUNEL staining of human intestinal epithelial HT-29 cells. After mock treatment or IFN-γ (50 ng/ml) treatment at the indicated times, in situ detection of apoptotic cells was performed on HT-29 cells cultured on coverslips by using an in situ cell death detection kit. Treatment with DNase I as a positive control (PC) or stained without terminal deoxynucleotide transferase as a negative control (NC). For the correlation of TUNEL with nuclear morphology, cultures were counterstained with DAPI (5 μg/ml). Red represents apoptosis positive cells. Images were viewed by fluorescence microscopy with excitation at 320–580 nm.

however, it had two sequences with a similarity to the STAT-1 consensus target sequence (Fig. 3.3 A). To quickly screen whether these two sequences arefunctional in the transcriptional repression of FcRn by IFN-γ, we set up a transient cell transfection assay using the FcRn promoter/luciferase reporter gene construct phFcRnLuc (146). We also generated constructs pM1 and pM2, each of which contains mutations of the putative GAS sequence in phFcRnLuc (Fig. 3.3 A). Transient transfection revealed that the phFcRnLuc or pM1 construct had decreased expression of luciferase in response to IFN-γ stimulation in wild-type 2fTGH cells (Fig. 3.3 B). However, transient transfection of the pM2 construct revealed that mutation of this putative GAS sequence significantly increased the luciferase activity in IFN-γ-stimulated cells to a similar level as that in mock-stimulated cells (Fig. 3.3 B). Hence, we conclude that the GAS sequence (TTCTTTGAA) in the human FcRn promoter is functional in response to IFN-γ stimulation (Table III. I).

To verify that this putative GAS sequence has the capability to directly bind STAT-1 protein in living cells, a ChIP assay was used to precipitate the STAT-1-DNA complexes with an Ab specific for STAT-1. After cross-linking the DNA with bound STAT-1 proteins in situ in IFN-γ-stimulated vs mock-stimulated HT-29 cells, the DNA fragments containing the STAT-1 sequences in FcRn promoter were precipitated with Ab and measured by PCR amplification. As shown in Fig.3.3 C, PCR with primers flanking the putative STAT-1 sequences generated a band from DNA coprecipitated with STAT-1 (*lanes 2* and *3*). In a negative control, immunoprecipitation with normal IgG did not generate any corresponding PCR

Table III.I Comparison of functional GAS element[a]

Gene	Species	GAS Sequence
c-*myc*	Mouse	**TTC**TGG**GAA**
ICAM-1	Human	**TTC**CCG**GAA**
IRF-1	Mouse	**TTC**CCC**GAA**
ICSBP[b]	Human	**TTC**TCG**GAA**
FcγR1	Human	**TTC**CCA**GAA**
IFP 53	Human	**TTC**TCA**GAA**
FcRn	Human	**TTC**TTT**GAA**
Consensus sequence		**TTC**NNN**GAA**

[a] Conserved nucleotides are set in boldface. N represents any nucleotide.
[b] IFN consensus sequence binding protein.

products (Fig. 3.3 C *lane 4*). The STAT-1 binding sequence in the ICAM-1 gene promoter (154) was used as a positive control. As expected, ChIP assays failed to detect DNA bands from U3A cells (Fig. 3.3 C, lanes 5 and 6).

To further visualize the capability of STAT-1 protein to directly bind to the putative FcRn GAS site identified from the ChIP assay, EMSAs were conducted to confirm the ChIP assay by using oligonucleotides containing the putative GAS sequence. As shown in Fig. 3.3 D, oligonucleotides formed a complex with extracts from IFN-γ-stimulated cells (*lane 2*) but not from mock-stimulated cells (*lane 1*). An oligonucleotide containing the GAS sequence from the c-*myc* promoter was used as a positive control (Fig. 3.3 D, *lane 9*). To verify whether the binding was specific, a competition assay was performed. The inducible band could be completely competed away by unlabeled oligonucleotides (*lane 3*). Supershift analysis revealed that the complex contains a factor that was recognized by Ab specific for the STAT-1 protein (*lane 4*) but not normal IgG (*lane 5*).

IFN-γ induces the in vivo association of p300 and STAT-1α, and overexpression of p300 reduces IFN-γ-mediated FcRn gene repression

Our data show that the nuclear translocation of STAT-1α correlated with IFN-γ -mediated down-regulation of FcRn gene transcription and that STAT-1α bound directly to the FcRn promoter (Fig. 3.3). It is possible that nuclear protein(s) interacting with STAT-1α may play a pivotal role in down-regulating FcRn gene

A.

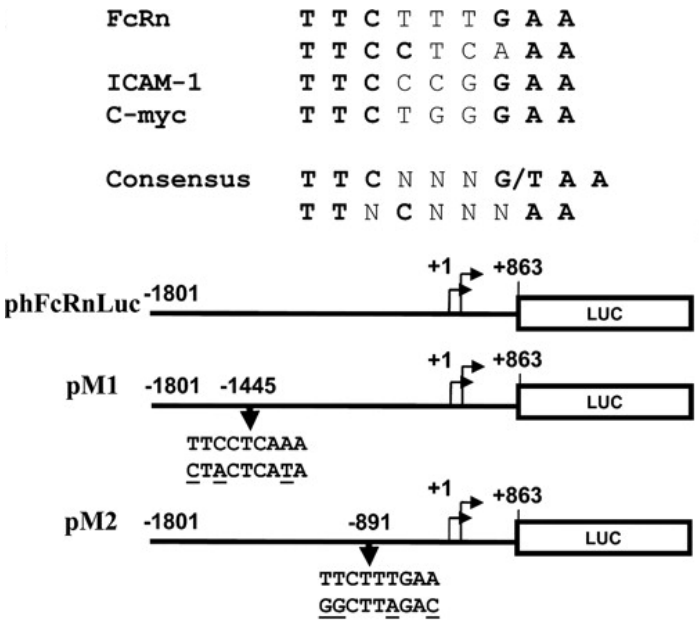
FcRn T T C T T T G A A
T T C C T C A A A
ICAM-1 T T C C C G G A A
C-myc T T C T G G G A A
Consensus T T C N N N G/T A A
T T N C N N N A A
phFcRnLuc
-1801
+1
+863
LUC
pM1
-1801 -1445
TTCCTCAAA
CTACTCATA
pM2
-1801
-891
TTCTTTGAA
GGCTTAGAC

B.

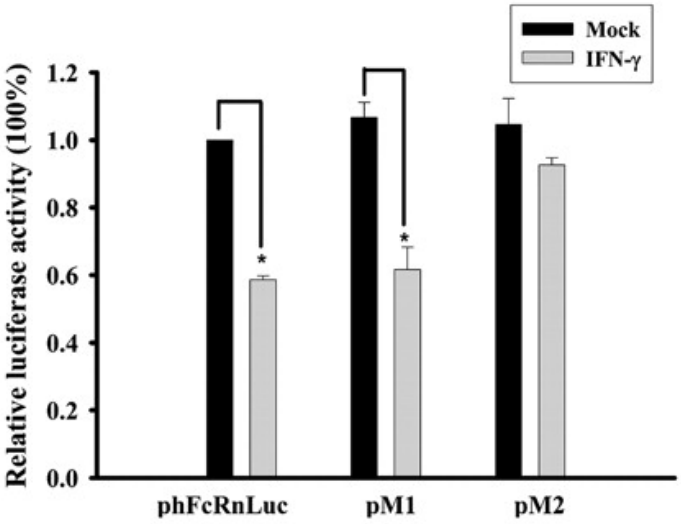
Mock
IFN-γ
Relative luciferase activity (100%)
1.2
1.0
0.8
0.6
0.4
0.2
0.0
*
*
phFcRnLuc
pM1
pM2

C.

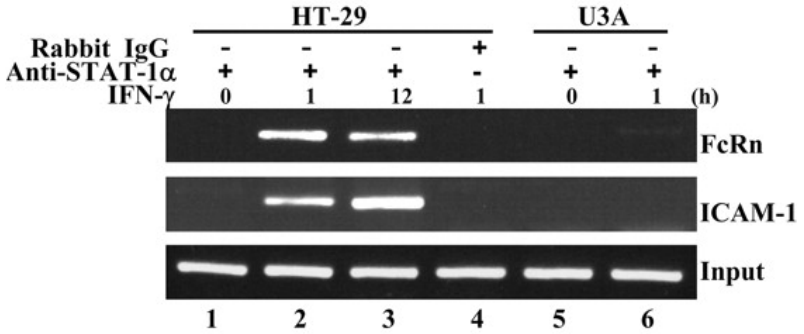
HT-29
U3A
Rabbit IgG - - - + - -
Anti-STAT-1α + + + - + +
IFN-γ 0 1 12 1 0 1 (h)
FcRn
ICAM-1
Input
1 2 3 4 5 6

D.

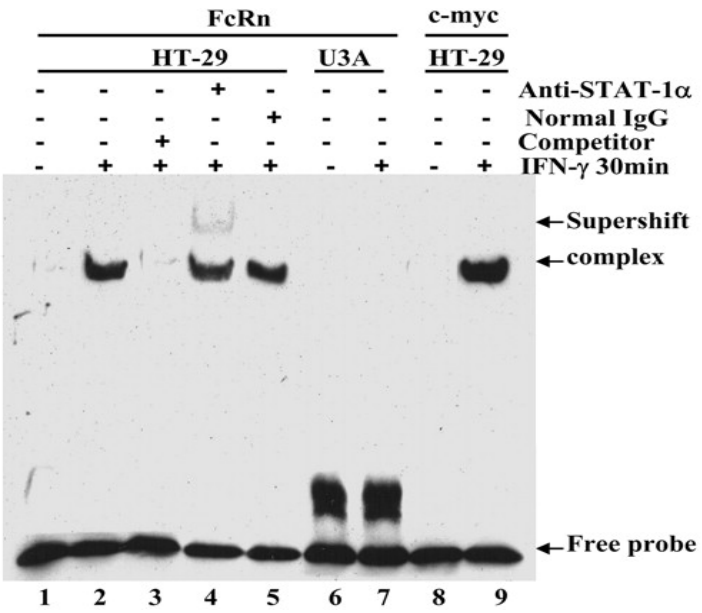

Figure 3.3 Identification of IFN-γ responsive element in human FcRn promoter.
A.The putative STAT-1 binding sequences in FcRn gene promoter. STAT-1 binding sequences from ICAM1 and c-*myc* as a positive control. The consensus STAT-1 sequence is in boldface. N represents any nucleotide. Reporter construct phFcRnLuc contains the FcRn promoter sequence from –1801 to +863 kb. The putative GAS mutations (underlined bases) in constructs pM1 and pM2 are also shown. Arrowheads indicate the position of the STAT-1 binding site in relation to the transcription start site of the FcRn gene. Luc, Luciferase. **B**. Identification of GAS sequence in response to IFN-γ stimulation. Wild-type 2fTGH cells were transiently transfected with phFcRnLuc, pM1, and pM2 constructs. Twenty-four hours after transfection, cells were either mock-treated (filled bar) or treated with IFN-γ (open bar) for 24 h. Cells were then harvested and protein extracts were prepared for the luciferase assay. **C**. Detection of the in vivo binding of STAT-1 protein to the human FcRn promoter in a ChIP assay. ChIP assays were performed using STAT-1-specific Abs (*lanes 1–3*, *5*, and *6*) or isotype-matched IgG (*lane 4*) as a negative control. **D.**EMSA analysis of binding activities of DNA probe with nuclear extracts from HT-29 cells treated with (+) or without (–) IFN-γ. A 26-bp fragment spanning the putative STAT-1 binding sequence corresponding to the GAS was used as a biotin-labeled probe. Binding specificity of these complexes was examined by competition assays with a 100-fold molar excess of unlabeled STAT-1-specific probe (*lane 3*). Supershift experiments were performed in the presence of the STAT-1 Ab, resulting in the formation of a slow migrating supershift band (*lane 4*).

expression. It is known that STAT-1α can bind CBP/p300 (147). Therefore, we further examined the possibility that the interaction between STAT-1α and CBP/p300 may lead to down-regulation of FcRn gene expression. Coimmunoprecipitation was used to examine the in vivo association of endogenous p300 and STAT-1α. The 2fTGH and U3A cells were incubated in the absence and presence of IFN-γ and nuclear extracts from these cells were subjected to immunoprecipitation with Ab against p300. The precipitated immune complexes were then blotted for the presence of STAT-1α. In IFN-γ-treated cells, anti-p300 Ab immunoprecipitated a significant amount of STAT-1α (Fig. 3.4 A *lane 2*) in comparison with mock-stimulated cells (*lane 1*). As a negative control, IgG did not immunoprecipitate STAT-1α (*lane 3*). These results suggest that STAT-1α does not associate with p300 in mock-stimulated cells; however, IFN-γ treatment can induce the in vivo association of STAT-1α and p300.

It is possible that STAT-1α suppresses FcRn gene activation by interfering with the binding of CBP/p300 to the FcRn promoter. Transient transfection assays were first used to examine whether overexpression of p300 could reverse IFN-γ-mediated FcRn suppression. Indeed, overexpression of p300 reversed IFN-γ-induced suppression of luciferase expression in a dose-dependent manner (Fig. 3.4 B). Therefore, these data suggest that the IFN-γ-induced interaction between STAT-1α and CBP/p300 is responsible for the down-regulation of FcRn expression by IFN-γ.

A.

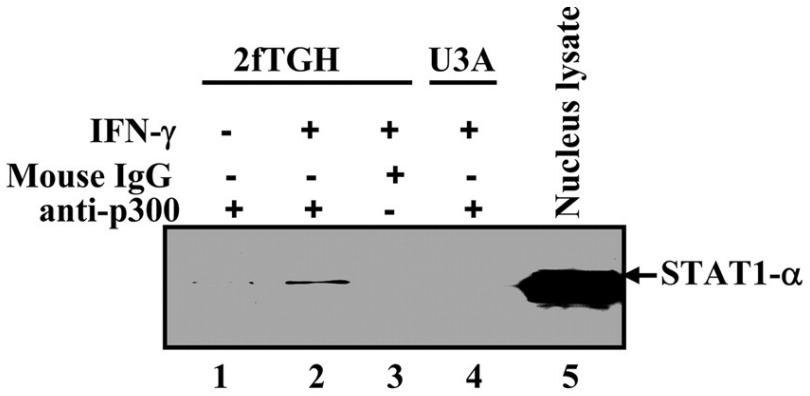

B.

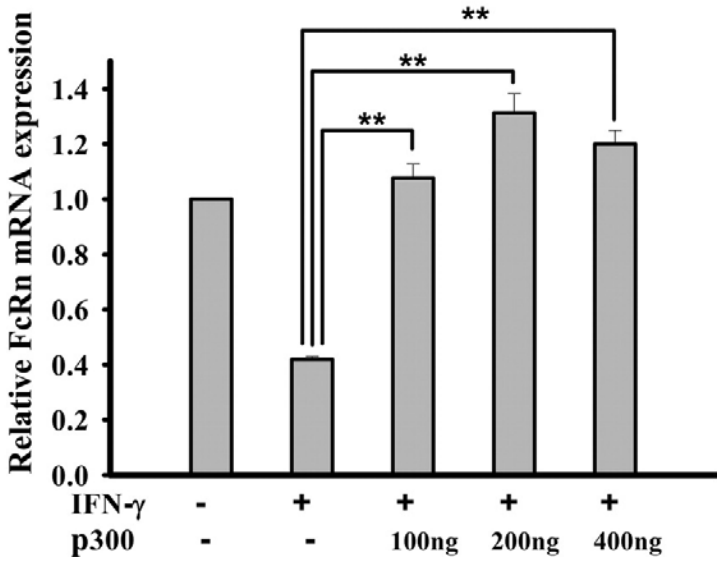

Figure 3.4 IFN-γ induces the in vivo association of p300 and STAT-1α, and overexpression of p300 blocks IFN-γ-mediated FcRn gene down-regulation. A. The 2fTGH (*lanes 1–3*) and U3A (*lane 4*) cells were treated with IFN-γ (10 ng/ml) or mock treated for 2 h and then nuclear extracts were obtained and subjected to immunoprecipitation. Anti-p300 mAb (*lanes 1*, *2*, and *4*) and isotype-matched IgG (*lane 3*) were used to immunoprecipitate the STAT-1α and p300 complex. **B.** HT-29 cells were transiently transfected with increasing amounts (0.1–0.4 μg) of a p300 construct, and the total amount of transfected DNA was normalized by pcDNA3. Transfected cells were treated with IFN-γ or mock treated for 14 h. FcRn mRNA was analyzed by quantitative real-time RT-PCR analysis.

IFN-γ reduced bidirectional transport of IgG in polarized lung epithelial monolayers

The FcRn protein has been shown to transport IgG bidirectionally in polarized epithelial cells, namely from the apical to the basolateral direction or vice versa (148). We therefore addressed the possibility that IFN-γ-stimulated epithelial cells have altered IgG transcytosis. Calu-3 cells have been previously shown to transcytose dimeric IgA in response to IFN-γ stimulation (155). We established the FcRnin Calu-3 cell lines and further verified the FcRn down-regulation by IFN-γ stimulation, as assessed by semiquantitative RT-PCR (Fig. 3.5 A).

In our transport experiment, after adding human IgG to the apical or basolateral surface of a Calu-3 cell monolayer, we assessed the IgG transported to the opposite basolateral or apical chamber following IFN-γ exposure, respectively. As expected, after 1 h at 37°C intact human IgG applied to the apical or basolateral side was transported across this monolayer. IgG H chain was detected in medium incubated at 37°C (Fig. 3.5 B, *upper row*). Importantly, IgG transport was decreased ~ 30% in the apical to basolateral direction (Fig. 3.5 B, *lane 3*), or 40% in the basolateral to apical direction (Fig. 3.5 B, *lane 5*) following IFN-γ stimulation, in comparison to the mock-treated monolayer (Fig. 8*C*, *lanes 2* and *4*). Treatment of Calu-3 monolayers with IFN-γ for 24 h might result in a leakage of IgG molecules, as shown in human intestinal epithelial cell line T84. Chicken IgY was used as a negative control because it is structurally similar to human IgG but does not bind to human FcRn. As shown in Fig. 3.5 B (*bottom panel*), chicken IgY was not transported

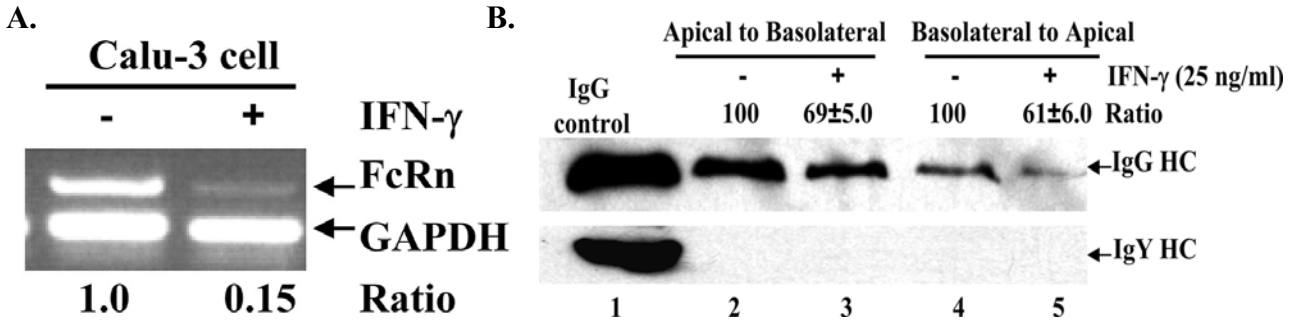

Figure 3.5 Effects of IFN-γ stimulation on the IgG transcytosis.
A. Semiquantitative RT-PCR analysis of FcRn mRNA in the human lung epithelial Calu-3 cell line. The Calu-3 cells were treated (+) with IFN-γ (25 ng/ml) (*right lane*) or left untreated (–) (*left lane*) for 24 h. **B.**Calu-3 cells (5 x 10^5/well) were grown in a 12-well Transwell plate. When the resistance of the monolayer reached 700-1000 ohms/cm^2, cells were stimulated with or without IFN-γ (25 ng/ml) for 24 h. Cells were loaded with human IgG (*top row*) or chicken IgY (*bottom row*) (0.5 mg/ml) at 4°C in either the apical (*lanes 2* and *3*) or basolateral (*lanes 4* and *5*) chamber. *Lane 1* represents an IgG or IgY H chain. Cells were warmed to 37°C to stimulate transcytosis, and medium was collected from the nonloading compartment 1 h later and subjected to Western blot-ECL analysis. The results are representative of at least three independent experiments. Band intensities of IgG heavy chain (HC) were compared by densitometry against IgG transported from mock-stimulated cells.

in either direction, suggesting that the transepithelial flux of Abs by passive diffusion through intercellular tight junctions or monolayer leaks does not contribute to the amount of the IgG we detect. Therefore, we concluded that IFN-γ stimulation decreased the IgG transport across the polarized epithelial cells.

DISCUSSION

Transcriptional regulation of genes hinges on the ordered recruitment of transcriptional polymerase, coactivators, repressors, chromatin modifiers/remodelers, and general transcriptional factors to the promoters of target genes. How the gene transcriptional machinery integrates signals from different biological signaling pathways is a central question for gene regulation. Exposure to IFN-γ can result in the regulation of up to 500 genes in either a positive or a negative way (134, 138). Genes that are negatively regulated by IFN-γ are fewer in number than those positively induced. Among the negatively regulated ones are some of the MMPs, stromelysin, type II collagen, HL-60, neu/HER-2, cell-cycle genes (c-*myc*, cyclin D, cyclin A), granulocyte chemotactic protein-2, IL-4, prolactin, perlecan, and the scavenger receptor A (SR-A) genes (138, 156-164). In this article we report, for the first time, the effect of IFN-γ on the transcriptional regulation of FcRn.

Activation of the IFN-γ signaling pathway down-regulates the expression of the human FcRn gene, and this down-regulation is dependent on the STAT-1 signaling pathway. This conclusion is supported by several pieces of evidence. First, our results showed that stimulation by IFN-γ decreased the FcRn expression in human intestinal

epithelial cells, Second, a nuclear run-on assay demonstrated that this down-regulation indeed occurred at transcription initiation (Fig. 3.2 B). Third, we have mapped an IFN-γ-responsive sequence, GAS, to the promoter region of the human FcRn gene by both EMSA and ChIP. Mutation of this GAS sequence abolished the inhibitory effect of IFN-γ on FcRn promoter (Fig. 3.3). Fourth, expression of luciferase activity driven by the FcRn promoter following IFN-γ exposure was not affected in STAT-1-null U3A in comparison with the wild-type cell 2fTGH. These results provided both biochemical and genetic support for the conclusion that increased phosphorylation of STAT-1 is the mechanism by which IFN-γ treatment leads to FcRn down-regulation. Recent studies have shown that IFN-γ can regulate gene expression by STAT-1-independent pathways(138). Among several genes that are inhibited by IFN-γ, c-*myc* has been shown to require STAT-1-dependent and STAT-1-independent pathways and, notably, there is a GAS element in the c-*myc* promoter that is necessary, but not sufficient, to confer the total inhibitory effects of IFN-γ. Therefore, our data support the conclusion that the down-regulation of human FcRn expression was mediated via a STAT-1-dependent pathway in response to IFN-γ. However, our data could not exclude the possibility that STAT-1 may bind to sites in other parts, such as introns, of the human FcRn gene. We considered the possibility that IFN-γ induces apoptosis(152) and regulates the expression of the gene at posttranscriptional level. However, several facts counter this conjecture. First, down-regulation of human FcRn and up-regulation of Ii occurred concomitantly in response to IFN-γ treatment (Fig. 1*A*). Second, we failed to detect any noticeable effect of IFN-γ on human FcRn half-life in actinomycin D-treated cells (Fig. 3.2), suggesting that

the half-life of FcRn mRNA was not affected by IFN-γ. Third, apoptosis was only detected after a 5-day period and then only in a few cells (Fig. 3.2 D). In addition, the level of IFN-γ repression (40–50%) on the reporter construct phFcRnLuc was similar to FcRn gene repression in cell lines; this would exclude the possibilities that the down-regulation of FcRn gene expression might be caused by apoptotic effects of IFN-γ or that IFN-γ affects the half-life and stability of FcRn mRNA. Therefore, these complementary experiments eliminate the concerns of apoptotic effects or stability of FcRn mRNA by IFN-γ.

The mechanism of STAT-1-mediated down-regulation of human FcRn expression might be through sequestering of the transcription activator CBP/p300. One potential mechanism by which IFN-γ might normally mediate the repression of FcRn transcription could be via STAT-1 interaction with either constitutive transcription factors or transcription factors that are activated upon exposure to IFN-γ. Although STAT-1 acts as an activator of transcription in numerous genes in response to IFN-γ stimulation, the detailed mechanisms by which STAT-1 switches on and off gene expression are still unclear. As shown in several elegant studies, although STAT-1 is necessary and sufficient to inhibit MMP-9, SR-A, and type II collagen gene transcription by IFN-γ, there are no GAS elements in the promoters of these genes (156, 165). Thus, suppression of the expression of these genes by IFN-γ -activated STAT-1 is probably not dependent on the direct binding of STAT-1 on the gene promoter of these genes. In contrast, the suppression of the MMP-9 or the SR-A gene depends on the ability of activated STAT-1 to interact with other nuclear proteins.

Indeed, STAT-1 can interact with a variety of other transcription factors, including STAT-2, CBP, p300, p300/CBP cointegrator protein (pCIP), histone deacetylase 1 (HDAC-1), N-Myc interactor (Nmi), and BRACA1 (166-169). Among these proteins, CBP/p300 serves as a scaffold in transcription complex formation in addition to functioning as histone acetyltransferases. Given the fact that the total amount of CBP/p300 is limited compared with the amount of other transcription regulators, a competition for using CBP/p300 in different signaling pathways has been proposed. In the case of the MMP-9, SR-A, neu/HER-2 genes, activated STAT-1 can competitively bind with CBP/p300, thereby resulting in decreased association of CBP/p300 in the gene promoter and interference with the assembly of functional transcription complexes (159, 165, 166). Our data showed that overexpression of CBP/p300 overcame the inhibitory effect of IFN-γ (Fig. 3.4 B). However, our data could not exclude the possibility of STAT-1 interacting with other transcription factors. For example, Y-box-binding protein YB-1, RFX5 complex, CIITA, IFN regulatory factor (IRF)-1, and IRF-2 are also involved in the gene repressions by IFN-γ (135, 161, 169, 170). Further work is underway to determine how STAT-1 actually mediates repression of FcRn gene expression.

To date, two biological functions have been attributed for FcRn: transcytosis of IgG across polarized epithelial cells and protection of IgG from degradation. The level of FcRn expression may be critical for the regulation of IgG levels in tissues and blood. First, mucosal Abs are important for mucosal infections, and epithelial cells that line mucosal surfaces in vivo express FcRn. Therefore, FcRn transports normal or

pathogen-specific neutralizing IgG across polarized cells such as placental or mucosal epithelial cells, potentially "seeding" maternal and mucosal immunity. From our findings, one might speculate whether IFN-γ dampening the expression of the FcRn receptor might lead to the lessening of IgG transport. In an in vitro Transwell model, our results clearly demonstrated that IFN-γ functionally decreased IgG transport in the polarized lung epithelial Calu-3 cell line (Fig. 3.5 B). Therefore, IFN-γ may dampen IgG-mediated mucosal immunity by reducing IgG transport in vivo. This result is in contrast to the fact that IFN-γ up-regulates pIgR expression, which is expected to enhance secretory IgA-mediated mucosal immunity (155, 171). Furthermore, our previous finding revealed that TNF-α and IL-1β, via activation of the NF-κB signaling pathway, can up-regulate the functional expression of FcRn. Because IFN-γ, TNF-α, and IL-1β are proinflammatory cytokines, FcRn levels may therefore be finely tuned by opposing negative and positive signaling in the maintenance of IgG homeostasis under pathophysiological conditions. Thus, regulation of FcRn expression in vivo likely involves the species, magnitudes, and coordinated actions of proinflammatory cytokines or other functional regulators. Secondly, by mediating the protection of IgG from catabolism, FcRn extends the half-life of pathogenic or autoimmune IgG, potentially promoting the progression of IgG-mediated autoimmune diseases (106). Therefore, by influencing the expression level of FcRn, IFN-γ may be directly coupled to the pathogenesis of IgG-mediated autoimmune diseases. Indeed, IFN-γ has been shown to regulate the intensity or the progression of several autoimmune diseases (172). However, it remains for further investigation whether its regulatory effect in the changing course of an autoimmune disease is, at least in part,

through the down-regulation of FcRn expression. This question merits further investigation in a murine model. Overall, by examining the molecular mechanisms by which IFN-γ regulates FcRn expression, our studies may contribute toward the general understanding of FcRn-mediated mucosal immunity and inflammation. The identification and understanding of IFN-regulated FcRn gene expression may lead to improved therapies for IgG-mediated autoimmune diseases.

Among MHC class I-related molecules, IFN-γ causes the up-regulations of the MHC genes HLA-A, HLA-B, HLA-C, HLA-F, HLA-G, HLA-H, HLA-E, and CD1 (141). The promoters of HLA-A, HLA-B, HLA-C genes contain a consensus ISRE sequence. IRF-1 is induced by IFN-γ and interacts with the ISRE in HLA gene promoters to stimulate transcription initiation (141). In the special case of HLA-E, although IFN-γ also induces HLA-E expression, the HLA-E gene promoter does not contain a functional ISRE. Instead, two distinct elements in the HLA-E promoter are termed the IFN response region (IRR) and the upstream IFN response region (UIRR). STAT-1 and GATA-1 bind to the IRR and UIRR, respectively, to stimulate transcription from the HLA-E promoter (173). Among the MHC class I-related genes, FcRn is an only molecule that is down-regulated by IFN-γ (Fig. 3.6). This scenario makes FcRn unique in the response to IFN regulation. Therefore, understanding differences in the mechanisms by which IFN-γ stimulates MHC-I genes and FcRn could be of great interest in the settings of immune responses and autoimmunity. Any differences in the signal transduction pathways leading to differential expression of

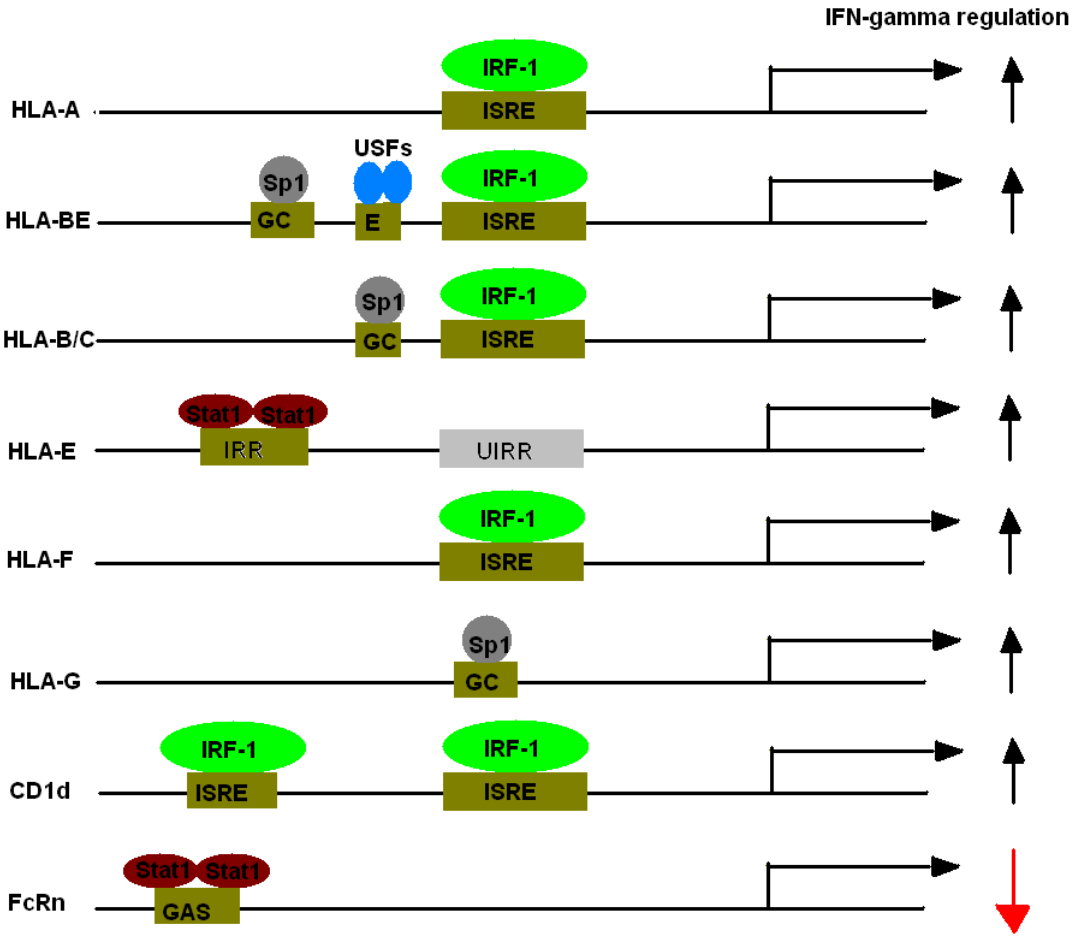

Figure 3.6. Schematic illustration of transcription factors binding to the promoter region of some MHC class I-related genes after IFN-γ treatment. The ISREs of HLA-A, HLA-B, HLA-C, and HLA-F bind IRF-1 upon IFN-γ exposure and regulate the IFN-γ-induced transactivation of these genes. The putative ISRE of HLA-E did not respond to IFN-γ-stimulation, whereas an upstream GAS sequence of HLA-E is responsive to IFN-γ through STAT-1 activation. HLA-G is responsive to IFN-γ via an upstream IFN-responsive regulatory sequence. Multiple putative ISREs of CD1D are predicted, but one is shown here. Human FcRn responds to IFN-γ through STAT-1 activation and binding to an upstream GAS sequence. In addition, several constitutive transcription factors are revealed to bind to the ISRE area. Sp1 binds to the GC-rich sequences in the ISRE areas of HLA-B, HLA-C, and HLA-G. The putative E box 5' of the ISRE in most HLA-BE alleles is bound by USF-1 and USF-2. Arrows represent the up- and down-regulation of gene expression upon IFN-γ exposure. The schematic structure of the gene promoter is not scaled.

the FcRn and MHC class I genes would be potential targets for therapeutic intervention aimed at selective activation of one or the other.

In summary, transcriptional repression of FcRn gene expression by IFN-γ is dependent on activated STAT-1 protein. These findings suggest that the biological consequence of IFN-γ -induced transcription of the FcRn gene is distinct from that of other MHC class I or related genes. Therefore, our observation that FcRn repression by IFN-γ is, to our knowledge, the first demonstration that MHC class I-related genes are regulated negatively by IFN-γ exposure. These results provide evidence that IFN-γ differentially modulates the expression of FcRn and MHC class I or its related genes, which generates opposing effects on cellular and humoral immunity. Further studies of STAT-1-mediated mechanism of transcriptional repression on FcRn will provide insights into understanding the inhibitory effects of IFN-γ on gene expression in general. Given the important role of FcRn in the maintenance of IgG concentration as well as transport of IgG across placenta and mucosal surfaces, the results from these studies would also provide new information on mucosal protection and vaccine development.

CHAPTER 4: FCRN MEDIATES EFFICIENT ANTIGEN PRESENTATION OF PHAGOSOMAL IMMUNE COMPLEXES IN MACROPHAGE, BUT NOT IN DENDRITIC CELL.

ABSTRACT

While Fc gamma receptors (FcγRs) facilitate MΦ and DC presenting IgG-restricted Immune complexes (ICs) onto MHC class II molecules efficiently, the role of another IgG Fc receptor, neonatal Fc receptor (FcRn) remains elusive. We now show that the phagosomal FcRn in MΦ binds to uptaken latex-ICs, prolongs the half life of latex-IC, and enhances the MHC-II-restricted antigen presentation. However, defective FcRn has no effects on the antigen processing and presentation of latex-ICs in DC both in vitro and in vivo. We show that phagosomes in MΦ are acidified very rapidly, that is required for the physical interaction of FcRn with IC. By contrast, DC maintains the neutral environment of phagosomes for a long time, which prohibits FcRn from binding to IC, consequently unable to affect the antigen process and antigen presentation. Our studies reveal a novel mechanism for FcRn to modulate the processing and presentation of IgG-complexed ICs antigen to MHC class II.

INTRODUCTION

Uptaking, processing and presenting exogenous antigens to T lymphocytes by professional antigen-presenting cells (APC) such as MΦ and DC is a crucial step to initiate the immune responses (99). MΦ and DC express FcγRs on their surfaces. Functionally analogous to the B cells receptor for antigen presentation, FcγRs could internalize antigen in the form of immune complexes and facilitate MHC class II-restricted antigen presentation and MHC class I-restricted cross-presentation (9, 174, 175). FcγRs-internalized IC are transported through endocytic pathway, to late endosomes or phagosomes, where IC is fragmented and loaded onto MHC class II molecules for presentation to T cells (175). Furthermore, the binding of IC to FcγRI and FcγRIII triggers the activation signaling through the γ subunit (FcRγ) that carries an immunoreceptor tyrosine-based activation motif (ITAM) (176). The signal through the FcγRs induces the maturation of DC and promotes antigen presentation (174).

The neonatal Fc receptor for IgG (FcRn) is structurally and functionally different from FcγRs. FcRn consists of one membrane-bound 45-50 kDa heavy chain and one 12 kDa light chain β_2-microglobulin (β_2m). The structure and sequence analysis show that FcRn shares homology with MHC class I molecule (26, 47). Despite of the structure similarity, the peptide groove of FcRn is occluded (28, 171). Instead, FcRn binds Fc portion of IgG on the outer face of the narrowed groove, which involves both heavy chain and β_2m. Several histidines residing in CH2 and CH3 domains of IgG are key residues directly contact FcRn, which are distinct from FcγR binding sites (26). FcRn was identified as a receptor to transport maternal IgG

to fetus or to the newborn across epithelial and endothelial barriers (36, 56). FcRn also can transport IgG and complexed antigens across intestine epithelium (177). This transcytosic function is accomplished by FcRn capturing IgG or ICs on the cell surface or in the endosomes, transporting them across the polarized cellular barriers. FcRn also acts as salvage receptors diverting the bound IgG away from lysosomal degradation and maintaining IgG homeostasis (67, 68, 178). These two functions of FcRn are dependent on the ability of FcRn to bind IgGs, which is pH restricted and only occurs at the pH $\leq$ 6.5 (27).

The pH value in the endocytic compartments of professional APCs plays a very important role to control the degradation of exogenous antigen following their uptake (179), as lysosomal degradation could destroy antigenic epitope for presentation. The high antigen presenting efficiency of DC is partially due to the pH regulation in different maturation stages and in different endocytic compartments. Particularly, the alkalinization of phagosomes provides DC the ability to control degradation for optimal presentation (101, 180). The rapid acidification of phagosomes in MΦ results in a strong activation of lysosomal proteases and effective protein degradation (181, 182). Our recent studies show that in DC and MΦ, FcRn localizes in late endosomes/lysosomes in addition to the early endosomes (183, 184). In this study, we compared the roles of FcRn in antigen processing and antigen presentation in DC and MΦ. We showed that FcRn can facilitate antigen presentation by stabilizing the IgG-complexed antigens in a pH-dependent manner, which provides a novel mechanism to explain the FcRn-mediated antigen presentation.

MATERAILS AND METHODS

Mice.

Seven-wk-old C57BL/6 mice were purchased from National Cancer Institute and Charles River Laboratories (Frederick, MD). Female B6.PL-Thy1a/CyJ (Thy1.1 congenic) WT mice and OT-II mice (B6 background) transgenic for $OVA_{323-339}$ were purchased from The Jackson Laboratory (Bar Harbor, ME). OT-I/RAG-/- (B6 background) mice transgenic for $OVA_{257-264}$ were kindly provided by ghost lab (NIAID, Bethesda, MD). MHC class II -/- mice on B6 background were purchased from Taconic (Rockville, MD). FcRn-/- B6 mice bearing Thy1.2 were used (68). Transgenic mice were bred and maintained in HEPA-filtered cages at the University of Maryland (College Park, MD). The studies detailed herein conform to the principles set forth by the IACUC guidelines for the care and use of animals in biomedical research.

Reagents.

OVA (grade VI) was purchased from Sigma-Aldrich (St. Louis, MO). Rabbit IgG poly-Ab to OVA were purchase from MP Biochemicals (Solon, Oh). Rabbit IgG-OVA immune complexes were made by mixing a 5:1 molar excess of anti-OVA: OVA at 37°C for 30min. Mouse IgG mono-Ab to OVA was purchased from Sigma. Mouse IgG-OVA immune complexes were made by mixing 1:1 of anti-OVA: OVA at 37°C for 30min. Latex beads (3μm, fluorescent or nonfluorescent) were purchased from Polyscience (Warrinton, PA). Latex beads were noncovalently conjugated with

OVA (10mg/ml) by incubation at 4°C for 48 hours. After then, the conjugated beads were washed with PBS for three times and stored in PBS at 4°C. Latex-OVA-ICs were made by mixing Latex-OVA with Rabbit anti-OVA at the ratio of 1:1. LPS from *Escherichia coli* type 0111.B4 was abtained from Sigma-Aldrich (St. Louis, MO). Rat mAb anti-LAMP-1 was from the Developmental Studies Hybridoma Bank (Iowa City, IA). mAb anti-EEA1, rat anti-mouse transferrin receptor were obtained from BD Biosciences. All secondary Abs were purchased from Invitrogen.

Bone marrow-derived DCs (BMDCs).

BMDCs were produced as described by Lutz et al (185) with minor modifications. In brief, bone marrow was flushed from the femurs of mice, and cells were plated in 100-mm petri dishes at a concentration of 1×10^6 cells/ml in RPMI 1640 supplemented with 10% FCS, penicillin/streptomycin, HEPES, glutamine, 50 μM 2-ME, and 10% GM-CSF-secreting J588L (kind gift from Dr. Kristin Tarbell, NIDDK) cell culture supernatant. On days 3 and 6, half of the medium was removed and replaced with fresh conditioned medium. On day 8, the suspension cells were harvested and analyzed by found flow cytometry. Cells contained > 80% CD11c+/ I-A/E positive cells.

Splenic DC (SPDC).

Spleen was digested by Collagenase D (Roache, IN) for 30 min at 37°C. Then, cells were passed through a strainer and washed with RPMI 1640. To separate DC, CD11c positive selection magnetic mcrio-beads (Miltenyi Biotec, CA) were used

following manufacture's instruction.

Bone marrow-derived macrophages (BMMs).

BMMs were prepared as described previously (186). bone marrow were obtained using a similar approach to that for BMDCs. Cells were plated in petri dishes in F12/DMEM Glutamax supplemented with 10% FCS, penicillin/streptomycin, glutamine, and 20% conditioned medium from the supernatant of M-CSF-secreting L929 fibroblasts. Media was replaced on day 3 and day6, and attached cells were used at 7-9 days for experiments.

Antigen Presentation Assays.

For MHC Class II–restricted antigen presentation assays. OVA, OVA-IC, and Latex-OVA-IC was separately added to Immature DCs or MΦ cells (1 x 10^5/well) in 96-well microtiter plates were incubated with antigen in the presence of LPS 200 ng/ml for 12 h. Cells were then washed with PBS before adding OT-II CD4+ T cells at a concentration of 2 x 10^5/well. CD4+ T cells were purified from OT-II TCR transgenic mice by negative selection using CD4+ cell isolation kit (Miltenyi Biotec, CA). T cell responses were monitored at 24 h by measuring IL-2 accumulation in the supernatant by ELISA (BD Biosciences, CA). Data are from triplicate cultures.

For MHC Class I–restricted antigen presentation assays. Presentation of OVA epitope 257-264 on K^b was detected using the T cell hybridoma B3Z or OT-I T cells. B3Z cells carry a β-galactosidase plasmid driven by NF-AT elements from the IL-2

promoter(187). OT-I CD8+ T cells were purified from OT-I/RAG-/- transgenic mice by negative selection using CD8+ T cell isolation kit (Miltenyi Biotec, CA). For antigen presentation assays, DC or MΦ were exposed to OVA-IC, at the concentration and for the periods of time specified, in the presence of the T cell hybridoma B3Z or OT-I CD8+ T cells. After incubation, B3Z cells were lysated, and a colorimetric assay using ONPG (sigma) as a substrate was used to detect LacZ activity in B3Z lysates. IL-2 production in supernatant was measured by ELISA kit following incubation with OT-I T cells.

Phagosomal pH measurement by confocol microscopy

Phagosomal pH was measured as previous description (188, 189). Briefly, BMMs or BMDCs ($2x10^5$cells/well) were plated in 4-well coverglass bottom chamber (Lab-Tek, Nunc, IL). After 80 % cells attached to the chambers, $1x10^6$ Latex-Beads coated with Dextran-Lysosensor Yellow/Blue (Invitrogen, CA) were added to each well and incubated with cells for indicated times, and then the cells were washed with warm PBS 5 min before the Confocal examination. The microscope (Zeiss LSM 510 Thornwood, NY) were used for the measurement at excitation laser 405 nm, and an emission filter at 450 nm and a longer emission between 505-530 nm. The ratios of 530/450 nm emission from phagocytosed beads were calculated by the software Zen 2007.

To obtain pH standard curve, cells were incubated with Lysosenor-coated beads for 5 h and then treated with 10 mM monensin and 20 mM nigericin. The

treated cells were equilibrated for 10 min with 25 mM MES (4-morpholineethanesulfonic acid) buffer containg 5 mM NaCl, 115 mM KCl, 1.2 mM $MgSO_4$ (from pH 5.0 to pH 7.5) prior to image acquirement.

Measurement of HRP-IC uptake and processing.

Horse radish peroxidase (HRP)-IC were generated by mixing HRP and rabbit anti-HRP (Sigma-Aldrich, MO) a 5:1 molar excess of anti-HRP:HRP at 37°C for 30min. After pulsed with HRP-IC for 3h at 37°C, cells were extensively washed and chased at 37°C for the indicated time point. The remaining HRP activities were represented by 450nm absorbance with TMB reagents.

Adoptive transfer with antigen-pulsed DC and MΦ.

Bone marrow derived DC or MΦ 5 x 10^5cells/ml were treated for 12 h in the presence of 100 μg/ml OVA, 10 μg/ml OVA-IC, and 10 μg/ml Latex-OVA-IC/ml in vitro. Free antigens were then removed from the cell cultures by washing about three times in cold PBS, each time followed by centrifugation for 10 min at 350 x *g* at 4°C. $OVA_{323-339}$ peptide pulsed cells as positive control, ICs-pulsed cells were resuspended in fresh medium at 1 x 10^6 cells/200 μl, and then injected either s.c. or i.v. into each mouse (190).

Analysis of CD4+ T cell proliferation ex vivo.

The T cell recall response was measured as previously described (191, 192). On day 0, DC or MΦ pulsed with the appropriate antigens were injected either s.c.or i.v.,

depending on the experiment. Nonpeptide-pulsed APCs were used as a negative control. On 5 days (DC immunization) or 15 days (MΦ immunization), CD4+ T cells were isolated from the spleen and lymph nodes of immunized mice and labeled with 1 μM CSFE (Invitrogen) for 10 min at 37°C. The cells were then washed once with HBSS without Mg^{2+} and Ca^{2+} (Fisher Scientific), supplemented with 5% FCS, followed by serum-free HBSS. 2×10^5/200ul CFSE-labeled CD4+ T cells were restimulated with spleenic DC bearing OVA peptide OVA323-339 in the 96-well plate. T cell proliferation was monitered with CFSE and PE-conjugated anti-Vα2 (BD Pharmingen) 3 days later by flow cytometry (193).

Immunofluorescence

Immunofluorescence patterns were visualized with confocal microscopy as described (184, 194) Briefly, cells were cultivated on Lab-Tek chamber (Nalge Nunc NY) for 12 h. Cells were pulsed with 1μg/ml OVA-DQ (Invitrogen)-ICs for 1h and then washed with PBS, cold fixed in 3.7% paraformaldehyde for 30 min at 4°C, and quenched with glycine for 10 min. After two washes with PBS, the cells were permeabilized in solution (PBS containing 0.2% Triton X-100) for 20 min and then blocked with PBS containing 10% normal goat serum. The mouse FcRn was detected using rabbit anti-FcRn-CT (184).

RESULTS

FcRn colocalizes with immune complexes (ICs) in the phagosomes of murine BMDC and BMM.

FcRn has been shown to locate in early endosome and lysosomes of DC and MΦ (184). We cultured bone marrow-derived DCs with J588L supernant and bone marrow-derived macrophages with L929 supernatant. In 8-10 days, FcRn was found highly distributed in early endosomes marked by Transferin receptor (TFR) of both BMDC and BMM by confocal microscope (Fig. 4.1 A), in agreement with the previous findings (72, 183, 184). When OVA-IC labeled in green florescence was loaded to BMDC and BMM, FcRn in red was found colocolized with OVA-IC (Fig. 4.1 B). To test if FcRn localizes in phagosomes, we feed BMDCs and BMMs with green florescent latex beads conjugated with OVA-ICs. We found that FcRn colocalized with latex beads, suggesting that FcRn was distributed to the phagosomes during the phagocytosis in DC and MΦ (Fig. 4.1C). This is in agreement with the observation that FcRn resides in the phagosomes of neutrophils (195).

In BMDC, FcRn enhances the presentation of endocytosed OVA-IC (mono), but not phagocytosed Latex-OVA-IC antigen through MHC class II.

To assess the role of FcRn in antigen presentation through MHC class II pathway, we compared IL-2 production from the OT-II CD4+ T cells activated either by wild-type BMDC or by FcRn-/- BMDC. OT-II CD4+ T cells isolated from OT-II transgenic mice can recognize OVA peptide 323-339 aa presented by the MHC class II molecules I-Ab (B6 background). When exposed to OVA, FcRn deficiency had no effect on the ability of DC to activate OT-II T cells (Fig. 4.2 D). As we know, soluble OVA was enocytosed into the cells and processed in the late endosome/lysosome as showed by OVA (Fig. 4.2 A). When monoclonal antiboby-

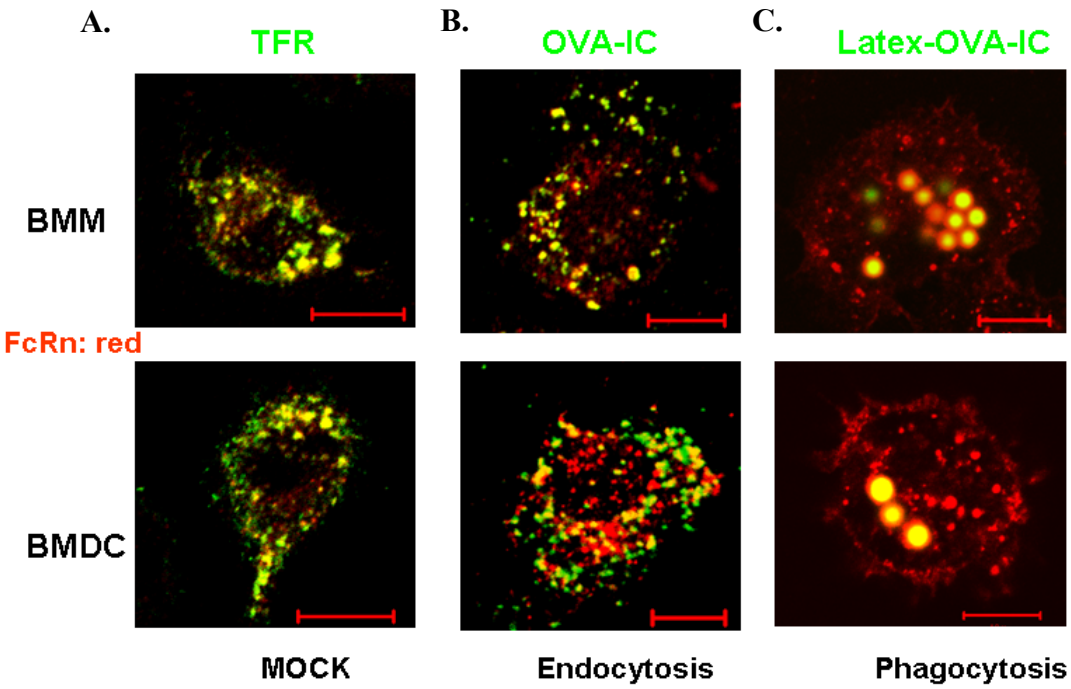

Figure 4.1 Localization of FcRn in endosomal compartments of murine bone marrow-derived DC and macrophage. BMMs (**top**) were isolated from 10th day culture in the presence of 10% J588L supernatant, and BMDCs (**bottom**) were isolated from 7th day culture with 20% L929 supernatant. The cells were fixed, permeabilized, stained, and analyzed by confocal microscopy. FcRn were visualized (red) using rabbit anti-FcRn-CT and Alexa 533-conjugated secondary antibodies. TFR (CD71) was detected by monoclonal rat-anti CD71 and Alexa 488-conjugated secondary antibodies. **A,** FcRn overlayed with early endosome marker TFR (green). **B**, some of the FcRn protein was colocalized with OVA-IC (green) in both BMM and BMDC.**C,** before the fixation, cells were pulsed with OVA-IC coated fluorescent Latex beads (green) for 2h, and then followed by the same staining procedure. Yellow, condistribution of two colors. Bar, represent 10μM.

restricted OVA-IC was exposed to the DCs, IL-2 production decreased modestly from OT-II T cell primed by FcRn-/- DC (Fig. 4.2 E) in comparison with WT DCs. These monoclonal IgG-restricted immune complexes also went through endosomes and lysosomes for antigen processing and presentation (Fig. 4.2 B). However, when DCs were incubated with latex beads conjugated with OVA-ICs, there was no difference on IL-2 production between WT DCs and FcRn-/- DCs primed T cells (Fig. 4.2 F), and these latex beads induced phagocytosis (Fig. 4.2 C). Similar results were obtained using polyclonal IgG-restricted immune complexs. Therefore, the expression of FcRn in BMDC promotes the presentation of antigen in ICs captured and processed through endocytosis, not through phagocytosis.

In BMM, FcRn enhances both endocytosed OVA-IC and phagocytosed Latex-OVA-IC to MHC class II.

To examine the roles of FcRn-mediated antigen presentation of MΦ, an in vitro T cell proliferation assay was conducted on BMM. BMM derived from WT and FcRn-/- bone marrow were pulsed with indicated concentrations of OVA-IC overnight, washed to remove extra ICs, and incubated with OT-II cells for 20 h. As shown in Fig. 4.3 E, the FcRn-/- BMM failed to prime the OT-II T cells. Similarly, the latex-OVA-ICs-treated FcRn-/- BMM also induced less IL-2 production in comparison with that of WT BMM (Fig. 4.3 F). In the control experiment, OVA loaded BMM, either WT or FcRn defective, activated CD4+ T to a similar level (Fig. 4.3 D). The trafficking patterns of immune complexes in MΦ and DC are similar (Fig. 4.3 A, 4.3 B, and 4.3 C).

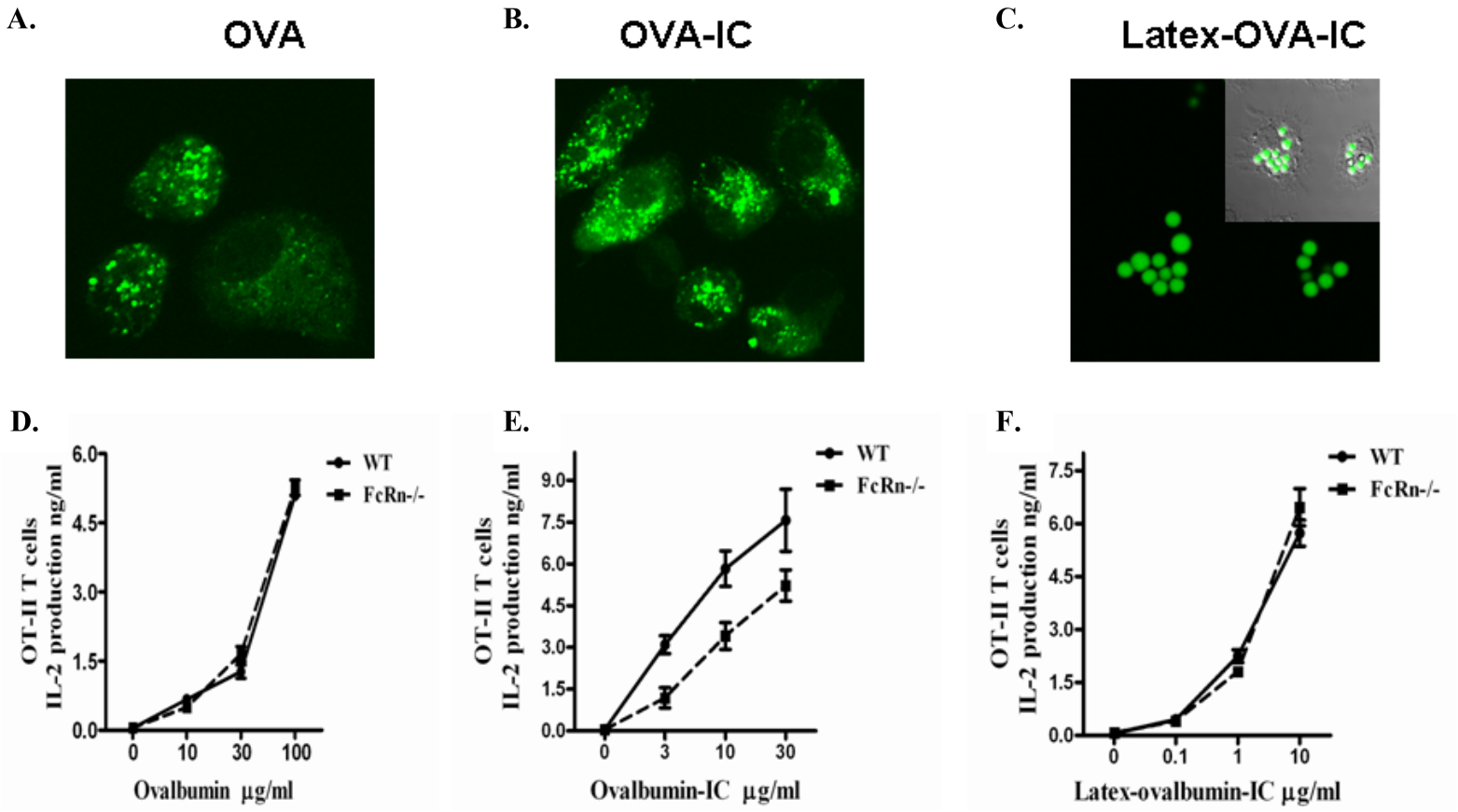

Figure 4. 2. FcRn deficiency in BMDC impaired OVA-IC antigen presentation to MHC class II, but not Latex-OVA-IC. BMDCs were incubated for 1 h at 37°C in the presence of , OVA **(A)**, OVA-ICs **(B)**, latex-OVA-IC **(C),** and then visualized by confocal microscopy. All of them were shown as green color. Bone marrow derived DCs were incubated for 12 h (**D, E** and **F**) in the presence of **D,** soluble OVA, **E,** OVA-ICs (mono), **F,** Latex-OVA-ICs at the indicated dosage. After washing with PBS, WT BMDCs (**solid line**) and FcRn-/-(**dashed line**) were incubated with OT-II CD4+ T cells for another 24h; IL-2 production from the supernatant was measured by ELISA kit. Data are the mean ± SD from experiment performed in triplicate.

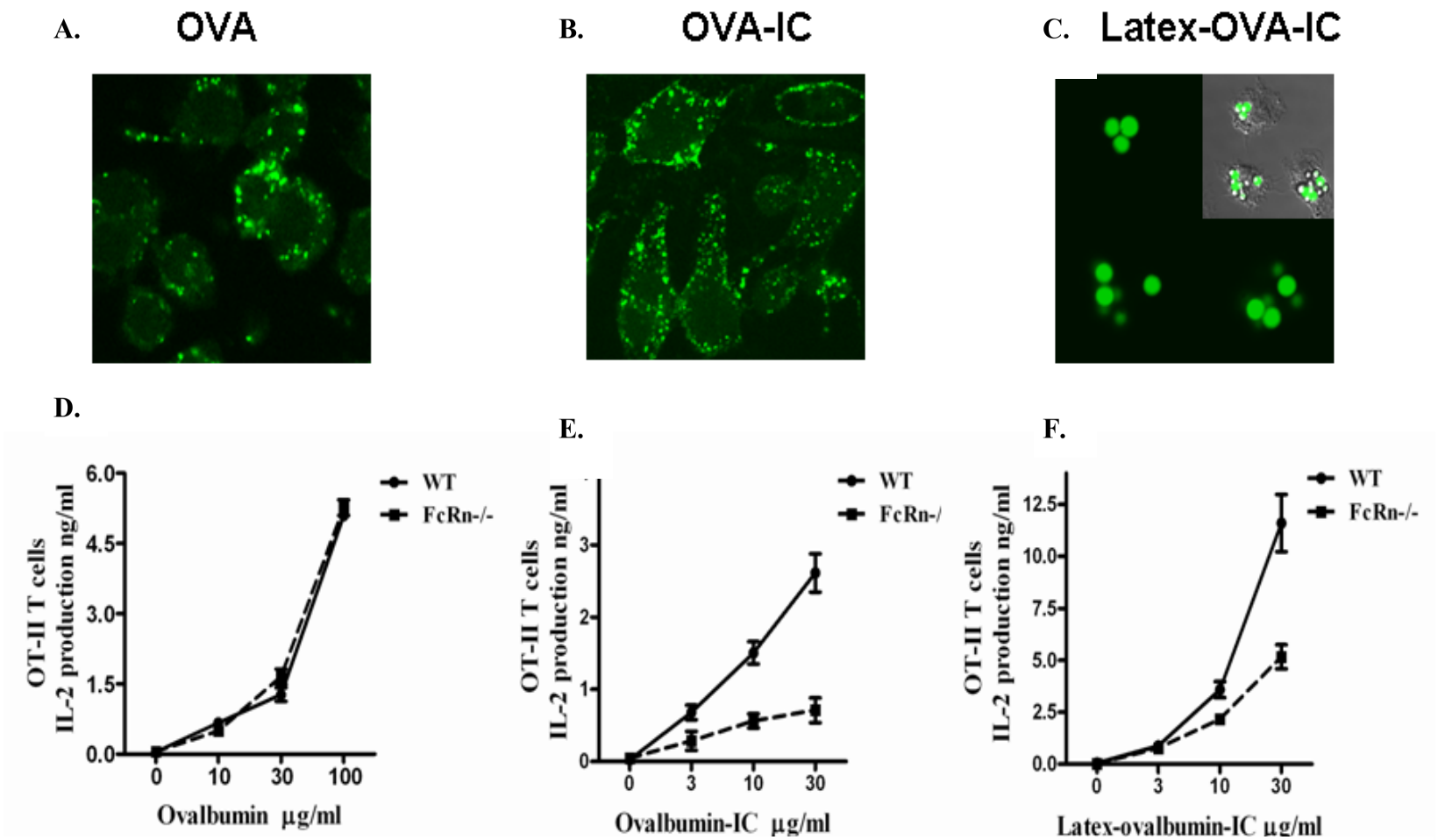

Figure 4.3 In BMM, FcRn enhances both endocytosed OVA-IC and phagocytosed Latex-OVA-IC to MHC class II. **I**ncubation of bone marrow derived macrophages for 1h at 37C in the presence of **A**, OVA, **B,** OVA-ICs , **C,** latex-OVA-IC, and then fixed for immunofluorescence, all of them were shown as green colors . IL-2 measurement by ELISA. BMMs were incubated for 12h in the presence of **D,** soluble OVA, **E,** OVA-ICs (mono), and **F,** Latex-OVA-ICs at the indicated dosage. After washing with PBS, WT BMDCs (**solid line**) and FcRn-/-(**dashed line**) were incubated with OT-II CD4+ T cells for another 24h. Supernatants from different samples were collected for IL-2 measurement. Data are the mean ± SD from experiment performed in triplicate.

FcRn does not affect the cross-antigen presentation by MHC class I.

The IC internalization through FcγRs in DC promotes both MHC class II and MHC class I restricted-antigen presentation (174, 196). We further addressed whether the FcRn-deficiency affected antigen cross-presentation in BMDC and BMM. CD8+ T cell hybridoma (B3Z) (187) were used to study presentation of exogenous OVA-ICs. This hybridoma recognizes the OVA 257-264 peptide presented by MHC class I (H-2K^b). When incubated with high concentration of OVA or low concentration of latex-OVA-ICs, WT and FcRn-/- BMDC efficiently activated B3Z cells (Fig. 4.4 A and C). WT and FcRn-/- BMDCs that were incubated with mAb-derived OVA-ICs, failed to activate of B3Z T cells (Fig. 4.4 B).

As shown previously (197), MΦ was able to present the exogenous OVA on MHC class I molecules and to initiate the CTL response. However, the ICs did not enhance this process (198). To determine whether FcRn affects the cross-antigen presentation in MΦ, B3Z T cells were primed with BMM. There was no contribution of FcγRs to BMM on the OVA-ICs cross-presentation as previously discussed (198), and the absent expression of FcRn in MΦ did not affect activation of B3Z (Fig. 4.4 D, E, and F). To confirm these results, all the assays on B3Z cells were repeated on OT-I T cells, the data were consistent with results from B3Z T cells. Therefore, we conclude that FcRn is not involved in the antigen cross-presentation in either DC or MΦ.

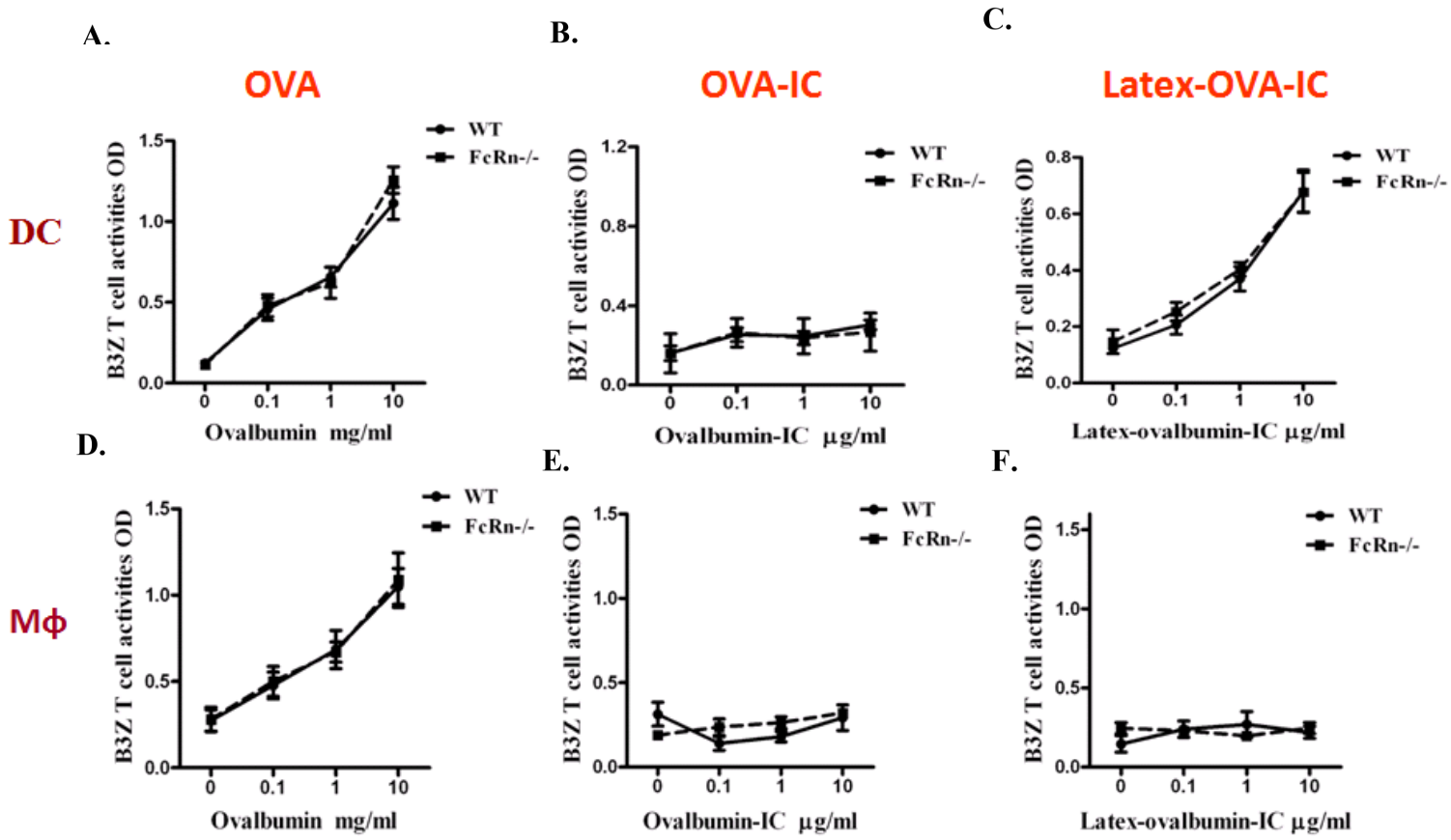

Figure 4.4 MHC class I-restricted antigen presentation is not affected by FcRn deficiency

In 96-well plate, $1X10^5$ cells/well C57BL/6 BMDCs (**A-C**) or BMMs (**D-F**) were cultured with LPS (200 ng/ml) for 12 h and increasing concentrations of soluble **OVA** (**A, D**), **OVA-ICs** (**B, E**) and **Latex-OVA-ICs** (**C, F**), washed, and incubated for an additional 18 h with B3Z ($2X10^5$/well). Medium was removed and washed softly with PBS, and then the WT (**solid line**) and FcRn-/- (**dashed line**) cells were exposed to substrate ONPG (10 µg/ml) combined with 0.5% Triton-X 100 in PBS. T cell activation was measured using a colorimetric assay at wavelength of 450 nm. Data are the mean ± SD from experiment performed in triplicate.

The phagosomal pH is different between BMM and BMDC; FcRn can stabilize the internalized ICs in the acidic compartments.

It was demonstrated that the phagosomal localizations of FcRn had distinctive effects on antigen presentations between DC and MΦ. We reasoned that the discrepancy might be related to phagosomal pH in DC and MΦ, based on the feature of FcRn binding to IgG at acidic pH.

To measure the phagosomal pH value in both MΦ and DC, we selected the pH sensor, soluble dextran-linked LysoSensor Blue/Yellow. This probe exhibits pH-dependent dual-emission spectra. At acidic condition, the probe emits at the wavelength of 530 nm maximally, whereas at neutral pH, the emission fluorescence at 450 nm is stronger (188). Thus, the pH value is equally translated to the ratio of fluorescence at 530 (Green) to 450 (Blue). After exposing the LysoSensor (1mg/ml) coupled latex-beads to BMM or BMDC for 5 hours, phagosomal pH values were measured. We found that the Green/Blue ratio obtained from phagosomes in BMM was 1.7 (Fig. 4.5 C). In contrast, phagosomes in BMDC displayed a Green/Blue ratio of 1.1 (Fig. 4.5 B). Using a pH standard curve (Fig. 4.5 A), we concluded that the phagosomal pH in MΦ was below 5.0, whereas phagosomal pH in DC was over 7.0.

We next asked how FcRn in BMDCs and BMMs regulated the presentation of IgG-restricted antigens. Because the antigen digestion rate correlates with the magnitude of antigen presentation, it is highly possible that FcRn protects uptaken antigen from rapid degradation through its binding with antigen, consequently,

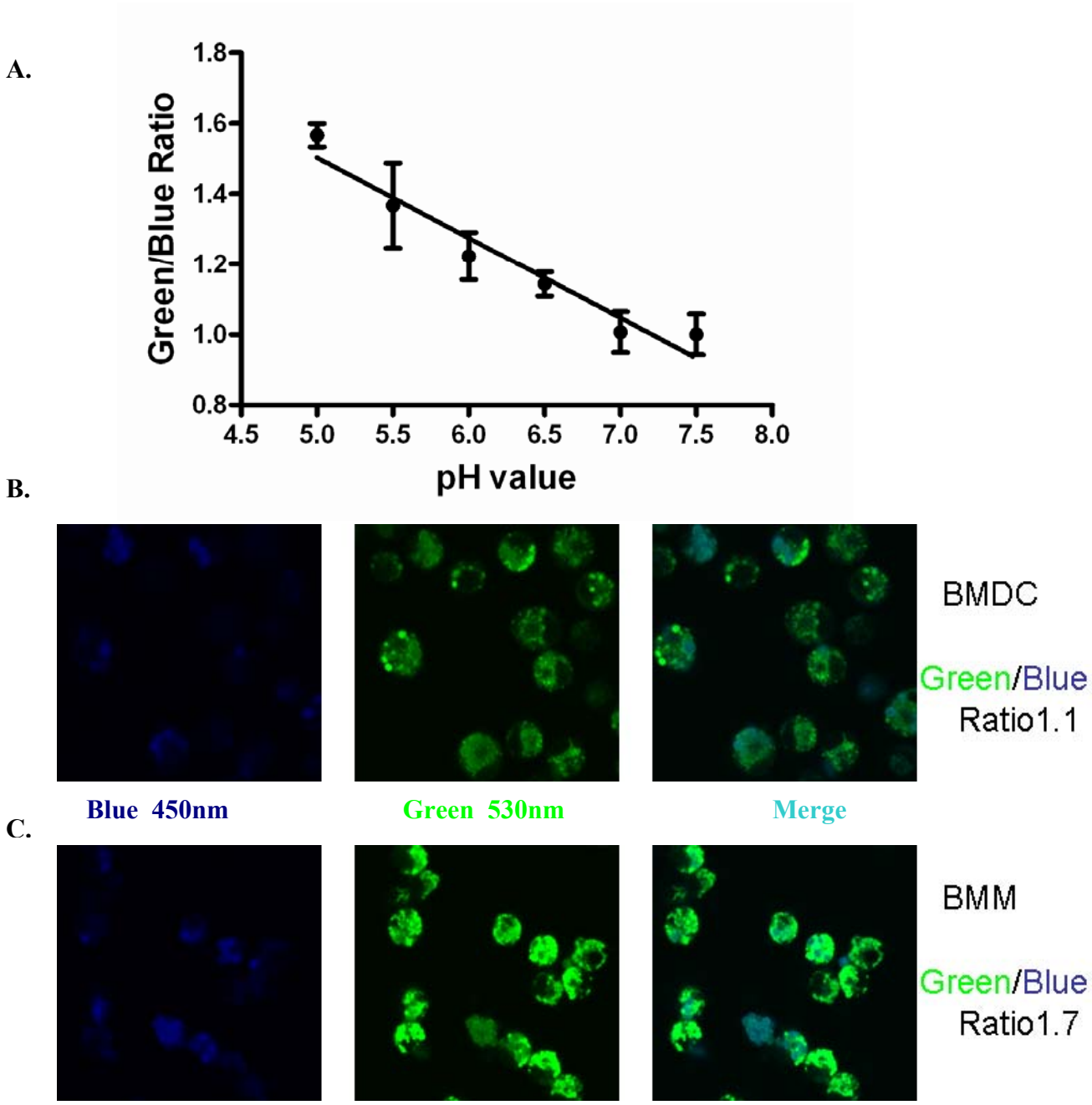

Figure 4.5 BMDC bears a phagosomal alkalinization, while phagosomes in BMM is acidic. BMDC (B), BMMs (C). A. Standard calibration curve for LysoSensor Blue/Yellow pH indicator. Day 9-BMDCs were incubated for 5h with Lysosensor Blue/Yellow (1mg/ml)-coupled latex beads (3μm) at 37°C, and equilibrated with MES buffers (pH value from 5.0 to 7.5) containing nigericin and monensin. Emissions at 450 nm and 530 nm from phagosomal beads were measured with confocal microscopy at exitation 405nm. The ratio of 530/450 nm fluorescence (Green/Blue) is measured as described in Materials and Methods. **B.** BMDCs were incubated with Lysosensor-coupled latex beads for 5h at 37°C, Emission at 450 nm was shown blue (*Left*); emission at 530 nm was displayed green (*Middle*); and the merged photo is on the right. The ratio of Green/Blue was calculated and shown on the right **C.** BMMs were exposed with Lysosensor-coupled latex beads for 5h, and the emissions were shown orderly as BMDC.

promotes the efficient epitopes loading onto the MHC class II molecules. To monitor the fates of internalized antigens in forms of ICs, Latex-beads-ICs or antigen alone in DC. We treated WT or FcRn-/- BMDCs with HRP, HRP-ICs and HRP-Beads-ICs separately for 3h, washed cells, and then chased HRP activities at indicated time points. After extensive washes with PBS (pH 5.0), the cells were lysated and applied for spectrophotometer measurement in TMB substrate at wavelength of 450 nm. The remaining activities of HRP were measured and recorded (Fig. 4.6). When BMDC was loaded with HRP-IC, the remaining activities of HRP (red line) from WT BMDC (Fig. 4.6 A) decreased slower than that from FcRn -/- BMDC (Fig. 4.6 B). When BMDC were loaded with HRP-beads-ICs or soluble HRP, the degradation rates (Blue line or Black line) in WT BMDC were similar to that in FcRn-/- BMDC (Fig. 4.6 A, B). In contrast, the degradation rates of HRP-ICs and HRP-Beads-ICs in WT BMM were much slower than that of FcRn-/- BMM (Fig. 4.6 C, D). Therefore, it is concluded that FcRn could stabablize the immune complex in acidic phagosomes in MΦ.

FcRn enhances the ICs antigen presentation ex vivo.

To further evaluate the contribution of FcRn mediated-antigen presentation in BMDC and BMM through MHC class II molecules ex vivo, we used an adoptive transfer system (175, 199). WT or FcRn-/- BMDC loaded with OVA, OVA-ICs or Latex-OVA-ICs were transferred to WT C57BL/6 mice. After 4 days, the draining lymph node (popliteal) was removed from these mice, and the CD4+ T cells were collected and stained with CFSE. T cells were restimulated with DC bearing peptides

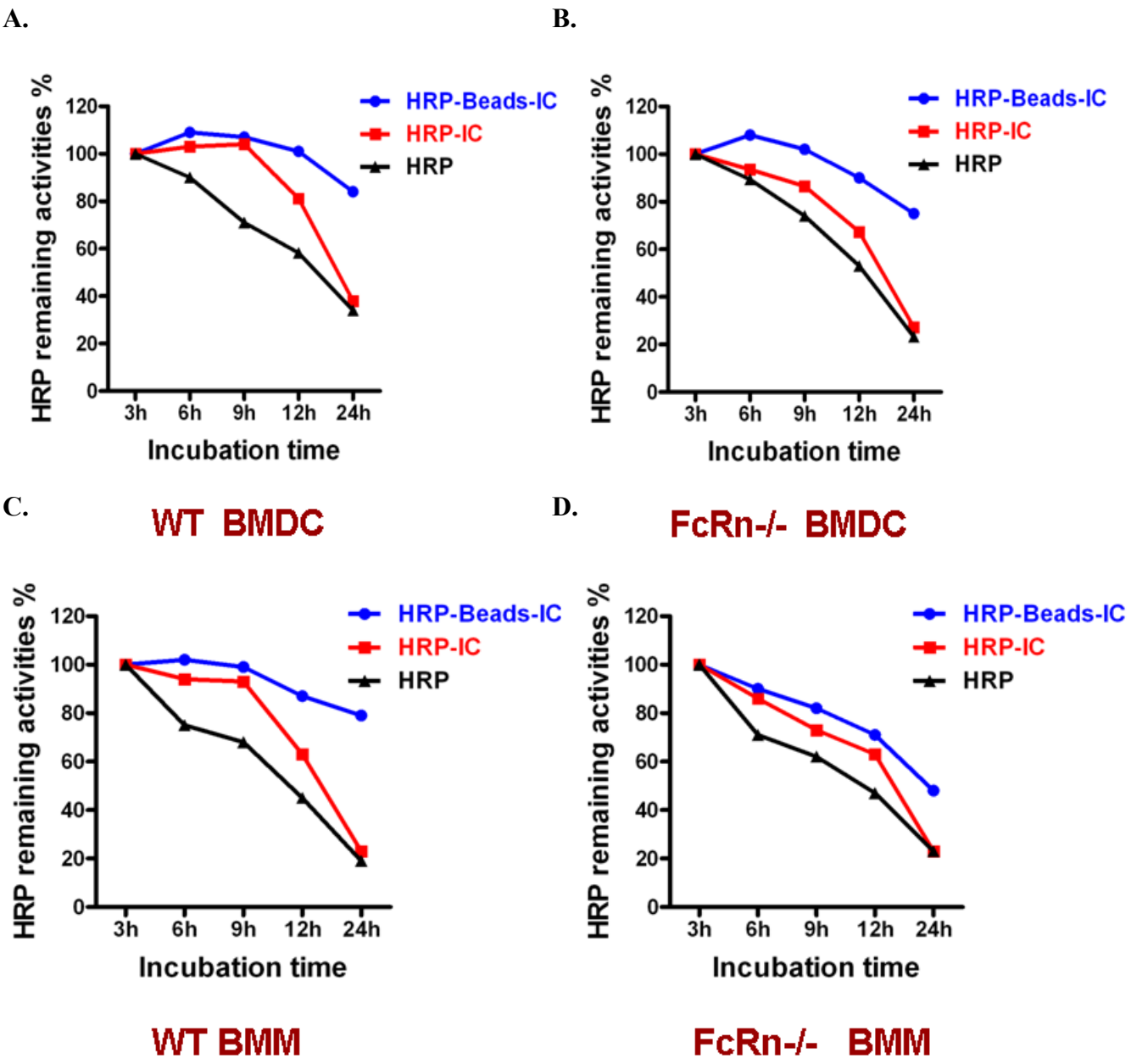

Figure 4.6 The dynamic degradation of HRP, HRP-IC, and HRP-Beads-IC in both macrophage and DC. WT BMDC **(A.)** and FcRn -/-BMDC **(B.)** was pulsed with HRP(▲), HRP-IC(■), and HRP-beads-IC(●) for 3 hours separately. After extensive washing, cells were incubated with fresh medium at 37°C for additional 3h, 6h, 9h, and 21h. The reaminning HRP activites were measured by exposing the cell lysis to TMB reagent, and subject to the cytometric quantification at 450nm. The readout of 3h-pulsed samples were assigned as 100%, and the values of chase samples were calculated in comparison with pulse samples. Following the same procedure, WT BMM **(C.)** and FcRn-/- **(D.)** were treated and measured as described above.

$OVA_{323-339}$. The T cells from animals immunized with IC-loaded WT BMDC proliferated better than in the mice immunized with ICs-loaded FcRn-/- BMDC (Fig. 4.7 A, *second panel from right*). In contrast, WT or FcRn-/- BMDCs loaded with Latex-OVA-ICs stimulated the CFSE-T cell proliferation to the similar extent (Fig. 4.8 A, *right panel*). These results are consistent with in vitro data. In addition, T cells stimulated by OVA-loaded BMDCs proliferated equally (Fig. 4.7 A, *second panel from left*)

To further assess whether the presence of FcRn in BMM affects the T cells activation ex vivo, WT or FcRn-/- BMM was pulsed with ICs or Latex-OVA-ICs for 4h, and then s.c.injected these loaded BMM to the C57BL/6 mice. CD4+ T cells isolated from the draining lymph nodes were labeled with CFSE and restimulated with OVA323-339 peptide. The results showed that FcRn in BMMs loaded with ICs or Latex-OVA-ICs enhanced the T cell proliferation (Fig. 4.7 B), in spite of the instensity of T cell proliferation was less than that of BMDC stimulation. Collectively, these data show that the binding of FcRn with IgG-restricted antigens in acidic pH is critical to allow DCs and MΦ to present antigen and to activate naïve T cells response in vivo.

DISCUSSION

This study establishes a novel mechanism of the enhanced antigen presentation of IgG-complexed ICs that is distinct from other ways which go through augmenting

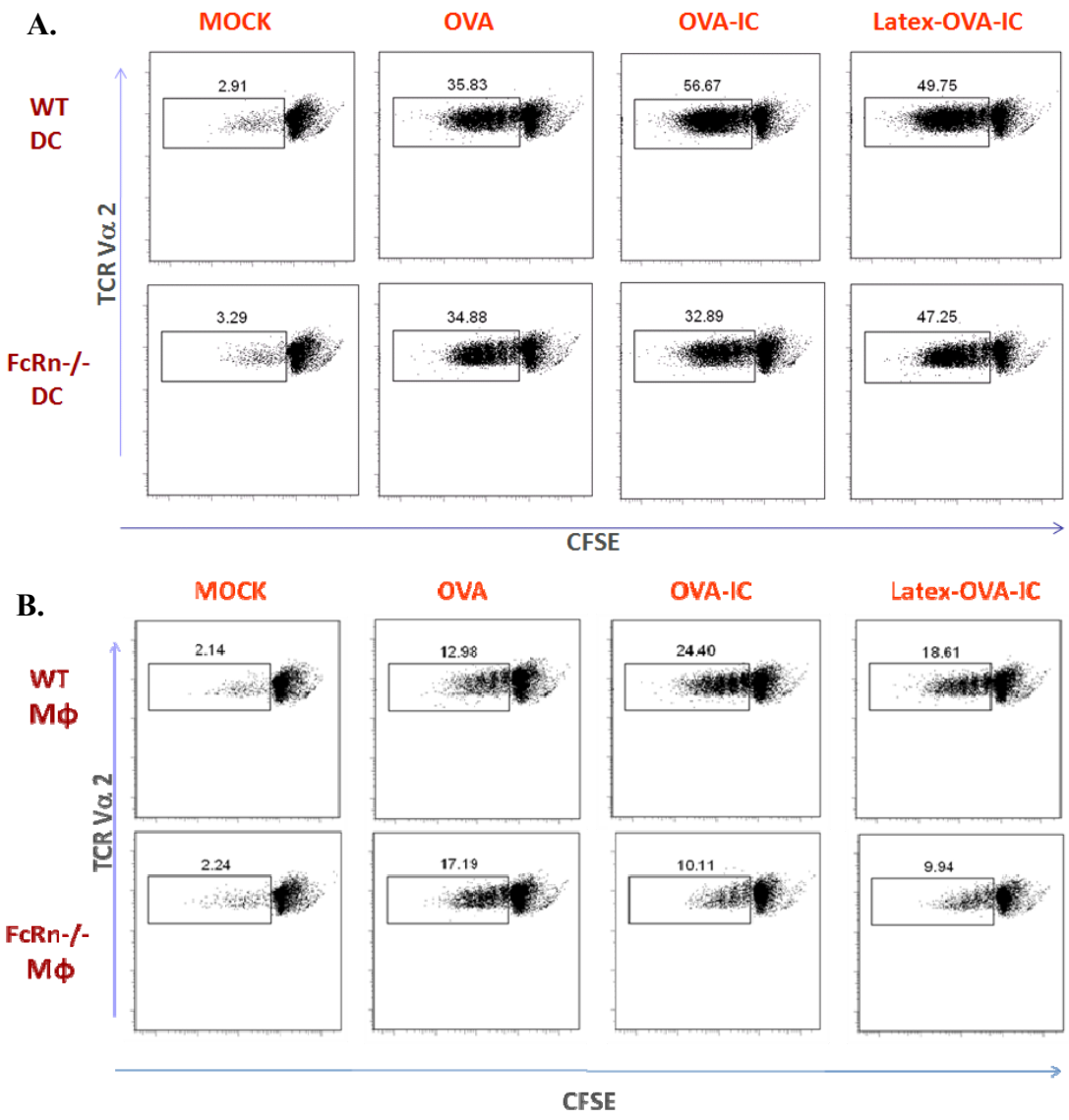

Figure 4.7 FcRn defective BMDC impairs the antigen presentation of endocytosed ICs to CD4+ T cell *ex vivo*, whereas FcRn defective BMM impair both endosomal and phagosomal antigen to CD4+ T cell . A. Day-9 BMDC (WT, *top panel* or FcRn KO *bottom panel*) was pulsed separately with OVA (*second left panel*), OVA-IC (*second right*), and Latex-OVA-IC (*right panel*) for 12 h at at 37°C, and then the antigen-loaded cells were washed with PBS for three times. Pretreated cells were injected s.c into syngenic C57BL/6. As control, non-antigen treated BMDC were injected. After four day, CD4+ T cells were isolated from different immunization and labeled with CFSE, the secondary anti-OVA proliferative responses were measured by repriming of CFSE-CD4+T cells with spleen DC bearing OVA specific peptide323-336. **B.** Day-7 BMM were treated with three forms of antigen and injected into C57BL/6 mice described as above. Two weeks later, CFSE-labelled CD4+ T cells proliferation were gated and measured.

antigen uptake and regulating maturation of APC cells. Our finding indicates that FcRn in endocytic compartments of DC and MΦ protects the ICs from rapid catabolism in lysosomes and leads to increasing efficiency of antigen processing and peptide loading onto the MHC class II molecules. These data extend upon the unique ability of FcRn binding to IgG by now demonstrating a new function of FcRn in DC and MΦ for antigen presentation, besides IgG protection and IgG transcytosis (57). We further demonstrated that FcRn in different endocytic compartments of DCs functioned differently during antigen presentation of IgG-ICs. It enhances antigen presentation of endocytosed ICs, but not phagocytosed ICs in DC. More interestingly, FcRn in MΦ boosts antigen presentation of ICs uptaken through both endocytosis and phagocytosis. Furthermore, this discrapancy is shown due to the different pH among endocytic organelles.

Phagosomes in DC and MΦ are considered as fully competent organelles for MHC class II and MHC class I antigen processing (175, 199). Efficient antigen processing in phagosomes requires the limited and controlled proteolysis of protein antigen. One of the most direct ways to control the activities of lysosomal proteases is the pH value adjustment. It has been shown in DC, that the recruitment of NADPH oxidase NOX2 to phagosomes mediates a sustained production of ROS, which consumes the proton in phagosomal lumen, causing the pH elevation to 7.4, even higher than the extracellular pH (180). This high pH in phagosomes provides DC with default control on proteases to digest the antigens properly. However, in MΦ, due to the low ROS production and high activity of V-ATPase, the phagosomes are acidified

very rapidly. This low pH facilitates FcRn binding with ICs and protect antigen from rapid degradation in MΦ. Regarding the endosomes/lysosomes, the pH in both MΦ and DC is acidic, which facilitates FcRn involving in the presentation of immume complexes antigen internalized through endosomes/lysosomes.

Although a variety of studies document the involvement of FcγRs in the receptor-mediated endocytosis (9), the mechanism of ICs internalization (endocytosis and phagocytosis) in DC and MΦ is still unclear. However, our results excluded the possibility that FcRn is required for ICs internalization. We demonstrated that the internalization of ICs in MΦ and DC was not affected by FcRn deficiency, this result is compatible with the fact that majority of FcRn is expressed in the endosomes/lysosomes of DC and MΦ (183, 184), and does not bind to IgG in neutral pH. Hence, ICs probably access to the endosomes or phagosomes through FcγRs-mediated endocytosis. In the endosomes, the FcγRs-ICs binding switches to FcRn-ICs binding. The binding of FcRn with ICs makes ICs less susceptible to protease digestion. This is demonstrated by the experiment that HRP alone is digested much easier in endosomes/lysosomes than HRP-IC (Fig. 4.6). Therefore it warrants more detailed studies on how the interaction of FcRn with ICs contributes to the stability of antigens.

In summary, the MHC class I-like molecule FcRn stabilizes the internalized ICs through the direct binding in acidic organelles, promotes the antigen presentation on MHC class II.

CHAPTER 5: CONCLUSION AND PERSPECTIVE

FcRn is an MHC class I-related Fc receptor for IgG. It binds IgG at acidic pH and releases IgG at neutral pH, which differs from other FcγRs. In addition to facilitating the transfer of maternal IgG to fetus or newborn, FcRn also acts as homeostatic receptor responsible for extending the serum half-life of IgG in adult. In IgG-related autoimmune diseases and infectious diseases, IgG plays a pivotal role for disease development and progression. As IgG level is correlated closely with the expression level of FcRn, understanding the function and regulation of FcRn will pave the road to better understand these diseases in another angle.

In this study (Chapter 2) (146), we have shown the rapid up-regulation of FcRn mRNA and FcRn protein in a human macrophage-like cell line, an intestinal epithelial cell line, and freshly isolated human monocytes after TNF-α or IL-1β treatment or in response to CpG or LPS. Stimulated FcRn mRNA levels were reduced in cells treated with the inhibitor of NF-κB p65 nuclear translocation (CAPE) or by overexpression of a dominantly negative IκBα. Three intronic NF-κB binding sites in human FcRn gene were identified by chromatin immunoprecipitation assays. A chromosome conformation capture assay demonstrated interactions between the NF-κB binding sequences and the FcRn promoter. Human IgG transcytosis on polarized human intestinal epithelial cells was also enhanced in both directions after exposure of the cells to TNF-α. Overall, these data indicate that FcRn expression in human cells stimulated by proinflammatory cytokines or TLR ligands is

regulated by NF-κB binding to three FcRn gene intronic regions.

However, several interesting questions still remain. First, how is FcRn regulated in patients with antoimmune disease or infectious disease? What is the application of FcRn upregulation? Such as, autoimmune skin blistering diseases, pemphigus and pemphigo, are characterized by subepidermal blisters, inflammatory cell infiltration, and the linear deposition of IgG autoantibodies at the basement membrane zone of skin. It is very interesting to know whether FcRn upregulation is involved in pemphigoid initiation and progression. The study by Zhi Liu and Derry, C. Roopenian's groups have shown that FcRn deficiency ameliorates pemphigus (200), which provides a direct link between pemphigus and FcRn. Second, during inflammatory cytokines or TLR ligands stimulation, what transcription factors are involved in the formation of loops between introns and promoter besides NF-κB? In our study, chromosome confirmation capture (3C) assay indicates that there are potential loops formed between human FcRn intronic elements and promoter region after TNF-α stimulation. Because of limitation of 3C assay, several issues still need to be clarified, where is the exact locations of loops? How many loops are formed during the transcription? What other factors are involved in the NF-kB mediated gene upregulation? What are the modifications on the epigenetic level? Third, regarding the fact that human FcRn gene is different from mouse FcRn gene, the transgenic mouse model containg the whole human FcRn locus will be very useful; it will serve as valuable tool to understand the FcRn regulation in the context of autoimmune diseases and infectious diseases, and to provide additional thoughts on mechanisms of disease initation and progression.

Many studies have shown that IFN-γ can upregulate MHC class I genes (141). In the present study (Chapter 3) (194), we demonstrated that MHC class I-related FcRn was down-regulated by IFN-γ stimulation, and this down-regulation is dependent on Jak1-Stat1 signaling pathway. One Stat1 binding site was identified in the human FcRn promoter by ChIP assay. The mutation of Stat1 binding site blocked the IFN-γ-induced down-regulation of luciferase activities that were driven by FcRn promoter. Most frequently, dimeric Stat1 translocates into the nucleus and binds to the GAS sequence to activate gene expression. However, in the case of FcRn, activated Stat1 bound to FcRn GAS sequence and blocked FcRn transcription. Similarly, gene suppression by Stat1 was also observed on MMP-9 or the SR-A gene, even though there are no GAS elements on these genes, and Stat1 was demonstrated to play an indirect role through interacting with other transcription factors (156, 165). Thus, it is very interesting to exploit the mechanism how Stat1 switchs on and off genes expression. In our study, an important transcription factor, p300/CBP was found recruited and sequestered by Stat1, which might result in the inhibition of FcRn transcriptional initiation. Furthermore, this block can be rescued by the overexpression of p300. Exploitation of p300-Stat1 interaction merits further study with the goals of understanding Stat1-mediated gene regulation on epigenic level. More interestingly, the GAS element (TTCTTTGAA) on human FcRn has stronger binding affinity with Stat4 (153). Also, we found that IFN-α/β can upregulate FcRn expression through non-IRES element, which coincide with the demonstration that Stat4 can be activiated by IFN-α/β directly (201-204). So, how type I interferon-inducible-Stat4 antagonizes Stat1 in FcRn regulation remains an interesting question.

Under normal development, the significant decrease of murine FcRn was found in the intestine tracts after the weaning (57). Exploitation of FcRn regulation holds promises for unveiling the finely tuned network of transcriptional factors and the full function of FcRn in the mucosal organs.

The involvement of FcRn in antigen presentation was recently discovered by Dr.Blumberg's group (76). In our study (Chapter 4), we described that FcRn in DC and MΦ can stabilize the input IgG-derived immune complexes in the acidic condition, slow down the antigen processing, and then promote the efficient peptide loading onto MHC class II molecules. In DC, the nearly neutral pH in phagosome fails FcRn to interact with uptaken immune complexes (IC -coupled beads), which results in non-effect on antigen presentation. However, in MΦ, the acidic pH in phagosomes facilitates the physical contact between FcRn and immune complexes, which enhances the efficient antigen processing and antigen presentation both in vitro and ex vivo. Therefore, the pH value in the specific organelle is the key to determine whether FcRn is able to involve in the antigen presentation of uptaken immune complexes. However, how FcRn plays its role to protect complexed-antigen from rapid proteolysis remains still a question. Since proteolysis is necessary for antigen presentation, it is interesting to determine how FcRn balances the antigen digestion and protection to efficiently produce antigenic epitope from an immune complex. These findings will provide basis and starting point for subunit vaccine engineering.

The trafficking of FcRn in epithelium has been well demonstrated (205, 206).

How FcRn is distributed in DC and MΦ remains elusive. Particularly, the expression of invariant chain in APC changes FcRn distribution (184). FcRn in turn is more prone to be delivered to the late endosome/lysosome in APC cells. In our study, we have also shown that FcRn traffics to the phagosome in APCs. Both late endosomes and phagosomes are competent organelles for antigen presentation. Therefore, understanding the traffic pattern of FcRn in APCs will further shed light on the mechanism of FcRn in antigen presentation.

It has been shown that the distribution pattern and fate of monovalent of IgG inside DC and MΦ are different from that of multivalent antigen-antibody complexes (207). Monovalent IgGs are easily recycled, whereas, multivalent antigen-antibody complexes are destinated for the degradation (207, 208). Inconsistently, immune complexes can also be recycled in DC to better activate B cells (75). So, the question of how FcRn cooperates with other FcγRs to mediate immune complex trafficking will provide insightful concept to solve the discrepancy. The role of FcRn in immune complex trafficking could also explain FcRn-mediated antigen presentation.

FcRn, the pH-dependent Fc receptor begins to be fully recognized on its functional importance. In addition of its critical role of IgG transport and homeostasis, FcRn is involved in the antigen presentation of IgG-restricted immue complexes from our study. The exploitation of FcRn will be a great benefit for better therapeutics and better vaccines.

REFERENCES LIST

1. William E., M.D.P.E. 2003.

2. Whitby, F.G., E.I. Masters, L. Kramer, J.R. Knowlton, and Y. Yao. 2000. Structural basis for the activation of 20S proteasomes by 11S regulators. *Nature* 408:115.

3. Brink, R., C.C. Goodnow, J. Crosbie, E. Adams, J. Eris, D.Y. Mason, S.B. Hartley, and A. Basten. 1992. Immunoglobulin M and D antigen receptors are both capable of mediating B lymphocyte activation, deletion, or anergy after interaction with specific antigen. *J. Exp. Med.* 176:991-1005.

4. Kett, K., P. Brandtzaeg, J. Radl, and J.J. Haaijman. 1986. Different subclass distribution of IgA-producing cells in human lymphoid organs and various secretory tissues. *J Immunol* 136:3631-3635.

5. Papadea, C., and I.J. Check. 1989. Human Immunoglobulin G and Immunoglobulin G Subclasses: Biochemical, Genetic, and Clinical Aspects. *Critical Reviews in Clinical Laboratory Sciences* 27:27-58.

6. Lal, R.B., I.M. Heiba, R.R. Dhawan, E.S. Smith, and P.L. Perine. 1991. IgG subclass responses to human immunodeficiency virus-1 antigens: Lack of IgG2 response to gp41 correlates with clinical manifestation of disease. *Clinical Immunology and Immunopathology* 58:267-277.

7. Perlmutter, R.M., D. Hansburg, D.E. Briles, R.A. Nicolotti, and J.M. David. 1978. Subclass Restriction of Murine Anti-Carbohydrate Antibodies. *J Immunol* 121:566-572.

8. Coutelier, J.P., J.T. van der Logt, F.W. Heessen, G. Warnier, and J. Van Snick. 1987. IgG2a restriction of murine antibodies elicited by viral infections. *J. Exp. Med.* 165:64-69.

9. Ravetch, J.V., and S. Bolland. 2001. IGG FC RECEPTORS. *Annual Review of Immunology* 19:275-290.

10. Nimmerjahn, F., P. Bruhns, K. Horiuchi, and J.V. Ravetch. 2005. Fc³RIV: A Novel FcR with Distinct IgG Subclass Specificity. 23:41-51.

11. Daeron, M. 1997. Fc RECEPTOR BIOLOGY. *Annual Review of Immunology* 15:203-234.

12. Kacskovics, I. 2004. Fc receptors in livestock species. *Veterinary Immunology and Immunopathology* 102:351-362.

13. Clynes, R., and J.V. Ravetch. 1995. Cytotoxic antibodies trigger inflammation through Fc receptors. *Immunity* 3:21-26.

14. Park, S.Y., S. Ueda, H. Ohno, Y. Hamano, M. Tanaka, T. Shiratori, T. Yamazaki, H. Arase, N. Arase, A. Karasawa, S. Sato, B. Ledermann, Y. Kondo, K. Okumura, C. Ra, and T. Saito. 1998. Resistance of Fc Receptor-deficient Mice to Fatal Glomerulonephritis. *J. Clin. Invest.* 102:1229-1238.

15. Watanabe, N., B. Akikusa, S.Y. Park, H. Ohno, L. Fossati, G. Vecchietti, J.E. Gessner, R.E. Schmidt, J.S. Verbeek, B. Ryffel, I. Iwamoto, S. Izui, and T. Saito. 1999. Mast Cells Induce Autoantibody-Mediated Vasculitis Syndrome Through Tumor Necrosis Factor Production Upon Triggering Fcgamma Receptors. *Blood* 94:3855-3863.

16. Anderson, C.F., and D.M. Mosser. 2002. Cutting Edge: Biasing Immune Responses by Directing Antigen to Macrophage Fc{gamma} Receptors. *J Immunol* 168:3697-3701.

17. Bheekha Escura R, W.E., Hammerschmid F, Pearce A, Kidd P, Mudde GC. 1995 Regulation and targeting of T-cell immune responses by IgE and IgG antibodies. *Immunology* 86(3):343-350.

18. Fanger, N.A., D. Voigtlaender, C. Liu, S. Swink, K. Wardwell, J. Fisher, R.F. Graziano, L.C. Pfefferkorn, and P.M. Guyre. 1997. Characterization of expression, cytokine regulation, and effector function of the high affinity IgG receptor Fc gamma RI (CD64) expressed on human blood dendritic cells. *J Immunol* 158:3090-3098.

19. Heijnen, I.A.F.M., M.J.v. Vugt, N.A. Fanger, R.F. Graziano, T.P.M.d. Wit, F.M.A. Hofhuis, P.M. Guyre, P.J.A. Capel, J.S. Verbeek, and J.G.J.v.d. Winkel. 1996. Antigen Targeting to Myeloid-specific Human Fcgamma RI/CD64 Triggers Enhanced Antibody Responses in Transgenic Mice. *J. Clin. Invest.* 97:331-338.

20. Watts, C., and A. Lanzavecchia. 1993. Suppressive effect of antibody on processing of T cell epitopes. *J. Exp. Med.* 178:1459-1463.

21. Barnes, N., A.L. Gavin, P.S. Tan, P. Mottram, F. Koentgen, and P.M. Hogarth. 2002. Fc[gamma]RI-Deficient Mice Show Multiple Alterations to Inflammatory and Immune Responses. *Immunity* 16:379-389.

22. Barrionuevo, P., M. Beigier-Bompadre, G.C. Fernandez, S. Gomez, M.F. Alves-Rosa, M.S. Palermo, and M.A. Isturiz. 2003. Immune complex-FcgammaR interaction modulates monocyte/macrophage molecules involved in inflammation and immune response. *Clinical and Experimental Immunology* 133:200-207.

23. Dai, Y., K.A. Carayanniotis, P. Eliades, P. Lymberi, P. Shepherd, Y.-c.M. Kong, and G. Carayanniotis. 1999. Enhancing or Suppressive Effects of Antibodies on Processing of a Pathogenic T Cell Epitope in Thyroglobulin. *J Immunol* 162:6987-6992.

24. Inaba, K., and R.M. Steinman. 1986. Accessory cell-T lymphocyte interactions. Antigen-dependent and -independent clustering. *J. Exp. Med.* 163:247.

25. Samuelsson, A., T.L. Towers, and J.V. Ravetch. 2001. Anti-inflammatory Activity of IVIG Mediated Through the Inhibitory Fc Receptor. *Science* 291:484-486.

26. Simister, N.E., and K.E. Mostov. 1989. An Fc receptor structurally related to MHC class I antigens. *Nature* 337:184-187.

27. Ghetie, V., and E.S. Ward. 2000. Multiple Roles for the Major Histocompatibility Complex Class I-Related Receptor FcRn. *Annual Review of Immunology* 18:739-766.

28. Burmeister, W.P., L.N. Gastinel, N.E. Simister, M.L. Blum, and P.J. Bjorkman. 1994. Crystal structure at 2.2 A resolution of the MHC-related neonatal Fc receptor. *Nature* 372:336-343.

29. Plaksin, D., K. Polakova, M.G. Mage, and D.H. Margulies. 1997. Rigidification of the alpha(2) helix of an MHC class I molecule by a valine to proline mutation in position 165 does not prevent peptide-specific antigen presentation. *Journal of Immunology* 159:4408-4414.

30. Plaksin, D., K. Polakova, M.G. Mage, and D.H. Margulies. 1997. Rigidification of the alpha2 helix of an MHC class I molecule by a valine to proline mutation in position 165 does not prevent peptide- specific antigen presentation. *J Immunol* 159:4408-4414.

31. Relloso, M., T.-Y. Cheng, J.S. Im, E. Parisini, C. Roura-Mir, C. DeBono, D.M. Zajonc, L.F. Murga, M.J. Ondrechen, I.A. Wilson, S.A. Porcelli, and D.B. Moody. 2008. pH-Dependent Interdomain Tethers of CD1b Regulate Its Antigen Capture. 28:774-786.

32. Ahouse, J.J., C.L. Hagerman, P. Mittal, D.J. Gilbert, N.G. Copeland, N.A. Jenkins, and N.E. Simister. 1993. Mouse MHC class I-like Fc receptor encoded outside the MHC. *J Immunol* 151:6076-6088.

33. Story, C.M., J.E. Mikulska, and N.E. Simister. 1994. A major histocompatibility complex class I-like Fc receptor cloned from human placenta: possible role in transfer of immunoglobulin G from mother to fetus. *J. Exp. Med.* 180:2377-2381.

34. Neil E. Simister, C.M.S.H.-L.C.J.S.H. 1996. An IgG-transporting Fc receptor expressed in the syncytiotrophoblast of human placenta. *European Journal of Immunology* 26:1527-1531.

35. Einar K. Kristoffersen, R.M. 1996. Co-localization of the neonatal Fcgamma receptor and IgG in human placental term syncytiotrophoblasts. *European Journal of Immunology* 26:1668-1671.

36. Leach, J.L., D.D. Sedmak, J.M. Osborne, B. Rahill, M.D. Lairmore, and C.L. Anderson. 1996. Isolation from human placenta of the IgG transporter, FcRn, and localization to the syncytiotrophoblast: implications for maternal- fetal antibody transport. *J Immunol* 157:3317-3322.

37. Kristoffersen, E.K. 1996. Human placental Fc [gamma]-binding proteins in the maternofetal transfer of IgG. *APMIS Suppl.* 64:5-36.

38. Jin-Kyoo Kim, M.F.C.G.R.C.-H.K.V.G.E.S.W. 1999. Mapping the site on human IgG for binding of the MHC class I-related receptor, FcRn. *European Journal of Immunology* 29:2819-2825.

39. Raghavan, M., V.R. Bonagura, S.L. Morrison, and P.J. Bjorkman. 1995. Analysis of the pH Dependence of the Neonatal Fc Receptor/Immunoglobulin G Interaction Using Antibody and Receptor Variants. *Biochemistry* 34:14649-14657.

40. Medesan, C., D. Matesoi, C. Radu, V. Ghetie, and E.S. Ward. 1997. Delineation of the amino acid residues involved in transcytosis and catabolism of mouse IgG1. *J Immunol* 158:2211-2217.

41. Raghavan, M., V.R. Bonagura, S.L. Morrison, and P.J. Bjorkman. 1995. Analysis of the pH dependence of the neonatal Fc receptor/immunoglobulin G interaction using antibody and receptor variants. *Biochemistry* 34:14649-14657.

42. Raghavan, M., M.Y. Chen, L.N. Gastinel, and P.J. Bjorkman. 1994. Investigation of the interaction between the class I MHC-related Fc receptor and its immunoglobulin G ligand. *Immunity* 1:303-315.

43. Vaughn, D.E., C.M. Milburn, D.M. Penny, W.L. Martin, J.L. Johnson, and P.J. Bjorkman. 1997. Identification of critical IgG binding epitopes on the neonatal Fc receptor. *Journal of Molecular Biology* 274:597-607.

44. Ahouse, J.J. 1993. Mouse MHC class I-like Fc receptor encoded outside the MHC. *J. Immunol.* 151:6076-6088.

45. Garcia, K.C., M. Degano, R.L. Stanfield, A. Brunmark, M.R. Jackson, P.A. Peterson, L. Teyton, and I.A. Wilson. 1996. An alpha beta T Cell Receptor Structure at 2.5 A and Its Orientation in the TCR-MHC Complex. *Science* 274:209-219.

46. Garboczi, D.N., P. Ghosh, U. Utz, Q.R. Fan, W.E. Biddison, and D.C. Wiley. 1996. Structure of the complex between human T-cell receptor, viral peptide and HLA-A2. *Nature* 384:134-141.

47. Burmeister, W.P., A.H. Huber, and P.J. Bjorkman. 1994. Crystal structure of the complex of rat neonatal Fc receptor with Fc. *Nature* 372:379-383.

48. Duncan, A.R., J.M. Woof, L.J. Partridge, D.R. Burton, and G. Winter. 1988. Localization of the binding site for the human high-affinity Fc receptor on IgG. *Nature* 332:563-564.

49. Canfield, S.M., and S.L. Morrison. 1991. The binding affinity of human IgG for its high affinity Fc receptor is determined by multiple amino acids in the CH2 domain and is modulated by the hinge region. *J. Exp. Med.* 173:1483-1491.

50. Lund, J., J.D. Pound, P.T. Jones, A.R. Duncan, T. Bentley, M. Goodall, B.A. Levine, R. Jefferis, and G. Winte. 1992. Multiple binding sites on the CH2 domain of IgG for mouse Fc[gamma]R11. *Molecular Immunology* 29:53-59.

51. Lund, J., G. Winter, P.T. Jones, J.D. Pound, T. Tanaka, M.R. Walker, P.J. Artymiuk, Y. Arata, D.R. Burton, R. Jefferis, and J.M. Woof. 1991. Human Fc gamma RI and Fc gamma RII interact with distinct but overlapping sites on human IgG. *J Immunol* 147:2657-2662.

52. Hogarth, P.M., L. Ierino Frank, and D. Hulett Mark. 1994. Characterization of FcR Ig-Binding Sites and Epitope Mapping. *ImmunoMethods* 4:17-24.

53. Tao, M.H., and S.L. Morrison. 1989. Studies of aglycosylated chimeric mouse-human IgG. Role of carbohydrate in the structure and effector functions mediated by the human IgG constant region. *J Immunol* 143:2595-2601.

54. Tsuchiya, N., T. Endo, K. Matsuta, S. Yoshinoya, T. Aikawa, E. Kosuge, F. Takeuchi, T. Miyamoto, and A. Kobata. 1989. Effects of Galactose Depletion from Oligosaccharide Chains on Immunological Activities of Human-Igg. *Journal of Rheumatology* 16:285-290.

55. Walker, M.R., J. Lund, K.M. Thompson, and R. Jefferis. 1989. Aglycosylation of Human Igg1 and Igg3 Monoclonal-Antibodies Can Eliminate Recognition by Human-Cells Expressing Fc-Gamma-Ri and or Fc-Gamma-Rii Receptors. *Biochemical Journal* 259:347-353.

56. Neil E. Simister, A.R.R. 1985. Isolation and characterization of an Fc receptor from neonatal rat small intestine. *European Journal of Immunology* 15:733-738.

57. Roopenian, D.C., and S. Akilesh. 2007. FcRn: the neonatal Fc receptor comes of age. *Nat Rev Immunol* 7:715-725.

58. Israel, E.J., V.K. Patel, S.F. Taylor, A. Marshak-Rothstein, and N.E. Simister. 1995. Requirement for a beta 2-microglobulin-associated Fc receptor for acquisition of maternal IgG by fetal and neonatal mice. *J Immunol* 154:6246-6251.

59. Roberts, D.M., M. Guenthert, and R. Rodewald. 1990. Isolation and characterization of the Fc receptor from the fetal yolk sac of the rat. *J. Cell Biol.* 111:1867-1876.

60. Shah, U., B.L. Dickinson, R.S. Blumberg, N.E. Simister, W.I. Lencer, and W.A. Walker. 2003. Distribution of the IgG Fc receptor, FcRn, in the human fetal intestine. *Pediatr. Res.* 53:295-301.

61. Israel, E.J., S. Taylor, Z. Wu, E. Mizoguchi, R.S. Blumberg, A. Bhan, and N.E. Simister. 1997. Expression of the neonatal Fc receptor, FcRn, on human intestinal epithelial cells. *Immunology* 92:69-74.

62. Ghetie, V., J.G. Hubbard, J.K. Kim, M.F. Tsen, Y.F. Lee, and E.S. Ward. 1996. Abnormally short serum half-lives of IgG in beta 2-microglobulin-deficient mice. *European Journal of Immunology* 26:690-696.

63. Yoshida, M., A. Masuda, T.T. Kuo, K. Kobayashi, S.M. Claypool, T. Takagawa, H. Kutsumi, T. Azuma, W.I. Lencer, and R.S. Blumberg. 2006.

IgG transport across mucosal barriers by neonatal Fc receptor for IgG and mucosal immunity. *Springer Semin. Immunopathol.* 28:397-403.

64. Spiekermann, G.M., P.W. Finn, E.S. Ward, J. Dumont, B.L. Dickinson, R.S. Blumberg, and W.I. Lencer. 2002. Receptor-mediated immunoglobulin G transport across mucosal barriers in adult life: Functional expression of FcRn in the mammalian lung. *Journal of Experimental Medicine* 196:303-310.

65. Victor Ghetie, J.G.H.J.-K.K.M.-F.T.Y.L.E.S.W. 1996. Abnormally short serum half-lives of IgG in beta 2-microglobulin-deficient mice. *European Journal of Immunology* 26:690-696.

66. Ghetie, V., S. Popov, J. Borvak, C. Radu, D. Matesoi, C. Medesan, R.J. Ober, and E.S. Ward. 1997. Increasing the serum persistence of an IgG fragment by random mutagenesis. *Nat Biotech* 15:637-640.

67. Junghans, R.P., and C.L. Anderson. 1996. The protection receptor for IgG catabolism is the beta 2-microglobulin-containing neonatal intestinal transport receptor. *PNAS* 93:5512-5516.

68. Roopenian, D.C., G.J. Christianson, T.J. Sproule, A.C. Brown, S. Akilesh, N. Jung, S. Petkova, L. Avanessian, E.Y. Choi, D.J. Shaffer, P.A. Eden, and C.L. Anderson. 2003. The MHC Class I-Like IgG Receptor Controls Perinatal IgG Transport, IgG Homeostasis, and Fate of IgG-Fc-Coupled Drugs. *J Immunol* 170:3528-3533.

69. Brambell FWR, H.W., Morris IG. 1964. A theoretical mode of gammaglobulin catabolism. *Nature* 203:1352-1355.

70. Ward, E.S., J. Zhou, V. Ghetie, and R.J. Ober. 2003. Evidence to support the cellular mechanism involved in serum IgG homeostasis in humans. *Int. Immunol.* 15:187-195.

71. Borvak, J. 1998. Functional expression of the MHC class I-related receptor, FcRn, in endothelial cells of mice. *Int. Immunol.* 10:1289-1298.

72. Akilesh, S., G.J. Christianson, D.C. Roopenian, and A.S. Shaw. 2007. Neonatal FcR Expression in Bone Marrow-Derived Cells Functions to Protect Serum IgG from Catabolism. *J Immunol* 179:4580-4588.

73. Zhu, X. 2001. MHC class I-related neonatal Fc receptor for IgG is functionally expressed in monocytes, intestinal macrophages, and dendritic cells. *J. Immunol.* 166:3266-3276.

74. Montoyo, H.c.P.r., C. Vaccaro, M. Hafner, R.J. Ober, W. Mueller, and E.S. Ward. 2009. Conditional deletion of the MHC class I-related receptor FcRn reveals the sites of IgG homeostasis in mice. *Proceedings of the National Academy of Sciences* 106:2788-2793.

75. Bergtold, A., D.D. Desai, A. Gavhane, and R. Clynes. 2005. Cell Surface Recycling of Internalized Antigen Permits Dendritic Cell Priming of B Cells. *Immunity* 23:503-514.

76. Qiao, S.-W., K. Kobayashi, F.-E. Johansen, L.M. Sollid, J.T. Andersen, E. Milford, D.C. Roopenian, W.I. Lencer, and R.S. Blumberg. 2008. Dependence of antibody-mediated presentation of antigen on FcRn. *Proceedings of the National Academy of Sciences* 105:9337-9342.

77. Yu, Z., and V.A. Lennon. 1999. Mechanism of intravenous immune globulin therapy in antibody-mediated autoimmune diseases. *N. Engl. J. Med.* 340:227-228.

78. Getman, K.E., and J.P. Balthasar. 2005. Pharmacokinetic effects of 4C9, an anti-FcRn antibody, in rats: implications for the use of FcRn inhibitors for the treatment of humoral autoimmune and alloimmune conditions. *J. Pharm. Sci.* 94:718-729.

79. Liu, L. 2007. Amelioration of experimental autoimmune myasthenia gravis in rats by neonatal FcR blockade. *J. Immunol.* 178:5390-5398.

80. Vaccaro, C., J. Zhou, R.J. Ober, and E.S. Ward. 2005. Engineering the Fc region of immunoglobulin G to modulate in vivo antibody levels. *Nature Biotechnol.* 23:1283-1288.

81. Ghosh, S., M.J. May, and E.B. Kopp. 1998. NF-Îº B AND REL PROTEINS: Evolutionarily Conserved Mediators of Immune Responses. *Annual Review of Immunology* 16:225-260.

82. Verma, I.M., J.K. Stevenson, E.M. Schwarz, D. Van Antwerp, and S. Miyamoto. 1995. Rel/NF-kappa B/I kappa B family: intimate tales of association and dissociation. *Genes & Development* 9:2723-2735.

83. Li, Q., and I.M. Verma. 2002. NF-[kappa]B regulation in the immune system. *Nat Rev Immunol* 2:725-734.

84. Chen, L.-F., and W.C. Greene. 2004. Shaping the nuclear action of NF-[kappa]B. *Nat Rev Mol Cell Biol* 5:392-401.

85. Akira, S., K. Takeda, and T. Kaisho. 2001. Toll-like receptors: critical proteins linking innate and acquired immunity. *Nat Immunol* 2:675-680.

86. Kopp, E., R. Medzhitov, J. Carothers, C. Xiao, I. Douglas, C.A. Janeway, and S. Ghosh. 1999. ECSIT is an evolutionarily conserved intermediate in the Toll/IL-1 signal transduction pathway. *Genes & Development* 13:2059-2071.

87. Takeda, K., T. Kaisho, and S. Akira. 2003. TOLL-LIKE RECEPTORS. *Annual Review of Immunology* 21:335-376.

88. Kelliher, M.A., S. Grimm, Y. Ishida, F. Kuo, B.Z. Stanger, and P. Leder. 1998. The Death Domain Kinase RIP Mediates the TNF-Induced NF-ºB Signal. 8:297-303.

89. Yang, J., Y. Lin, Z. Guo, J. Cheng, J. Huang, L. Deng, W. Liao, Z. Chen, Z.-g. Liu, and B. Su. 2001. The essential role of MEKK3 in TNF-induced NF-[kappa]B activation. *Nat Immunol* 2:620-624.

90. Platanias, L.C. 2005. Mechanisms of type-I- and type-II-interferon-mediated signalling. *Nat Rev Immunol* 5:375-386.

91. Leonard, W.J., and J.J. O'Shea. 1998. JAKS AND STATS: Biological Implications*. *Annual Review of Immunology* 16:293.

92. Darnell, J.E., I.M. Kerr, and G.R. Stark. 1994. JAK-STAT PATHWAYS AND TRANSCRIPTIONAL ACTIVATION IN RESPONSE TO IFNS AND OTHER EXTRACELLULAR SIGNALING PROTEINS. *Science* 264:1415-1421.

93. Darnell, J.E. 1997. STATs and gene regulation. *Science* 277:1630-1635.

94. Wen, Z.L., Z. Zhong, and J.E. Darnell. 1995. MAXIMAL ACTIVATION OF TRANSCRIPTION BY STAT1 AND STAT3 REQUIRES BOTH TYROSINE AND SERINE PHOSPHORYLATION. *Cell* 82:241-250.

95. Wen, Z.L., and J.E. Darnell. 1997. Mapping of Stat3 serine phosphorylation to a single residue (727) and evidence that serine phosphorylation has no influence on DNA binding of Stat1 and Stat3. *Nucleic Acids Research* 25:2062-2067.

96. Shuai, K., and B. Liu. 2003. Regulation of JAK-STAT signalling in the immune system. *Nat Rev Immunol* 3:900-911.

97. Hebbes, T.R., A.W. Thorne, and C. Cranerobinson. 1988. A DIRECT LINK BETWEEN CORE HISTONE ACETYLATION AND

TRANSCRIPTIONALLY ACTIVE CHROMATIN. *Embo Journal* 7:1395-1402.

98. Cresswell, P., N. Bangia, T. Dick, and G. Diedrich. 1999. The nature of the MHC class I peptide loading complex. *Immunol. Rev.* 172:21-28.

99. Trombetta, E.S., and I. Mellman. 2005. CELL BIOLOGY OF ANTIGEN PROCESSING IN VITRO AND IN VIVO. *Annual Review of Immunology* 23:975-1028.

100. Trombetta, E.S., M. Ebersold, W. Garrett, M. Pypaert, and I. Mellman. 2003. Activation of lysosomal function during dendritic cell maturation. *Science* 299:1400-1403.

101. Mellman, I., and R.M. Steinman. 2001. Dendritic Cells: Specialized and Regulated Antigen Processing Machines. *Cell* 106:255-258.

102. Steinman, R.M., and J. Swanson. 1995. THE ENDOCYTIC ACTIVITY OF DENDRITIC CELLS. *Journal of Experimental Medicine* 182:283-288.

103. Chaudhury, C. 2003. The major histocompatibility complex-related Fc receptor for IgG (FcRn) binds albumin and prolongs its lifespan. *J. Exp. Med.* 197:315-322.

104. Brambell, F.W.R., W.A. Hemmings, and I.G. Morris. 1964. A Theoretical Model of [gamma]-Globulin Catabolism. *Nature* 203:1352-1355.

105. Roopenian, D.C. 2003. The MHC class I-like IgG receptor controls perinatal IgG transport, IgG homeostasis, and fate of IgG-Fc-coupled drugs. *J. Immunol.* 170:3528-3533.

106. Petkova, S.B., S. Akilesh, T.J. Sproule, G.J. Christianson, H. Al Khabbaz, A.C. Brown, L.G. Presta, Y.G. Meng, and D.C. Roopenian. 2006. Enhanced half-life of genetically engineered human IgG1 antibodies in a humanized FcRn mouse model: potential application in humorally mediated autoimmune disease. *Int. Immunol.* 18:1759-1769.

107. Akilesh, S. 2004. The MHC class I-like Fc receptor promotes humorally mediated autoimmune disease. *J. Clin. Invest.* 113:1328-1333.

108. Zhu, X., J. Peng, D. Chen, X. Liu, L. Ye, H. Iijima, K. Kadavil, W.I. Lencer, and R.S. Blumberg. 2005. Calnexin and ERp57 Facilitate the Assembly of the Neonatal Fc Receptor for IgG with {beta}2-Microglobulin in the Endoplasmic Reticulum. *J Immunol* 175:967-976.

109. DiDonato, J., F. Mercurio, C. Rosette, J. Wu-Li, H. Suyang, S. Ghosh, and M. Karin. 1996. Mapping of the inducible IkappaB phosphorylation sites that signal its ubiquitination and degradation. *Mol. Cell. Biol.* 16:1295-1304.

110. Karin, M., and Y. Ben-Neriah. 2000. Phosphorylation Meets Ubiquitination: The Control of NF-ÎºB Activity. *Annual Review of Immunology* 18:621-663.

111. Zhu, X., J. Peng, R. Raychowdhury, A. Nakajima, W. Lencer, and R. Blumberg. 2002. The heavy chain of neonatal Fc receptor for IgG is

sequestered in endoplasmic reticulum by forming oligomers in the absence of beta 2-microglobulin association. *Biochem J* 367:703-714

112. Dekker, J., K. Rippe, M. Dekker, and N. Kleckner. 2002. Capturing Chromosome Conformation. *Science* 295:1306-1311.

113. Eivazova, E.R., and T.M. Aune. 2004. Dynamic alterations in the conformation of the Ifng gene region during T helper cell differentiation. *Proceedings of the National Academy of Sciences of the United States of America* 101:251-256.

114. Schjerven, H., P. Brandtzaeg, and F.-E. Johansen. 2001. A Novel NF-{kappa}B/Rel Site in Intron 1 Cooperates with Proximal Promoter Elements to Mediate TNF-{alpha}-Induced Transcription of the Human Polymeric Ig Receptor. *J Immunol* 167:6412-6420.

115. Medzhitov, R. 2001. Toll-like receptors and innate immunity. *Nat Rev Immunol* 1:135-145.

116. Hmama, Z., D. Nandan, L. Sly, K.L. Knutson, P. Herrera-Velit, and N.E. Reiner. 1999. 1{alpha},25-Dihydroxyvitamin D3-induced Myeloid Cell Differentiation Is Regulated by a Vitamin D Receptor-Phosphatidylinositol 3-Kinase Signaling Complex. *J. Exp. Med.* 190:1583-1594.

117. Natarajan, K., S. Singh, T.R. Burke, D. Grunberger, and B.B. Aggarwal. 1996. Caffeic acid phenethyl ester is a potent and specific inhibitor of activation of nuclear transcription factor NF-kappa B. *Proceedings of the National Academy of Sciences of the United States of America* 93:9090-9095.

118. Guo, Z., G.H. Boekhoudt, and J.M. Boss. 2003. Role of the Intronic Enhancer in Tumor Necrosis Factor-mediated Induction of Manganous Superoxide Dismutase. *J. Biol. Chem.* 278:23570-23578.

119. Molinero, L.L., M.B. Fuertes, M.V. Girart, L. Fainboim, G.A. Rabinovich, M.A. Costas, and N.W. Zwirner. 2004. NF-{kappa}B Regulates Expression of the MHC Class I-Related Chain A Gene in Activated T Lymphocytes. *J Immunol* 173:5583-5590.

120. Kvale, D., D. Lovhaug, L.M. Sollid, and P. Brandtzaeg. 1988. Tumor necrosis factor-alpha up-regulates expression of secretory component, the epithelial receptor for polymeric Ig. *J Immunol* 140:3086-3089.

121. Covert, M.W., T.H. Leung, J.E. Gaston, and D. Baltimore. 2005. Achieving Stability of Lipopolysaccharide-Induced NF-{kappa}B Activation. *Science* 309:1854-1857.

122. Lee, J.Y., N.A. Kim, A. Sanford, and K.E. Sullivan. 2003. Histone acetylation and chromatin conformation are regulated separately at the TNF-{alpha} promoter in monocytes and macrophages. *J Leukoc Biol* 73:862-871.

123. Gobin, S.J.P., P. Biesta, and P.J. Van den Elsen. 2003. Regulation of human beta 2-microglobulin transactivation in hematopoietic cells. *Blood* 101:3058-3064.

124. Martone, R., G. Euskirchen, P. Bertone, S. Hartman, T.E. Royce, N.M. Luscombe, J.L. Rinn, F.K. Nelson, P. Miller, M. Gerstein, S. Weissman, and M. Snyder. 2003. Distribution of NF-ÎºB-binding sites across human chromosome 22. *Proceedings of the National Academy of Sciences of the United States of America* 100:12247-12252.

125. Ge, B., O. Li, P. Wilder, A. Rizzino, and T.W. McKeithan. 2003. NF-{kappa}B Regulates BCL3 Transcription in T Lymphocytes Through an Intronic Enhancer. *J Immunol* 171:4210-4218.

126. Leung, T.H., A. Hoffmann, and D. Baltimore. 2004. One Nucleotide in a ºB Site Can Determine Cofactor Specificity for NF-ºB Dimers. 118:453-464.

127. Ping, D., G. Boekhoudt, F. Zhang, A. Morris, S. Philipsen, S.T. Warren, and J.M. Boss. 2000. Sp1 Binding Is Critical for Promoter Assembly and Activation of the MCP-1 Gene by Tumor Necrosis Factor. *J. Biol. Chem.* 275:1708-1714.

128. Boekhoudt, G.H., Z. Guo, G.W. Beresford, and J.M. Boss. 2003. Communication Between NF-{kappa}B and Sp1 Controls Histone Acetylation Within the Proximal Promoter of the Monocyte Chemoattractant Protein 1 Gene. *J Immunol* 170:4139-4147.

129. Kunsch, C., R.K. Lang, C.A. Rosen, and M.F. Shannon. 1994. Synergistic transcriptional activation of the IL-8 gene by NF-kappa B p65 (RelA) and NF-IL-6. *J Immunol* 153:153-164.

130. Tomaras, G.D., D.A. Foster, C.M. Burrer, and S.M. Taffet. 1999. ETS transcription factors regulate an enhancer activity in the third intron of TNF-alpha. *J Leukoc Biol* 66:183-193.

131. Kandil, E., M. Noguchi, T. Ishibashi, and M. Kasahara. 1995. Structural and phylogenetic analysis of the MHC class I-like Fc receptor gene. *J Immunol* 154:5907-5918.

132. Jiang, L., J. Wang, R.S. Solorzano-Vargas, H.V. Tsai, E.M. Gutierrez, L.O. Ontiveros, P.R. Kiela, S.V. Wu, and M.G. Martin. 2004. Characterization of the rat intestinal Fc receptor (FcRn) promoter: transcriptional regulation of FcRn gene by the Sp family of transcription factors. *Am J Physiol Gastrointest Liver Physiol* 286:G922-931.

133. Svenungsson, E., G.Z. Fei, K. Jensen-Urstad, U. de Faire, A. Hamsten, and J. Frostegard. 2003. TNF-{alpha}: a link between hypertriglyceridaemia and inflammation in SLE patients with cardiovascular disease. *Lupus* 12:454-461.

134. Stark, G.R., I.M. Kerr, B.R.G. Williams, R.H. Silverman, and R.D. Schreiber. 1998. HOW CELLS RESPOND TO INTERFERONS. *Annual Review of Biochemistry* 67:227-264.

135. Eilers, A., D. Georgellis, B. Klose, C. Schindler, A. Ziemiecki, A.G. Harpur, A.F. Wilks, and T. Decker. 1995. Differentiation-regulated serine phosphorylation of STAT1 promotes GAF activation in macrophages. *Mol. Cell. Biol.* 15:3579-3586.

136. Wen, Z., Z. Zhong, and J.E. Darnell. 1995. Maximal activation of transcription by statl and stat3 requires both tyrosine and serine phosphorylation. *Cell* 82:241-250.

137. Varinou, L., K. Ramsauer, M. Karaghiosoff, T. Kolbe, K. Pfeffer, M. Müller, and T. Decker. 2003. Phosphorylation of the Stat1 Transactivation Domain Is Required for Full-Fledged IFN-[gamma]-Dependent Innate Immunity. *Immunity* 19:793-802.

138. Ramana, C.V., M.P. Gil, R.D. Schreiber, and G.R. Stark. 2002. Stat1-dependent and -independent pathways in IFN-[gamma]-dependent signaling. *Trends in Immunology* 23:96-101.

139. Gough, D.J., K. Sabapathy, E.Y.-N. Ko, H.A. Arthur, R.D. Schreiber, J.A. Trapani, C.J.P. Clarke, and R.W. Johnstone. 2007. A Novel c-Jun-dependent Signal Transduction Pathway Necessary for the Transcriptional Activation of Interferon {gamma} Response Genes. *J. Biol. Chem.* 282:938-946.

140. Colgan, S.P., V.M. Morales, J.L. Madara, J.E. Polischuk, S.P. Balk, and R.S. Blumberg. 1996. IFN-gamma modulates CD1d surface expression on intestinal epithelia. *Am J Physiol Cell Physiol* 271:C276-283.

141. Gobin, S.J.P., M.v. Zutphen, A.M. Woltman, and P.J.v.d. Elsen. 1999. Transactivation of Classical and Nonclassical HLA Class I Genes Through the IFN-Stimulated Response Element. *J Immunol* 163:1428-1434.

142. Yang, Y., W. Chu, D.E. Geraghty, and J.S. Hunt. 1996. Expression of HLA-G in human mononuclear phagocytes and selective induction by IFN-gamma. *J Immunol* 156:4224-4231.

143. Lefebvre, S., P. Moreau, V. Guiard, E.C. Ibrahim, F. Adrian-Cabestre, C. Menier, J. Dausset, E.D. Carosella, and P. Paul. 1999. Molecular mechanisms controlling constitutive and IFN-[gamma]-inducible HLA-G expression in various cell types. *Journal of Reproductive Immunology* 43:213-224.

144. Wainwright, S.D., P.A. Biro, and C.H. Holmes. 2000. HLA-F Is a Predominantly Empty, Intracellular, TAP-Associated MHC Class Ib Protein with a Restricted Expression Pattern. *J Immunol* 164:319-328.

145. Barrett, D.M., K.S. Gustafson, J. Wang, S.Z. Wang, and G.D. Ginder. 2004. A GATA Factor Mediates Cell Type-Restricted Induction of HLA-E Gene Transcription by Gamma Interferon. *Mol. Cell. Biol.* 24:6194-6204.

146. Liu, X., L. Ye, G.J. Christianson, J.-Q. Yang, D.C. Roopenian, and X. Zhu. 2007. NF-{kappa}B Signaling Regulates Functional Expression of the MHC Class I-Related Neonatal Fc Receptor for IgG via Intronic Binding Sequences. *J Immunol* 179:2999-3011.

147. Nguyen, V.T., and E.N. Benveniste. 2000. IL-4-Activated STAT-6 Inhibits IFN-{gamma}-Induced CD40 Gene Expression in Macrophages/Microglia. *J Immunol* 165:6235-6243.

148. Pongratz, G., J.W. McAlees, D.H. Conrad, R.S. Erbe, K.M. Haas, and V.M. Sanders. 2006. The Level of IgE Produced by a B Cell Is Regulated by Norepinephrine in a p38 MAPK- and CD23-Dependent Manner. *J Immunol* 177:2926-2938.

149. Dickinson, B.L., K. Badizadegan, Z. Wu, J.C. Ahouse, X. Zhu, N.E. Simister, R.S. Blumberg, and W.I. Lencer. 1999. Bidirectional FcRn-dependent IgG transport in a polarized human intestinal epithelial cell line. *J. Clin. Invest.* 104:903-911.

150. McCarthy, K.M., Y. Yoong, and N.E. Simister. 2000. Bidirectional transcytosis of IgG by the rat neonatal Fc receptor expressed in a rat kidney cell line: a system to study protein transport across epithelia. *J Cell Sci* 113:1277-1285.

151. Iozzo, R.V., and J.R. Hassell. 1989. Identification of the precursor protein for the heparan sulfate proteoglycan of human colon carcinoma cells and its post-translational modifications. *Archives of Biochemistry and Biophysics* 269:239-249.

152. Chin, Y.E., M. Kitagawa, K. Kuida, R.A. Flavell, and X.Y. Fu. 1997. Activation of the STAT signaling pathway can cause expression of caspase 1 and apoptosis. *Mol. Cell. Biol.* 17:5328-5337.

153. Ehret, G.B., P. Reichenbach, U. Schindler, C.M. Horvath, S. Fritz, M. Nabholz, and P. Bucher. 2001. DNA Binding Specificity of Different STAT Proteins. COMPARISON OF IN VITRO SPECIFICITY WITH NATURAL TARGET SITES. *J. Biol. Chem.* 276:6675-6688.

154. Chang, Y.-J., M.J. Holtzman, and C.-C. Chen. 2002. Interferon-gamma - induced Epithelial ICAM-1 Expression and Monocyte Adhesion. INVOLVEMENT OF PROTEIN KINASE C-DEPENDENT c-Src TYROSINE KINASE ACTIVATION PATHWAY. *J. Biol. Chem.* 277:7118-7126.

155. Loman, S., J. Radl, H.M. Jansen, T.A. Out, and R. Lutter. 1997. Vectorial transcytosis of dimeric IgA by the Calu-3 human lung epithelial cell line: upregulation by IFN-gamma. *Am J Physiol Lung Cell Mol Physiol* 272:L951-958.

156. Ma, Z., H. Qin, and E.N. Benveniste. 2001. Transcriptional Suppression of Matrix Metalloproteinase-9 Gene Expression by IFN-{gamma} and IFN-{beta}: Critical Role of STAT-1{alpha}. *J Immunol* 167:5150-5159.

157. Venkataraman, C., S. Leung, A. Salvekar, H. Mano, and U. Schindler. 1999. Repression of IL-4-Induced Gene Expression by IFN-{gamma} Requires Stat1 Activation. *J Immunol* 162:4053-4061.

158. Sharma, B., and R.V. Iozzo. 1998. Transcriptional Silencing of Perlecan Gene Expression by Interferon-gamma. *J. Biol. Chem.* 273:4642-4646.

159. Kominsky, S.L., A.C. Hobeika, F.A. Lake, B.A. Torres, and H.M. Johnson. 2000. Down-Regulation of neu/HER-2 by Interferon-{{gamma}} in Prostate Cancer Cells. *Cancer Res* 60:3904-3908.

160. Elser, B., M. Lohoff, S. Kock, M. Giaisi, S. Kirchhoff, P.H. Krammer, and M. Li-Weber. 2002. IFN-³ Represses IL-4 Expression via IRF-1 and IRF-2. 17:703-712.

161. Xu, Y., L. Wang, G. Buttice, P.K. Sengupta, and B.D. Smith. 2003. Interferon {gamma} Repression of Collagen (COL1A2) Transcription Is Mediated by the RFX5 Complex. *J. Biol. Chem.* 278:49134-49144.

162. Bui, J.D., L.N. Carayannopoulos, L.L. Lanier, W.M. Yokoyama, and R.D. Schreiber. 2006. IFN-Dependent Down-Regulation of the NKG2D Ligand H60 on Tumors. *J Immunol* 176:905-913.

163. Jeffrey B. VanDeusen,
Manisha H.S.B.B.Bradley W.B.Amy K.F.Gerard J.N.Brian M.M.A.J.D.Micha el A.C. 2006. STAT-1-mediated repression of monocyte interleukin-10 gene expression <I>in vivo</I>. *European Journal of Immunology* 36:623-630.

164. Kelchtermans, H., S. Struyf, B. De Klerck, T. Mitera, M. Alen, L. Geboes, M. Van Balen, C. Dillen, W. Put, C. Gysemans, A. Billiau, J. Van Damme, and P. Matthys. 2007. Protective role of IFN-{gamma} in collagen-induced arthritis conferred by inhibition of mycobacteria-induced granulocyte chemotactic protein-2 production. *J Leukoc Biol* 81:1044-1053.

165. Horvai, A.E., L. Xu, E. Korzus, G. Brard, D. Kalafus, T.-M. Mullen, D.W. Rose, M.G. Rosenfeld, and C.K. Glass. 1997. Nuclear integration of JAK/STAT and Ras/AP-1 signaling by CBPâ€‰andâ€‰p300. *Proceedings of the National Academy of Sciences of the United States of America* 94:1074-1079.

166. Ma, Z., M.J. Chang, R.C. Shah, and E.N. Benveniste. 2005. Interferon-{gamma}-activated STAT-1{alpha} suppresses MMP-9 gene transcription by sequestration of the coactivators CBP/p300. *J Leukoc Biol* 78:515-523.

167. Chatterjee-Kishore, M., F.v.d. Akker, and G.R. Stark. 2000. Association of STATs with relatives and friends. *Trends in Cell Biology* 10:106-111.

168. Nusinzon, I., and C.M. Horvath. 2003. Interferon-stimulated transcription and innate antiviral immunity require deacetylase activity and histone deacetylase 1. *Proceedings of the National Academy of Sciences of the United States of America* 100:14742-14747.

169. Zhu, X.-S., and J.P.Y. Ting. 2001. A 36-Amino-Acid Region of CIITA Is an Effective Inhibitor of CBP: Novel Mechanism of Gamma Interferon-Mediated

Suppression of Collagen {alpha}2(I) and Other Promoters. *Mol. Cell. Biol.* 21:7078-7088.

170. Higashi, K., Y. Inagaki, N. Suzuki, S. Mitsui, A. Mauviel, H. Kaneko, and I. Nakatsuka. 2003. Y-box-binding Protein YB-1 Mediates Transcriptional Repression of Human alpha 2(I) Collagen Gene Expression by Interferon-gamma. *J. Biol. Chem.* 278:5156-5162.

171. Piskurich, J.F., K.R. Youngman, K.M. Phillips, P.M. Hempen, M.H. Blanchard, J.A. France, and C.S. Kaetzel. 1997. Transcriptional regulation of the human polymeric immunoglobulin receptor gene by interferon-[gamma]. *Molecular Immunology* 34:75-91.

172. Park-Min, K.-H., N.V. Serbina, W. Yang, X. Ma, G. Krystal, B.G. Neel, S.L. Nutt, X. Hu, and L.B. Ivashkiv. 2007. Fc³RIII-Dependent Inhibition of Interferon-³ Responses Mediates Suppressive Effects of Intravenous Immune Globulin. 26:67-78.

173. Gustafson, K.S., and G.D. Ginder. 1996. Interferon-gamma Induction of the Human Leukocyte Antigen-E Gene Is Mediated through Binding of a Complex Containing STAT1alpha to a Distinct Interferon-gamma -responsive Element. *J. Biol. Chem.* 271:20035-20046.

174. Regnault, A., D. Lankar, V. Lacabanne, A. Rodriguez, C. Thery, M. Rescigno, T. Saito, S. Verbeek, C. Bonnerot, P. Ricciardi-Castagnoli, and S. Amigorena. 1999. Fcgamma Receptor-mediated Induction of Dendritic Cell Maturation

and Major Histocompatibility Complex Class I-restricted Antigen Presentation after Immune Complex Internalization. *J. Exp. Med.* 189:371-380.

175. Houde, M., S. Bertholet, E. Gagnon, S. Brunet, G. Goyette, A. Laplante, M.F. Princiotta, P. Thibault, D. Sacks, and M. Desjardins. 2003. Phagosomes are competent organelles for antigen cross-presentation. *Nature* 425:402-406.

176. Amigorena, S., J. Salamero, J. Davoust, W.H. Fridman, and C. Bonnerot. 1992. Tyrosine-containing motif that transduces cell activation signals also determines internalization and antigen presentation via type III receptors for IgG. *Nature* 358:337-341.

177. Yoshida, M., S.M. Claypool, J.S. Wagner, E. Mizoguchi, and A. Mizoguchi. 2004. Human neonatal Fc receptor mediates transport of IgG into luminal secretions for delivery of antigens to mucosal dendritic cells. *Immunity* 20:769.

178. Chaudhury, C., S. Mehnaz, J.M. Robinson, W.L. Hayton, D.K. Pearl, D.C. Roopenian, and C.L. Anderson. 2003. The Major Histocompatibility Complex-related Fc Receptor for IgG (FcRn) Binds Albumin and Prolongs Its Lifespan. *J. Exp. Med.* 197:315-322.

179. Trombetta, E.S., M. Ebersold, W. Garrett, M. Pypaert, and I. Mellman. 2003. Activation of lysosomal function during dendritic cell maturation. *Science* 299:1400.

180. Savina, A., C. Jancic, S. Hugues, P. Guermonprez, P. Vargas, I.C. Moura, A.-M. Lennon-Duménil, M.C. Seabra, G. Raposo, and S. Amigorena. 2006. NOX2 Controls Phagosomal pH to Regulate Antigen Processing during Crosspresentation by Dendritic Cells. *Cell* 126:205-218.

181. Hackam, D.J., O.D. Rotstein, W. Zhang, S. Gruenheid, P. Gros, and S. Grinstein. 1998. Host resistance to intracellular infection: Mutation of natural resistance-associated macrophage protein 1 (Nramp1) impairs phagosomal acidification. *J. Exp. Med.* 188:351.

182. Yates, R.M., and D.G. Russell. 2005. Phagosome Maturation Proceeds Independently of Stimulation of Toll-like Receptors 2 and 4. *Immunity* 23:409-417.

183. Zhu, X., G. Meng, B.L. Dickinson, X. Li, E. Mizoguchi, L. Miao, Y. Wang, C. Robert, B. Wu, P.D. Smith, W.I. Lencer, and R.S. Blumberg. 2001. MHC Class I-Related Neonatal Fc Receptor for IgG Is Functionally Expressed in Monocytes, Intestinal Macrophages, and Dendritic Cells. *J Immunol* 166:3266-3276.

184. Ye, L., X. Liu, S.N. Rout, Z. Li, Y. Yan, L. Lu, T. Kamala, N.K. Nanda, W. Song, S.K. Samal, and X. Zhu. 2008. The MHC Class II-Associated Invariant Chain Interacts with the Neonatal Fc{gamma} Receptor and Modulates Its Trafficking to Endosomal/Lysosomal Compartments. *J Immunol* 181:2572-2585.

185. Lutz, M.B., N. Kukutsch, A.L.J. Ogilvie, S. Rößner, F. Koch, N. Romani, and G. Schuler. 1999. An advanced culture method for generating large quantities of highly pure dendritic cells from mouse bone marrow. *Journal of Immunological Methods* 223:77-92.

186. Sutterwala, F.S., G.J. Noel, R. Clynes, and D.M. Mosser. 1997. Selective Suppression of Interleukin-12 Induction after Macrophage Receptor Ligation. *J. Exp. Med.* 185:1977-1985.

187. Sanderson, S., and N. Shastri. 1994. LacZ inducible, antigen/MHC-specific T cell hybrids. *Int. Immunol.* 6:369-376.

188. Diwu, Z., C.-S. Chen, C. Zhang, D.H. Klaubert, and R.P. Haugland. 1999. A novel acidotropic pH indicator and its potential application in labeling acidic organelles of live cells. *Chemistry & Biology* 6:411-418.

189. Chen, Q.-R., L. Zhang, P.W. Luther, and A.J. Mixson. 2002. Optimal transfection with the HK polymer depends on its degree of branching and the pH of endocytic vesicles. *Nucl. Acids Res.* 30:1338-1345.

190. Ingulli, E., A. Mondino, A. Khoruts, and M.K. Jenkins. 1997. In Vivo Detection of Dendritic Cell Antigen Presentation to CD4+ T Cells. *J. Exp. Med.* 185:2133-2141.

191. Desmedt, M., P. Rottiers, H. Dooms, W. Fiers, and J. Grooten. 1998. Macrophages Induce Cellular Immunity by Activating Th1 Cell Responses and Suppressing Th2 Cell Responses. In 5300-5308.

192. Trumpfheller, C., J.S. Finke, C.B. Lopez, T.M. Moran, B. Moltedo, H. Soares, Y. Huang, S.J. Schlesinger, C.G. Park, M.C. Nussenzweig, A. Granelli-Piperno, and R.M. Steinman. 2006. Intensified and protective CD4+ T cell immunity in mice with anti-dendritic cell HIV gag fusion antibody vaccine. *J. Exp. Med.* 203:607-617.

193. Quah, B.J.C., H.S. Warren, and C.R. Parish. 2007. Monitoring lymphocyte proliferation in vitro and in vivo with the intracellular fluorescent dye carboxyfluorescein diacetate succinimidyl ester. *Nat. Protocols* 2:2049-2056.

194. Liu, X., L. Ye, Y. Bai, H. Mojidi, N.E. Simister, and X. Zhu. 2008. Activation of the JAK/STAT-1 Signaling Pathway by IFN-{gamma} Can Down-Regulate Functional Expression of the MHC Class I-Related Neonatal Fc Receptor for IgG. *J Immunol* 181:449-463.

195. Vidarsson, G., A.M. Stemerding, N.M. Stapleton, S.E. Spliethoff, H. Janssen, F.E. Rebers, M. de Haas, and J.G. van de Winkel. 2006. FcRn: an IgG receptor on phagocytes with a novel role in phagocytosis. *Blood* 108:3573-3579.

196. Sallusto, F., and A. Lanzavecchia. 1994. Efficient presentation of soluble antigen by cultured human dendritic cells is maintained by granulocyte/macrophage colony-stimulating factor plus interleukin 4 and downregulated by tumor necrosis factor alpha. *J. Exp. Med.* 179:1109-1118.

197. Reis e Sousa, C., and R.N. Germain. 1995. Major histocompatibility complex class I presentation of peptides derived from soluble exogenous antigen by a subset of cells engaged in phagocytosis. *J. Exp. Med.* 182:841-851.

198. Rodriguez, A., A. Regnault, M. Kleijmeer, P. Ricciardi-Castagnoli, and S. Amigorena. 1999. Selective transport of internalized antigens to the cytosol for MHC class I presentation in dendritic cells. *Nat Cell Biol* 1:362-368.

199. Ramachandra, L., R. Song, and C.V. Harding. 1999. Phagosomes Are Fully Competent Antigen-Processing Organelles That Mediate the Formation of Peptide:Class II MHC Complexes. *J Immunol* 162:3263-3272.

200. Ning, L., Z. Minglang, J. Hilario-Vargas, P. Prisayanh, S. Warren, L.A. Diaz, D.C. Roopenian, and L. Zhi. 2005. Complete FcRn dependence for intravenous Ig therapy in autoimmune skin blistering diseases. *Journal of Clinical Investigation* 115:3440.

201. Farrar, J.D., J.D. Smith, T.L. Murphy, and K.M. Murphy. 2000. Recruitment of Stat4 to the Human Interferon-alpha /beta Receptor Requires Activated Stat2. *J. Biol. Chem.* 275:2693-2697.

202. Berenson, L.S., M. Gavrieli, J.D. Farrar, T.L. Murphy, and K.M. Murphy. 2006. Distinct Characteristics of Murine STAT4 Activation in Response to IL-12 and IFN-{alpha}. *J Immunol* 177:5195-5203.

203. Miyagi, T., M.P. Gil, X. Wang, J. Louten, W.-M. Chu, and C.A. Biron. 2007. High basal STAT4 balanced by STAT1 induction to control type 1 interferon effects in natural killer cells. *J. Exp. Med.* 204:2383-2396.

204. Nguyen, K.B., W.T. Watford, R. Salomon, S.R. Hofmann, G.C. Pien, A. Morinobu, M. Gadina, J.J. O'Shea, and C.A. Biron. 2002. Critical Role for STAT4 Activation by Type 1 Interferons in the Interferon-gamma Response to Viral Infection. *Science* 297:2063-2066.

205. Zhuo Gan, S.R.C.V.R.J.O.E.S.W. 2009. Analyses of the Recycling Receptor, FcRn, in Live Cells Reveal Novel Pathways for Lysosomal Delivery. *Traffic* 10:600-614.

206. He, W., M.S. Ladinsky, K.E. Huey-Tubman, G.J. Jensen, J.R. McIntosh, and P.J. Bjorkman. 2008. FcRn-mediated antibody transport across epithelial cells revealed by electron tomography. *Nature* 455:542-546.

207. Ukkonen, P., V. Lewis, M. Marsh, A. Helenius, and I. Mellman. 1986. Transport of macrophage Fc receptors and Fc receptor-bound ligands to lysosomes. *J. Exp. Med.* 163:952-971.

208. Hamano, Y., H. Arase, H. Saisho, and T. Saito. 2000. Immune Complex and Fc Receptor-Mediated Augmentation of Antigen Presentation for in Vivo Th Cell Responses. *J Immunol* 164:6113-6119.